

# TRYPTOPHAN CATABOLISM BY GUT MICROBIOTA:

A BRIDGE CONNECTING FOOD  
SCIENCE AND HUMAN NUTRITION

ZHAN HUANG

黄展



## **Propositions**

1. The food matrix has direct effects on the amount of tryptophan available in the intestinal lumen and indirect effects on the gut microbiome composition and function.

(this thesis)

2. The gut microbiome function is more important for intestinal health than its composition.

(this thesis)

3. Statistical significance cuts out many interesting topics in scientific publications.

4. The system of special issues in open access journals should be rejected by every researcher.

5. Making good relationships comes from what you do, not from what you say.

6. Propositions are useless for a PhD thesis.

Propositions belonging to the thesis, entitled

Tryptophan catabolism by gut microbiota: a bridge connecting food science and human nutrition

Zhan Huang

Wageningen, 7 February 2023

Tryptophan catabolism by gut microbiota: a bridge  
connecting food science and human nutrition

Zhan Huang

## **Thesis committee**

### **Promoters**

Prof. Dr V. Fogliano

Professor of Food Quality and Design

Wageningen University & Research

Prof. Dr J. M. Wells

Professor of Host-Microbe Interactomics

Wageningen University & Research

### **Co-promotor**

Dr E. Capuano

Associate professor of Food Quality and Design

Wageningen University & Research

### **Other members**

Prof. Dr H. Smidt, Wageningen University & Research

Prof. Dr K. Venema, Maastricht University

Dr J. J. Mes, Wageningen University & Research

Dr N. Bosco, Lesaffre Group, Marcq-en-Barœul, France

This research was conducted under the auspices of VLAG Graduate School (Biobased, Biomolecular, Chemical, Food and Nutrition Sciences).



Tryptophan catabolism by gut microbiota: a bridge connecting food  
science and human nutrition

Zhan Huang

**Thesis**

submitted in fulfilment of the requirements for the degree of doctor  
at Wageningen University  
by the authority of the Rector Magnificus,  
Prof. Dr A.P.J. Mol,  
in the presence of the  
Thesis Committee appointed by the Academic Board  
to be defended in public  
on Tuesday 7 February 2023  
at 4 p.m. in the Omnia Auditorium.

Zhan Huang

Tryptophan catabolism by gut microbiota: a bridge connecting food science and human nutrition

228 pages

PhD thesis Wageningen University, Wageningen, The Netherlands (2023)

With references, with summary in English

ISBN: 978-94-6447-524-1

DOI: <https://doi.org/10.18174/583090>

# Table of Contents

<b>Chapter 1</b> .....	7
General introduction	
<b>Chapter 2</b> .....	41
Whole food modulates tryptophan-derived aryl hydrocarbon receptor ligands production in the intestine: a study in growing pigs	
<b>Chapter 3</b> .....	75
Substrate-driven differences in tryptophan catabolism by gut microbiota and Aryl hydrocarbon Receptor activation	
<b>Chapter 4</b> .....	109
Distinct effects of fiber and colon segment on microbiota-derived indoles and short-chain fatty acids	
<b>Chapter 5</b> .....	137
Impact of high-fiber or high-protein diet on the capacity of human gut microbiota to produce tryptophan catabolites	
<b>Chapter 6</b> .....	183
General discussion	
<b>Appendix</b> .....	209
Summary	
Acknowledgements	
About the author	



## CHAPTER 1







# General introduction



# 1 Introduction to the thesis

Over the past two decades, gut microbiota has been intensively studied for the purpose of understanding its role in host health and pathophysiology of disease.<sup>1</sup> A large array of microbiota-derived metabolites involved in host-microbiota interactions have been identified,<sup>2</sup> of which the most well-researched is short-chain fatty acid mainly generated by microbial fermentation of undigested carbohydrates. Microbial fermentation of proteins is generally considered detrimental for host health, as it produces potentially toxic metabolites, such as ammonia, amines, phenols, and hydrogen sulfide.<sup>3</sup> However, in recent years, emerging evidence shows that microbiota-derived catabolites from tryptophan (Trp), an essential amino acid, have positive impact on host health.<sup>4</sup> These catabolites are suggested to be able to activate the intestinal immune system through binding to aryl hydrocarbon receptor,<sup>5</sup> enhance the intestinal barrier functions,<sup>6,7</sup> stimulate the secretion of gut hormones,<sup>8</sup> and influence the gut microbial community structure.<sup>9</sup> Disruptions in Trp catabolism by gut microbiota are reported in individuals with obesity, type 2 diabetes, metabolic syndrome, irritable bowel syndrome, inflammatory bowel disease, celiac disease, and colorectal cancer, showing reduced microbial production of Trp catabolites.<sup>10–14</sup> Together with their biological effects, Trp catabolism by gut microbiota is therefore considered to open a new way for novel therapeutic opportunities and pharmacological developments in treating disease.

A number of bacteria capable of catabolizing Trp have been identified,<sup>14</sup> but we still do not know the main contributors of Trp catabolism in the human gut, as there are no studies linking the relative abundance of specific bacterial taxa with amounts of different Trp catabolites in human stool samples. Diet is recognized as a major driver of microbiota composition and function and the main source of Trp for humans,<sup>15–17</sup> but few studies have investigated the potential to modulate the microbial catabolism of Trp through diet. A recent study examined the correlation between dietary habits and circulating levels of microbiota-derived Trp catabolites.<sup>18</sup> It was concluded that intake of fiber-rich foods was positively associated with serum indole-3-propionic acid level,<sup>18</sup> but the underlying mechanisms remain unclear.

This thesis aims at adding on to the existing knowledge regarding Trp catabolism by gut microbiota with a focus on its dietary modulations by food matrix, food components, and habitual diets. The results presented in this thesis will contribute to future strategies linking dietary interventions and microbial production of beneficial Trp catabolites.

## 2 Dietary tryptophan

Trp is an essential amino acid composed of an  $\alpha$ -amino group, an  $\alpha$ -carboxylic acid group, and a side chain of indole (Figure 1.1). It is among the less common amino acids found in proteins and cells, but in the human body, Trp is an important biochemical precursor to a large number of endogenous and microbiota-derived metabolites.<sup>19</sup>

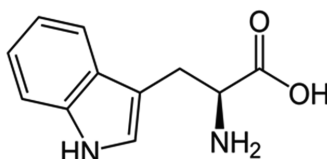


**Figure 1.1** The chemical structure of tryptophan.

Given Trp cannot be synthesized by animal cells, humans rely on exogenous intake, mostly from the foods in the diet. In general, Trp is abundant in protein-rich foods, like meat, fish, eggs, milk, and legumes.<sup>20,21</sup> After consumption, the proteolytic digestion of proteins in the small intestine leads to the release of Trp, which can be absorbed by intestinal epithelium. Once inside a cell, in addition to serving as a substrate for peptide synthesis, approximately 95% of Trp is metabolized by the host kynurenine (Kyn) pathway to produce Kyn, quinolinic acid, niacin, and kynurenic acid, and approximately 1-2% of Trp is converted to serotonin (5-HT) and melatonin via 5-HT pathway.<sup>13</sup> These endogenous Trp metabolites play important roles in the regulation of many biological processes involving neurotransmission, inflammation, and the immune response.<sup>22</sup>

Although the majority of ingested proteins or Trp is digested and absorbed in the small intestine, still significant amounts of proteins may reach the colon, where a range of commensal bacteria degrade them by secreting proteases and peptidases,<sup>23</sup> and produce a variety of Trp catabolites.<sup>24</sup> This chapter aims at providing a description of the Trp catabolism by gut microbiota and the physiological effects of Trp catabolites, as well as the influence of dietary factors.

### 3 Tryptophan catabolism by gut microbiota

It is estimated that 60-90 g of solid matter containing around 20% proteins, as well as a small fraction of free Trp that escapes absorption in the small intestine, can reach the colon every day.<sup>25</sup> Besides proteins, solid matter also contains a significant amount of dietary fibers. Gut microbiota preferentially utilizes fermentable carbohydrates over proteins as the energy source,<sup>26</sup> and therefore, microbial fermentation of proteins mainly occurs in the distal part of the colon, where the fermentable carbohydrates are depleted.<sup>27</sup> Protein fermentation in the distal colon leads to the release of Trp, which is further converted by gut microbiota via different metabolic pathways (Figure 1.2 and Table 1.2). However, the conversion of Trp is not limited to proteolytic specialists or to the distal colon. For example, Trp catabolism by bacterial species from *Lactobacillus* has been reported in the stomach and ileum of mice.<sup>28</sup> In addition, several microbiota-derived Trp catabolites have been identified in ileal fluid samples of ileostomy patients.<sup>29</sup> To date, only little is known about the microbial catabolism of Trp in the stomach or small intestine; hence, we focus on the Trp catabolites in faeces which are discussed in more details below.

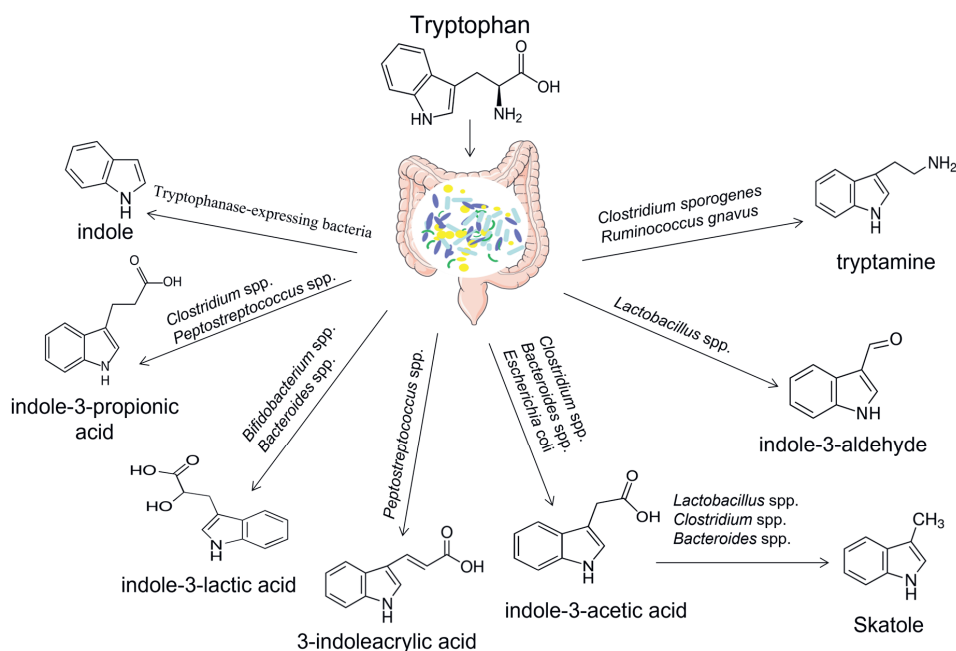


**Figure 1.2** Microbiota-associated production of tryptophan catabolites in the intestine.

**Table 1.1** Intestinal bacterial species and their enzymes involved in tryptophan catabolism

Catabolite	Enzymes	Producers	References
Indole	Tryptophanase	<i>Escherichia coli</i> <i>Clostridium</i> spp. <i>Bacteroides</i> spp. ...for more see <sup>9</sup>	9
Indole-3-lactic acid	Indolelactate dehydrogenase	<i>Lactobacillus murinus</i> <i>Lactobacillus paracasei</i> <i>Lactobacillus reuteri</i> <i>Bifidobacterium bifidum</i>	30–33
3-Indoleacrylic acid	Phenyllactate dehydratase	<i>Clostridium sporogenes</i> <i>Peptostreptococcus russellii</i>	30,34
Indole-3-propionic acid	Acyl-CoA dehydrogenase	<i>Clostridium sporogenes</i> <i>Clostridium cadvareris</i> <i>Peptostreptococcus russellii</i> <i>Peptostreptococcus stomatis</i>	30,34–36
Indole-3-acetic acid	Tryptophan monooxygenase Indole pyruvate decarboxylase Aldehyde dehydrogenase Indole acetaldehyde oxidase	<i>Eubacterium hallii</i> <i>Clostridium bartlettii</i> <i>Bacteroides ovatus</i> <i>Parabacteroides distasonis</i> <i>Bifidobacterium adolescentis</i>	14,36,37
Indole-3-aldehyde	Aminotransferase	<i>Lactobacillus reuteri</i> <i>Lactobacillus murinus</i> <i>Lactobacillus acidophilus</i>	28,31
Skatole	Indoleacetate decarboxylase	<i>Bacteroides thetaiotaomicron</i> <i>Clostridium bartlettii</i> <i>Clostridium scatologenes</i> <i>Clostridium drakei</i> <i>Lactobacillus</i> spp.	38,39
Tryptamine	Tryptophan decarboxylase	<i>Clostridium sporogenes</i> <i>Ruminococcus gnavus</i>	40
Oxindole	Cytochrome P450 2A6	<i>Desulfobacterium indolicum</i>	41
Kynurenine	Kynurenine formamidase Tryptophan 2,3 dioxygenase	<i>Ralstonia metallidurans</i> <i>Pseudomonas fluorescen</i> <i>Lactobacillus</i> spp.	2,42
Serotonin	Tryptophan hydroxylase	<i>Alistipes</i> spp. <i>Akkermansia</i> spp. <i>Roseburia</i> spp. ...for more see <sup>43</sup>	43,44



### 3.1 Indole and oxindole

Indole (Ind) is the most abundant Trp catabolite identified in human faeces, with a concentration of 300–6600  $\mu\text{mol/L}$ .<sup>45,46</sup> The generation of Ind is catalyzed via a single-step reaction by a specific enzyme tryptophanase (*TnaA*),<sup>48</sup> and only bacteria encoding a *TnaA* gene homolog can synthesize Ind from Trp. Available data show that more than 85 Gram-positive and Gram-negative bacterial species are identified as the Ind-producing bacteria in the intestine, including *Clostridium* spp., *Bacteroides* spp., and several pathogenic bacteria.<sup>9</sup>

Compared to Ind, much less is known regarding the microbial production of oxindole (Oxi), but it can be measured in human faeces at a concentration of 2–800  $\mu\text{mol/L}$ .<sup>46</sup> This suggests the existence of a microbial pathway for Oxi production in the intestine. To date, one sulphate-reducing bacterial species, *Desulfobacterium indolicum*, has been shown capable of metabolizing Ind to Oxi.<sup>41</sup> Another metabolic pathway of Ind degradation was identified in an endophytic fungus, *Phomopsis liquidambari*, which utilizes Ind as carbon and nitrogen source to produce Oxi.<sup>49</sup>

### 3.2 Indole-3-acetic acid, indole-3-aldehyde, and skatole

In the intestine, a portion of Trp can be catabolized to indole-3-acetic acid (IAA) by some commensal species from *Bacteroides* and *Clostridium*.<sup>36,37</sup> IAA has a concentration of 2–10  $\mu\text{mol/L}$  in human faeces.<sup>10</sup> Unlike Ind, multiple metabolic pathways are responsible for the formation of IAA, including the indole-3-acetamide pathway via tryptophan monooxygenase and indole-3-acetamide hydrolase, and the indole-3-pyruvate pathway via indole pyruvate decarboxylase and indole acetaldehyde oxidase.<sup>50,51</sup>

IAA can be further converted to indole-3-aldehyde (I3A) and skatole (Ska). The indole-3-pyruvate pathway is the main pathway for I3A synthesis, which is catalyzed by aromatic amino acid aminotransferase.<sup>28,52</sup> It is the key enzyme phylogenetically conserved in many *Lactobacillus* species.<sup>28,31,32</sup> In addition, I3A can also be produced through the peroxidase-catalyzed aerobic oxidation of IAA, but this typically happens in plants.<sup>53</sup> Ska is synthesized from IAA via decarboxylation by a few species mainly from *Bacteroides*, *Clostridium*, and *Lactobacillus*.<sup>38,39</sup> It is produced in large quantities in the hindgut of pigs,<sup>54</sup> but in humans, the level of Ska produced is usually low and highly variable.<sup>13</sup> This could be due to the two-step process for Ska production, in which the level of precursor IAA is the rate-limiting factor.<sup>55</sup>

### 3.3 Indole-3-lactic acid, 3-indoleacrylic acid, and indole-3-propionic acid

Indole-3-lactic acid (ILA), 3-indoleacrylic acid (IA), and indole-3-propionic acid (IPA) are produced from the reductive metabolism of Trp.<sup>30</sup> Firstly, Trp is reduced to indole-3-pyruvate by aromatic amino acid aminotransferase. Next, indole-3-pyruvate is converted to ILA via indolelactate dehydrogenase. Then, ILA is catalyzed to IA by phenyllactate dehydratase. In the end, IA is further converted to IPA in the presence of acyl-CoA dehydrogenase.

Microbial production of IPA is completely dependent on the presence of microbiota and can be established by the colonization with *Clostridium sporogenes*.<sup>35</sup> Besides *Clostridium* spp., several *Peptostreptococcus* spp., like *P. russellii*, can also synthesize IPA and IA.<sup>34</sup> Many *Bifidobacterium* spp. and *Lactobacillus* spp. are reported to convert Trp to ILA.<sup>31,33</sup> The concentration of ILA, IA and IPA in human faeces is approximately 45  $\mu\text{mol/L}$ ,<sup>11</sup> 5  $\mu\text{mol/L}$ ,<sup>46</sup> and 0.7  $\mu\text{mol/L}$ ,<sup>56</sup> respectively.

### 3.4 Tryptamine

Tryptamine (TA) is present at concentrations of 0.5-1.5  $\mu\text{mol/L}$  in human faeces.<sup>12</sup> Similar to Ind, the production of TA from Trp is also a single-step reaction of decarboxylation, which is catalyzed by Trp decarboxylase.<sup>40</sup> This enzyme is common in the plant kingdom,<sup>57</sup> but it is an exceedingly rare activity among bacteria. In the intestine, only two known commensal Firmicutes, *Ruminococcus gnavus* and *Clostridium sporogenes*, can convert Trp to TA.<sup>40</sup> However, the NIH Human Microbiome Project revealed that the Trp decarboxylase homologs are present in 9-17% of gut metagenomes of a random population of healthy individuals.<sup>40</sup> This suggests that the generation and physiological role of TA in the intestine is important and more studies are needed to identify the TA-producing bacterial species.

### 3.5 Kynurenine and serotonin

Kyn and 5-HT are two well-known endogenous Trp metabolites, but accumulating evidence from human fecal samples and *in vitro* fermentation by *ex vivo* human gut microbiota indicates that these two endogenous metabolites can also be produced by gut microbiota.<sup>12,46,58,59</sup> In human faeces, Kyn has a concentration of 10-60  $\mu\text{mol/L}$  and 5-HT has a concentration of 5-40  $\mu\text{mol/L}$ .<sup>12,46</sup> Trp 2,3 dioxygenase and Kyn formamidase are the two enzymes participating in the conversion of Trp to Kyn and their encoding genes are in the genomes of *Cupriavidus metallidurans* (*Ralstonia metallidurans*).<sup>60</sup> In addition, several members of the mammalian gut

microbiota, like *Lactobacillus* spp. and pathogenic *Pseudomonas* spp., also have the genomic capacity to produce Kyn.<sup>2</sup>

The biosynthetic pathways of 5-HT in gut microbiota are not yet fully elucidated, but two metabolic routes have been proposed: plant-like pathway (decarboxylation of Trp to TA followed by hydroxylation) and animal-like pathway (hydroxylation to 5-hydroxytryptophan and then decarboxylation).<sup>61</sup> Analysis of human gut-associated microbial genomes showed that the plant-like pathway was characterized as rare in human gut microbiome, but the animal-like pathway was present in almost 20% of gut-associated genomes, including *Akkermansia*, *Alistipes*, *Clostridium*, *Bacteroides*, and *Roseburia*.<sup>43</sup>

### 3.6 Conclusive remarks

In summary, the Trp catabolism by gut microbiota is a very complex process involving multiple members of the microbiota and metabolic pathways, in which *Bacteroides*, *Clostridium*, *Bifidobacterium*, and *Lactobacillus* are active Trp-degrading bacterial genera in the intestine. Given the large abundance and extensive metabolic capacity of gut microbiota, many strains that possess catalytic enzymes for Trp catabolism and their derived catabolites remain unknown. Studies linking bacterial abundance with concentrations of Trp catabolites in human stool samples followed by *in vitro* and *in silico* verifications are needed to identify the main producers of Trp catabolites in the intestine. Importantly, besides bacteria, the fungal microbiome is beginning to gain recognition as a fundamental part of the human gut microbiome,<sup>62</sup> in particular several fungi have been shown capable of degrading Trp to Ind derivatives.<sup>63,64</sup> Therefore, fungal metabolic roles or pathways regarding Trp catabolism warrant further study.

## 4 Physiological functions of tryptophan catabolites

The intense interest in Trp catabolism by gut microbiota is in relation to its contribution to the intestinal and systemic homeostasis. A growing body of literature demonstrates the various beneficial effects of microbiota-derived Trp catabolites on host physiology, with a focus on gut health (Figure 1.3).<sup>4,13,14</sup> Several mechanisms of action of Trp catabolites have been elucidated, in which the most documented is the activation of aryl hydrocarbon receptor (AhR). AhR is a ligand-activated transcription factor expressed by the epithelial and immune cells in the intestine, which is able to tune local and distant host functions including immune homeostasis and barrier physiology.<sup>5,65,66</sup> The activation of pregnane X receptor (PXR), known as a master regulator of drug metabolism,<sup>67</sup> is also of particular interest. Moreover, Trp catabolites also have profound effects on gut microbiota through quorum sensing mechanisms.<sup>13,14</sup>

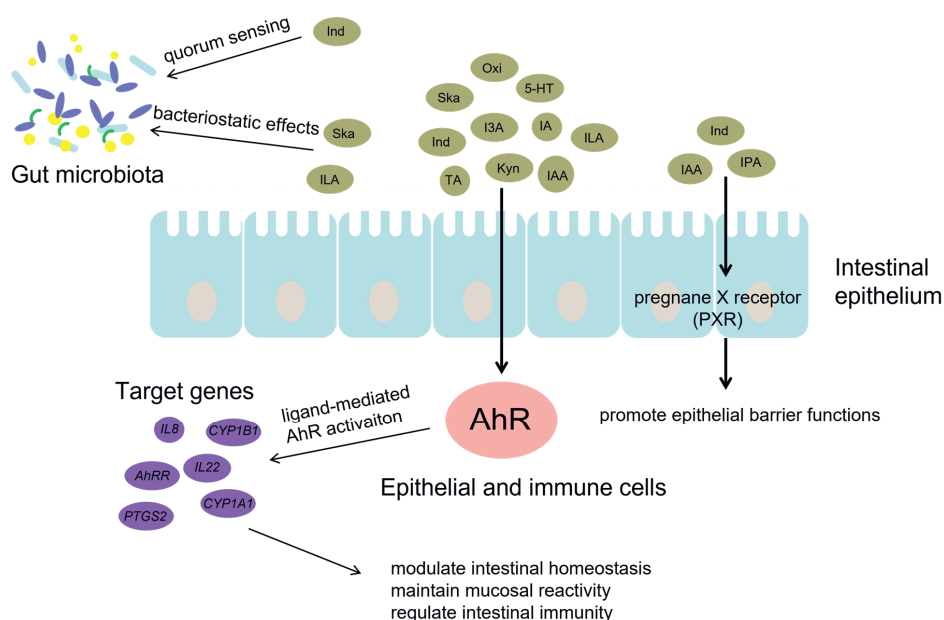


**Figure 1.3** The beneficial effect of bacterial tryptophan catabolites on gut health.

Ind: indole; Ska: skatole; ILA: indole-3-lactic acid; Oxi: oxindole; 5-HT: serotonin; I3A: indole-3-aldehyde; TA: tryptamine; Kyn: kynurenine; IAA: indole-3-acetic acid; IA: 3-indoleacrylic acid; IPA: indole-3-propionic acid; AhR: aryl hydrocarbon receptor; IL-8: interleukin 8; IL-22: interleukin 22; CYP1B1: cytochrome P450 family-1 subfamily-B polypeptide-1; CYP1A1: cytochrome P450 family-1 subfamily-A polypeptide-1; AhRR: aryl hydrocarbon receptor repressor; PTGS2: prostaglandin-endoperoxide synthase 2.

## 4.1 Tryptophan catabolites as aryl hydrocarbon receptor activators

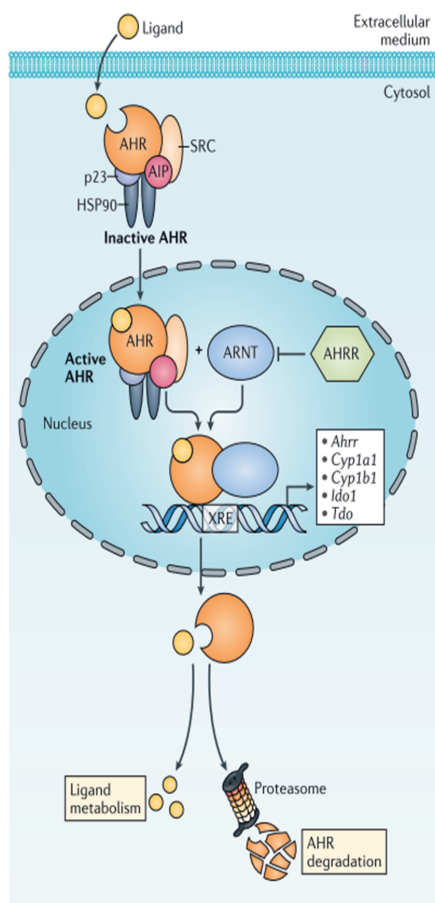


**Figure 1.4** The signaling pathway of aryl hydrocarbon receptor.<sup>65</sup>

AhR: aryl hydrocarbon receptor; p23: co-chaperone p23; HSP90: 90-kDa heat shock protein; AIP: aryl hydrocarbon receptor-interacting protein; SRC: Proto-oncogene tyrosine-protein kinase; ARNT: aryl hydrocarbon receptor nuclear translocator; AHRR: aryl hydrocarbon receptor repressor; XRE: xenobiotic response element; CYP1: cytochrome P450 family-1; A1: subfamily-A polypeptide-1; B1: subfamily-B polypeptide-1; Ido1: indoleamine 2,3-dioxygenase 1; Tdo: tryptophan-2,3-dioxygenase

AhR is a member of basic HLH (helix-loop-helix)/PER (periodic circadian protein)–ARNT (AhR nuclear translocator)–SIM (single-minded protein) (PAS) superfamily of transcription factors that are involved in the sensing of both endogenous and exogenous factors.<sup>65</sup> It is the only bHLH/PAS transcription factor that is known to be ligand activated.<sup>66</sup> In its inactive state, AhR is present in the cytosol as part of a protein complex that contains 90-kDa heat shock protein (HSP90), AhR-interacting protein (AIP), proto-oncogene tyrosine-protein kinase (SRC), and co-chaperone p23 (Figure 1.4). Upon binding of an agonist ligand, the AhR-ligand complex is translocated to the nucleus, where AhR, along with its ligand, is released from the complex and forms a heterodimer with AhR nuclear translocator (ARNT). The AhR:ligand:ARNT complex eventually binds to the xenobiotic response element (XRE), which is situated upstream of the AhR target genes (for more details see<sup>65</sup>).

The AhR signaling pathway is negatively controlled by three different feedback loops including degradation of AhR by proteasome, ligand metabolism by cytochrome P450 (CYP) 1A1, and disruption of the interaction between AhR-ligand complex and ARNT by AhR repressor (AHRR) (Figure 1.4).<sup>66</sup> The AhR activation is featured by ligand-specific, cell-type-specific, and context-specific binding,<sup>65</sup>

which means differential AhR action or outcome exists across different ligands, species, and circumstances.

In the intestine, Trp catabolism by gut microbiota is an important physiological source of endogenous AhR ligands. Although Trp itself cannot activate AhR,<sup>58,68</sup> many of Trp catabolites, such as Ind, IAA, TA, I3A, IA, and ILA, have been demonstrated to be AhR ligands.<sup>14</sup> In the AhR activation, Trp catabolites have varying levels of binding affinity and capacity to activate AhR. A recent study on a reporter cell line constructed from human HepG2 cells showed that the activation of AhR by Trp catabolites is dose-dependent and the most AhR-active Trp catabolites are Ind, Ska, and TA.<sup>69,70</sup> IAA, I3A, IPA, and ILA are low-efficacy AhR agonists.<sup>70</sup> Microbiota-derived Oxi, Kyn, and 5-HT are also identified as AhR activators,<sup>71–73</sup> but their physiological significance is currently unknown. Unlike other Trp catabolites reported to directly activate AhR, 5-HT is an indirect activator through interfering with CYP1A1-mediated ligand clearance,<sup>74</sup> suggesting a synergistic effect of 5-HT in activating AhR in the presence of an AhR ligand.

AhR expression and activation in the gastrointestinal tract have been shown to contribute to the intestinal homeostasis.<sup>75</sup> Recent studies have underlined that Trp-derived AhR ligands are immunomodulators in the intestine that modify the activity of immune system and decrease the inflammatory response.<sup>13</sup> In intestinal epithelial cell lines, ILA interacts with AhR to prevent the transcription of inflammatory cytokine interleukin (IL)-8,<sup>76,77</sup> which causes excessive inflammation in the premature intestine. ILA, along with I3A, also leads to the down-regulation of Thpok, a key regulator of T cell development and function, and reprogramming of intraepithelial CD4<sup>+</sup> T cells into immunoregulatory T cells by activating AhR.<sup>31</sup> In rodent studies, I3A and IAA are found to activate AhR to induce IL-22 and thereby to inhibit inflammation in the intestine.<sup>28,78,79</sup> IL-22 also stimulates protective responses in intestinal epithelial cells and provides colonization resistance against the fungus *Candida albicans*.<sup>28,80,81</sup> In a murine model of multiple sclerosis, TA was found to shift the T cell landscape toward an immunosuppressive state and directly interact with myelin-reactive T cells to inhibit neuroinflammation in an AhR dependent manner.<sup>82</sup> IA has been recently shown to promote the intestinal epithelial barrier functions and mitigate inflammatory response in mice by activating AhR to enhance goblet cell function and mucin gene expression.<sup>34</sup> I3A protects against increased gut permeability in a mouse model of colitis by maintaining the integrity of the apical junctional complex and its associated actin regulatory proteins and these effects are dependent on the AhR.<sup>6</sup> I3A also increases the proliferation of epithelial cells and promotes goblet cell



differentiation via increasing the expression of cytokine IL-10 by AhR activation.<sup>83</sup> Taken together, these AhR-driven immunomodulatory benefits of Trp catabolites suggest that they can be therapeutic targets, which can be directly achieved by the use of Trp catabolites,<sup>10,78,83</sup> or indirectly by using the high AhR ligand-producing bacteria, like *Lactobacillus reuteri*, *Lactobacillus murinus*, and *Peptostreptococcus* spp.<sup>12,34,84</sup>

## 4.2 Tryptophan catabolites as Pregnane X receptor activators

PXR is a member of the nuclear receptor superfamily of ligand-activated transcription factors, which is highly expressed in the intestine and liver.<sup>85</sup> It plays a critical role in the inflammatory response and the intermediary metabolism of drugs, lipids, glucose, and bile acids.<sup>86–88</sup> Upon ligand binding, the PXR-ligand complex is translocated to the nucleus and forms a heterodimer with the retinoid X receptor (RXR) before stabilization by coactivators including peroxisome proliferator-activated receptor- $\gamma$  coactivator 1 $\alpha$  (PGC-1 $\alpha$ ), hepatocyte nuclear factor 4 $\alpha$  (HNF4 $\alpha$ ), and steroid receptor coactivator 1 (SRC-1) (Figure 1.5). This complex then binds to the xenobiotic responsive enhancer molecule (XREM)/PXR response elements (PXRE) located in the 5'-flanking regions of PXR target genes, resulting in their transcriptional activation. The coactivators can also transcribe the orphan nuclear receptor, such as small heterodimer partner (SHP) and silencing mediator of retinoid and thyroid hormone receptors (SMRT), to inhibit the transcription of PXR target genes, but this process can be blocked by ligand-activated PXR.<sup>89</sup>

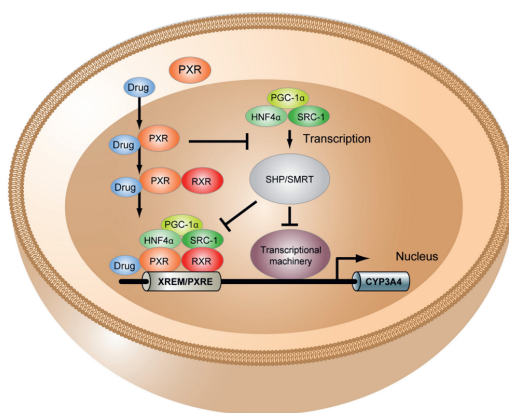


**Figure 1.5** The signaling pathway of pregnane X receptor.<sup>89</sup>

PXR: pregnane X receptor; RXR: retinoid X receptor; PGC-1 $\alpha$ : peroxisome proliferator-activated receptor- $\gamma$  coactivator 1 $\alpha$ ; HNF4 $\alpha$ : Hepatocyte nuclear factor 4 $\alpha$ ; SRC-1: steroid receptor coactivator 1; XREM: xenobiotic responsive enhancer molecule; PXRE: pregnane X receptor response element; SHP: small heterodimer partner; SMRT: silencing mediator of retinoid and thyroid hormone receptors; CYP3A4: cytochrome P450 family-3 subfamily-A polypeptide-4.

The role of Trp catabolites in the activation of PXR is less reported than AhR. Only a small fraction of Trp catabolites has been shown capable of activating PXR, such as IAA, IPA, and Ind. IPA and IAA are identified as weak PXR agonists and their activations can be highly potentiated in the presence of Ind.<sup>7</sup> In a follow-up study using a reporter gene assay, Ind was identified as a PXR agonist, which directly binds to the receptor and results in the transcriptional activation of PXR target genes, like CYP3A4 and MDR1.<sup>90</sup>

In the intestine, PXR plays an important role in abrogating intestinal inflammation and protecting the barrier function.<sup>91–93</sup> As a ligand of PXR, IPA, particularly in the presence of Ind, was found to regulate intestinal barrier function *in vivo* in mice by downregulating enterocyte-mediated inflammatory cytokine tumor necrosis factor- $\alpha$  (TNF- $\alpha$ ) and upregulating junctional protein-coding mRNAs.<sup>7</sup> IPA also attenuates hematopoietic system and gastrointestinal tract injuries intertwined with radiation exposure without precipitating tumor growth in mice via PXR/acyl-CoA-binding protein signaling pathway.<sup>94</sup> However, the physiological importance of IAA and Ind as PXR ligands in the intestine is currently unknown.

### 4.3 Tryptophan catabolites as modulators of gut microbiota

Several Trp catabolites have been shown capable of modulating the gut microbial composition.<sup>13</sup> Ind is a well-described quorum-sensing molecule that can regulate bacterial motility, spore formation, plasmid stability, antibiotic resistance, biofilm formation, and virulence.<sup>9</sup> Ind-producing bacteria appears to use Ind to survive against other non-Ind-producing bacteria and eukaryotes.<sup>9</sup> Ska is reported to be responsible for the growth and reproduction of certain intestinal bacteria and to have a bacteriostatic effect on Gram-negative enterobacteria, such as *Aerobacter*, *Escherichia*, *Proteus*, *Salmonella*, *Eberthella* and *Shigella*.<sup>13,95</sup> Ska also inhibits the growth and fermentation of *Lactobacillus acidophilus*.<sup>96</sup> Similar antibacterial and antifungal effects were also observed for ILA.<sup>97,98</sup>

### 4.4 Conclusive remarks

Besides AhR, PXR, and bacterial physiology, Trp catabolites are also involved in other pathways that positively impact the host physiology.<sup>24</sup> TA acts on a G-protein-coupled receptor to accelerate the gastrointestinal transit by increasing ionic flux and fluid secretion in the proximal colon of mice.<sup>99</sup> ILA dose-dependently inhibits the mouse polarization of T helper 17 cells, which plays a deleterious role in autoimmune diseases.<sup>32</sup> Ind modulates the production of glucagon-like peptide-1 from intestinal enteroendocrine L cells to stimulate the secretion of gut

hormones.<sup>8</sup> Collectively, these observations suggest a considerable role of Trp catabolites in host health and disease. However, most of these studies are on mice. As with any animal study, there are certain limitations, like the affinities of Trp catabolites for AhR and PXR differ between mice and humans,<sup>46,100</sup> that need to be considered and further validated when translating results from mouse models to humans.

## 5 Dietary factors affecting tryptophan catabolism by gut microbiota

In the intestine, the microbial production of Trp catabolites is affected by the amount of Trp available to gut microbiota. An *in vitro* study showed that the supplementation of Trp in colonic fermentation increases the microbial production of Trp catabolites.<sup>58</sup> This is also verified in mice and pig studies using a Trp-rich diet.<sup>11,101,102</sup> Therefore, food products with a high level of Trp would have advantages in the microbial production of Trp catabolites. In general, animal protein has a higher level of Trp than plant protein, but it also has a high digestibility.<sup>21</sup> In the small intestine, animal protein is directly digested by digestive enzymes and absorbed by the intestinal epithelium, whereas an intact plant cell wall is resistant to digestive enzymes, thereby preventing the encapsulated plant protein from digestion and absorption.<sup>103</sup> However, small intestine, especially the distal part, also hosts a considerable number of bacteria ( $\sim 10^{7-8}$  bacteria per gram of intestinal content),<sup>104</sup> which are able to compete with animal cells for nutrients.<sup>105</sup> This suggests that the high digestibility of animal protein may increase the availability of Trp to small bowel microbiota and drive the microbial production of Trp catabolites in the small intestine.

The low digestibility of plant protein in the upper gastrointestinal tract results in a relatively high fraction of plant protein reaching the colon, but this is also affected by the processing of plant foods which can break the plant cell wall.<sup>106</sup> Compared with small intestine, the bacterial load is  $1 \times 10^6$  fold greater in the colon.<sup>104</sup> Many commensal species in this niche possess carbohydrate-active enzymes that are able to break down the plant cell wall.<sup>107</sup> Unlike in the small intestine, the Trp released from bacterial proteolysis in the colon, cannot be rapidly absorbed by the epithelium and thus is utilized by bacteria.<sup>23</sup> Therefore, consumption of plant foods, especially those rich in Trp with intact plant cell wall, would seem a suitable strategy for delivering Trp to colonic microbiota.

Besides Trp, other food components can also modulate the microbial catabolism of Trp by interacting with gut microbiota. For example, mulberry-derived 1-deoxynojirimycin can increase the population of *Akkermansia* and *Clostridium* group bacteria and promote the microbial production of IPA.<sup>108</sup> Fuzhuan brick tea polysaccharide promotes the proliferation of beneficial bacteria, such as *Lactobacillus* and *Akkermansia*, and elevates the mouse fecal level

of I3A and IAA.<sup>109</sup> Similar effects were also observed for turmeric polysaccharides and *Lycium barbarum* polysaccharide.<sup>110,111</sup>

Probiotics act as health-promoting ingredients in the food products, which can improve the intestinal microbial balance by modulating the composition and metabolism of gut microbiota.<sup>112</sup> In recent years, probiotics have been reported to exert beneficial effects via metabolic pathway regarding Trp metabolism.<sup>4</sup> On the one hand, probiotics, such as species from *Lactobacillus* and *Bifidobacterium*, can directly convert Trp into I3A, ILA, and IAA.<sup>14</sup> On the other hand, some probiotics, such as *Lactobacillus casei* and *Lactobacillus fermentum*, can indirectly promote the intestinal synthesis of Kyn and 5-HT by increasing the expression of Trp hydroxylase 1 (TPH1) and indoleamine 2,3-dioxygenase 1 (IDO1).<sup>113,114</sup>

Habitual diets are a mixture of various food components that are continuously and indefinitely delivered to the intestinal ecosystem,<sup>115</sup> which have a wide influence on gut microbiota and of course the related microbial catabolism of Trp.<sup>24</sup> Poor dietary habits, like high intake of salt,<sup>32</sup> cholesterol,<sup>116</sup> and fat,<sup>117</sup> have been reported to be associated with a reduced production of microbiota-derived Trp catabolites including IAA, ILA, IPA, I3A, and TA in mouse models. Conversely, intakes of fiber or polyphenol rich foods can increase the circulating level of IPA in humans,<sup>18,118</sup> but potentially inhibit the production of Ind.<sup>119</sup> In line with this, a human crossover pilot study showed that compared with a fast food diet (i.e. burgers and fries), a Mediterranean diet, which is rich in vegetables, whole grains, olive oil, nuts, and fish, can increase the plasma concentration of IAA, ILA, and IPA.<sup>120</sup> Interestingly, chicken-eaters and pork-eaters also have different profiles of Trp catabolites, in which chicken-eaters have higher fecal concentration of Ind and Ska than the pork-eaters.<sup>121</sup> However, the mechanisms whereby the manipulation of the gut microbiota affect the Trp catabolism are not yet fully understood. Globally, these observations suggest that dietary factors can modulate the Trp catabolism by gut microbiota.

## 6 Aim and outline of this thesis

To extend the current knowledge on Trp catabolism by gut microbiota, especially the knowledge on its dietary modulating factors, this thesis investigated the effect of different foods, food matrix, food components, and habitual diets on the microbial production of Trp catabolites in the intestine, with particular attention to the colon (Figure 1.6). We hypothesized that (1) small bowel microbiota may play a role in the catabolism of Trp; (2) dietary factors could modulate the availability of Trp to microbiota and the microbiota composition and function regarding Trp catabolism; and (3) microbiota-associated shifts in Trp catabolism could potentially be a novel mechanism for microbiota-targeted diets that positively impact host physiology.

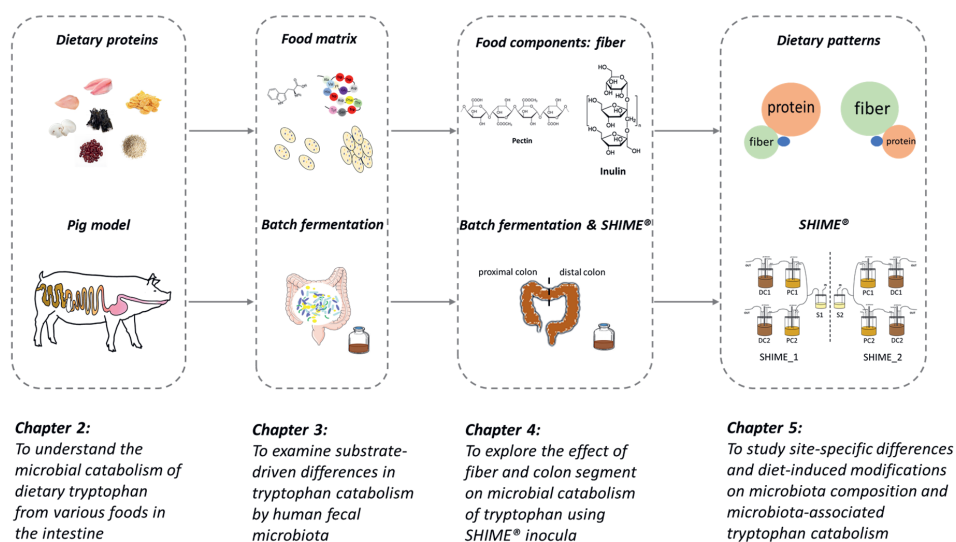


**Figure 1.6** Schematic of the thesis chapters.

SHIME: Simulator of Human Intestinal Microbial Ecosystem; S1/S2: stomach/small intestine compartment; PC: proximal colon compartment; DC: distal colon compartment

To test and verify these hypotheses, both *in vivo* and *in vitro* experimental approaches were employed in this thesis. In the *in vivo* study to understand the microbial catabolism of Trp in the intestine (i.e. small intestine and colon), an animal model of growing pigs was used given the high anatomical and physiological similarity between the human and porcine gastrointestinal tracts.<sup>122</sup> In the *in vitro* study to understand the effect and possible mechanisms



of dietary factors on the modulation of Trp catabolism by gut microbiota, static batch fermentation model and dynamic continuous culture system (Simulator of Human Intestinal Microbial Ecosystem, SHIME®) were used. Batch fermentation, usually carried out in small vessels, is relatively convenient and enables many samples to be studied at once and within a short period of 24-48 h.<sup>123</sup> The SHIME® model comprised of multiple connected vessels is complex but can mimic the entire human intestine, in which the environmental conditions are controlled to resemble the *in vivo* physiological conditions.<sup>124</sup> It is considered the best model to study the effect of long-term dietary interventions on human gut microbiome.

Specifically, in **Chapter 2**, we fed growing pigs with various foods, including algae, fungi, seeds, cereals, animal products, and potato protein. We collected ileal digesta and faeces of pigs to understand the microbial catabolism of Trp in the small intestine and colon. We found that colon is the main site for Trp catabolites production, in which plant foods tend to be more effective than animal foods. Therefore, in **Chapter 3**, plant-based materials (i.e. soybean protein, single and clustered soybean cells) containing an equimolar amount of Trp, but with a different accessibility were used in the static batch fermentation inoculated with human fecal microbiota to examine the substrate-driven differences in Trp catabolism by gut microbiota. Interestingly, we found that the polysaccharides in the plant cell wall potentially modulate the microbial catabolism of Trp, and thus in **Chapter 4**, we further studied the effect of pectin, inulin, and their combination on the microbial production of Trp catabolites. As the composition and function of gut microbiota vary along the colon with proximal colon (PC) being the major location for saccharolytic fermentation and distal colon (DC) for proteolytic fermentation,<sup>27</sup> we inoculated the *ex vivo* human gut microbiota from PC and DC compartments of SHIME® into the batch vessels to also evaluate the differences between these two colon segments in Trp catabolites production. Finally, in **Chapter 5**, we used SHIME® to explore the effect of two different habitual diets, high-fiber-low-protein diet and high-protein-low-fiber diet, on microbiota composition and function regarding Trp catabolism. We monitored the microbial production of Trp catabolites before, during, and after dietary interventions and combined this with amplicon sequencing and shotgun metagenomics to reveal the underlying mechanisms and to identify the potential main producers of Trp catabolites in the intestine.

To conclude and summarize, **Chapter 6** presents the general discussion of all the results obtained, as well as some results from our further investigations of Trp catabolites-mediated AhR and PXR pathways on porcine intestinal organoids. In the end, the scientific challenges and future recommendations regarding the topic of this thesis are also presented.

## Reference

1. Cani PD. Human gut microbiome: Hopes, threats and promises. *Gut*. 2018;67(9):1716-1725. doi:10.1136/gutjnl-2018-316723
2. Krautkramer KA, Fan J, Bäckhed F. Gut microbial metabolites as multi-kingdom intermediates. *Nat Rev Microbiol*. 2021;19(2):77-94. doi:10.1038/s41579-020-0438-4
3. Windey K, De Preter V, Verbeke K. Relevance of protein fermentation to gut health. *Mol Nutr Food Res*. 2012;56(1):184-196. doi:10.1002/mnfr.201100542
4. Agus A, Planchais J, Sokol H. Gut Microbiota Regulation of Tryptophan Metabolism in Health and Disease. *Cell Host Microbe*. 2018;23(6):716-724. doi:10.1016/j.chom.2018.05.003
5. Gutiérrez-Vázquez C, Quintana FJ. Regulation of the Immune Response by the Aryl Hydrocarbon Receptor. *Immunity*. 2018;48(1):19-33. doi:10.1016/j.immuni.2017.12.012
6. Scott SA, Fu J, Chang P V. Microbial tryptophan metabolites regulate gut barrier function via the aryl hydrocarbon receptor. *Proc Natl Acad Sci*. 2020;117(32):19376-19387. doi:10.1073/pnas.2000047117
7. Venkatesh M, Mukherjee S, Wang H, et al. Symbiotic bacterial metabolites regulate gastrointestinal barrier function via the xenobiotic sensor PXR and toll-like receptor 4. *Immunity*. 2014;41(2):296-310. doi:10.1016/j.immuni.2014.06.014
8. Chimere C, Emery E, Summers DK, Keyser U, Gribble FM, Reimann F. Bacterial Metabolite Indole Modulates Incretin Secretion from Intestinal Enteroendocrine L Cells. *Cell Rep*. 2014;9(4):1202-1208. doi:10.1016/j.celrep.2014.10.032
9. Lee J-H, Lee J. Indole as an intercellular signal in microbial communities. *FEMS Microbiol Rev*. 2010;34(4):426-444. doi:10.1111/j.1574-6976.2009.00204.x
10. Lamas B, Richard ML, Leducq V, et al. CARD9 impacts colitis by altering gut microbiota metabolism of tryptophan into aryl hydrocarbon receptor ligands. *Nat Med*. 2016;22(6):598-605. doi:10.1038/nm.4102
11. Lamas B, Hernandez-Galan L, Galipeau HJ, et al. Aryl hydrocarbon receptor ligand production by the gut microbiota is decreased in celiac disease leading to intestinal inflammation. *Sci Transl Med*. 2020;12(566):eaba0624. doi:10.1126/scitranslmed.aba0624
12. Natividad JM, Agus A, Planchais J, et al. Impaired Aryl Hydrocarbon Receptor Ligand Production by the Gut Microbiota Is a Key Factor in Metabolic Syndrome. *Cell Metab*.

- 2018;28(5):737-749.e4. doi:10.1016/j.cmet.2018.07.001
13. Gao J, Xu K, Liu H, et al. Impact of the gut microbiota on intestinal immunity mediated by tryptophan metabolism. *Front Cell Infect Microbiol.* 2018;8(13):1-22. doi:10.3389/fcimb.2018.00013
  14. Roager HM, Licht TR. Microbial tryptophan catabolites in health and disease. *Nat Commun.* 2018;9(1):1-10. doi:10.1038/s41467-018-05470-4
  15. Kolodziejczyk AA, Zheng D, Elinav E. Diet–microbiota interactions and personalized nutrition. *Nat Rev Microbiol.* 2019;17(12):742-753. doi:10.1038/s41579-019-0256-8
  16. David LA, Maurice CF, Carmody RN, et al. Diet rapidly and reproducibly alters the human gut microbiome. *Nature.* 2014;505(7484):559-563. doi:10.1038/nature12820
  17. Muegge BD, Kuczynski J, Knights D, et al. Diet drives convergence in gut microbiome functions across mammalian phylogeny and within humans. *Science (80- ).* 2011;332(6032):970-974. doi:10.1126/science.1198719
  18. Qi Q, Li J, Yu B, et al. Host and gut microbial tryptophan metabolism and type 2 diabetes: an integrative analysis of host genetics, diet, gut microbiome and circulating metabolites in cohort studies. *Gut.* 2022;71(6):1095-1105. doi:10.1136/gutjnl-2021-324053
  19. Moffett JR, Namboodiri MA. Tryptophan and the immune response. *Immunol Cell Biol.* 2003;81(4):247-265. doi:10.1046/j.1440-1711.2003.t01-1-01177.x
  20. Kałużna-Czaplińska J, Gątarek P, Chirumbolo S, Chartrand MS, Björklund G. How important is tryptophan in human health? *Crit Rev Food Sci Nutr.* 2019;59(1):72-88. doi:10.1080/10408398.2017.1357534
  21. Day L, Cakebread JA, Loveday SM. Food proteins from animals and plants: Differences in the nutritional and functional properties. *Trends Food Sci Technol.* 2022;119:428-442. doi:10.1016/j.tifs.2021.12.020
  22. Opitz CA, Somarribas Patterson LF, Mohapatra SR, et al. The therapeutic potential of targeting tryptophan catabolism in cancer. *Br J Cancer.* 2020;122(1):30-44. doi:10.1038/s41416-019-0664-6
  23. Portune KJ, Beaumont M, Davila AM, Tomé D, Blachier F, Sanz Y. Gut microbiota role in dietary protein metabolism and health-related outcomes: The two sides of the coin. *Trends Food Sci Technol.* 2016;57:213-232. doi:10.1016/j.tifs.2016.08.011
  24. Li X, Zhang B, Hu Y, Zhao Y. New Insights Into Gut-Bacteria-Derived Indole and Its Derivatives in Intestinal and Liver Diseases. *Front Pharmacol.* 2021;12. doi:10.3389/fphar.2021.769501

25. Silvester KR, Englyst HN, Cummings JH. Ileal recovery of starch from whole diets containing resistant starch measured in vitro and fermentation of ileal effluent. *Am J Clin Nutr.* 1995;62(2):403-411. doi:10.1093/ajcn/62.2.403
26. Oliphant K, Allen-Vercoe E. Macronutrient metabolism by the human gut microbiome: major fermentation by-products and their impact on host health. *Microbiome.* 2019;7(1):91. doi:10.1186/s40168-019-0704-8
27. Hamer HM, De Preter V, Windey K, Verbeke K. Functional analysis of colonic bacterial metabolism: relevant to health? *Am J Physiol Liver Physiol.* 2012;302(1):G1-G9. doi:10.1152/ajpgi.00048.2011
28. Zelante T, Iannitti RG, Cunha C, et al. Tryptophan Catabolites from Microbiota Engage Aryl Hydrocarbon Receptor and Balance Mucosal Reactivity via Interleukin-22. *Immunity.* 2013;39(2):372-385. doi:10.1016/j.immuni.2013.08.003
29. Koper JEB, Kortekaas M, Loonen LMP, et al. Aryl hydrocarbon Receptor activation during in vitro and in vivo digestion of raw and cooked broccoli ( *brassica oleracea* var. *Italica* ). *Food Funct.* 2020;11(5):4026-4037. doi:10.1039/D0FO00472C
30. Dodd D, Spitzer MH, Van Treuren W, et al. A gut bacterial pathway metabolizes aromatic amino acids into nine circulating metabolites. *Nature.* 2017;551(7682):648-652. doi:10.1038/nature24661
31. Cervantes-Barragan L, Chai JN, Tianero MD, et al. *Lactobacillus reuteri* induces gut intraepithelial CD4 + CD8 $\alpha\alpha$  + T cells. *Science (80- ).* 2017;357(6353):806-810. doi:10.1126/science.aah5825
32. Wilck N, Matus MG, Kearney SM, et al. Salt-responsive gut commensal modulates TH17 axis and disease. *Nature.* 2017;551(7682):585-589. doi:10.1038/nature24628
33. Aragozzini F, Ferrari A, Pacini N, Gualandris R. Indole-3-lactic acid as a tryptophan metabolite produced by *Bifidobacterium* spp. *Appl Environ Microbiol.* 1979;38(3):544-546. doi:10.1128/aem.38.3.544-546.1979
34. Wlodarska M, Luo C, Kolde R, et al. Indoleacrylic Acid Produced by Commensal *Peptostreptococcus* Species Suppresses Inflammation. *Cell Host Microbe.* 2017;22(1):25-37.e6. doi:10.1016/j.chom.2017.06.007
35. Wikoff WR, Anfora AT, Liu J, et al. Metabolomics analysis reveals large effects of gut microflora on mammalian blood metabolites. *Proc Natl Acad Sci U S A.* 2009;106(10):3698-3703. doi:10.1073/pnas.0812874106
36. Elsdon SR, Hilton MG, Waller JM. The end products of the metabolism of aromatic amino acids by clostridia. *Arch Microbiol.* 1976;107(3):283-288.

- doi:10.1007/BF00425340
37. Russell WR, Duncan SH, Scobbie L, et al. Major phenylpropanoid-derived metabolites in the human gut can arise from microbial fermentation of protein. *Mol Nutr Food Res*. 2013;57(3):523-535. doi:10.1002/mnfr.201200594
  38. Whitehead TR, Price NP, Drake HL, Cotta MA. Catabolic Pathway for the Production of Skatole and Indoleacetic Acid by the Acetogen *Clostridium drakei*, *Clostridium scatologenes*, and Swine Manure. *Appl Environ Microbiol*. 2008;74(6):1950-1953. doi:10.1128/AEM.02458-07
  39. Honeyfield DC, Carlson JR. Effect of indoleacetic acid and related indoles on *Lactobacillus* sp. strain 11201 growth, indoleacetic acid catabolism, and 3-methylindole formation. *Appl Environ Microbiol*. 1990;56(5):1373-1377. doi:10.1128/aem.56.5.1373-1377.1990
  40. Williams BB, Van Benschoten AH, Cimermancic P, et al. Discovery and Characterization of Gut Microbiota Decarboxylases that Can Produce the Neurotransmitter Tryptamine. *Cell Host Microbe*. 2014;16(4):495-503. doi:10.1016/j.chom.2014.09.001
  41. Licht D, Johansen SS, Arvin E, Ahring BK. Transformation of indole and quinoline by *Desulfobacterium indolicum* (DSM 3383). *Appl Microbiol Biotechnol*. 1997;47(2):167-172. doi:10.1007/s002530050907
  42. Kaur H, Bose C, Mande SS. Tryptophan Metabolism by Gut Microbiome and Gut-Brain-Axis: An in silico Analysis. *Front Neurosci*. 2019;13(1365):1-17. doi:10.3389/fnins.2019.01365
  43. Valles-Colomer M, Falony G, Darzi Y, et al. The neuroactive potential of the human gut microbiota in quality of life and depression. *Nat Microbiol*. 2019;4(4):623-632. doi:10.1038/s41564-018-0337-x
  44. O'Mahony SM, Clarke G, Borre YE, Dinan TG, Cryan JF. Serotonin, tryptophan metabolism and the brain-gut-microbiome axis. *Behav Brain Res*. 2015;277:32-48. doi:10.1016/j.bbr.2014.07.027
  45. Darkoh C, Chappell C, Gonzales C, Okhuysen P. A rapid and specific method for the detection of indole in complex biological samples. Schloss PD, ed. *Appl Environ Microbiol*. 2015;81(23):8093-8097. doi:10.1128/AEM.02787-15
  46. Dong F, Hao F, Murray IA, et al. Intestinal microbiota-derived tryptophan metabolites are predictive of Ah receptor activity. *Gut Microbes*. 2020;12(1):1788899. doi:10.1080/19490976.2020.1788899

47. Smith T. A modification of the method for determining the production of indol by bacteria. *J Exp Med.* 1897;2(5):543-547. doi:10.1084/jem.2.5.543
48. Snell EE. Tryptophanase: Structure, Catalytic Activities, and Mechanism of Action. *Adv Enzymol Relat Areas Mol Biol.* 1975;42:287-333. doi:10.1002/9780470122877.ch6
49. Chen Y, Xie XG, Ren CG, Dai CC. Degradation of N-heterocyclic indole by a novel endophytic fungus *Phomopsis liquidambari*. *Bioresour Technol.* 2013;129:568-574. doi:10.1016/j.biortech.2012.11.100
50. Malhotra M, Srivastava S. Organization of the ipdC region regulates IAA levels in different *Azospirillum brasilense* strains: Molecular and functional analysis of ipdC in strain SM. *Environ Microbiol.* 2008;10(5):1365-1373. doi:10.1111/j.1462-2920.2007.01529.x
51. Hubbard TD, Murray IA, Perdew GH. Indole and tryptophan metabolism: Endogenous and dietary routes to ah receptor activation. *Drug Metab Dispos.* 2015;43(10):1522-1535. doi:10.1124/dmd.115.064246
52. Zelante T, Puccetti M, Giovagnoli S, Romani L. Regulation of host physiology and immunity by microbial indole-3-aldehyde. *Curr Opin Immunol.* 2021;70:27-32. doi:10.1016/j.coi.2020.12.004
53. De Mello MP, De Toledo SM, Haun M, Durán N, Cilento G. Excited Indole-3-Aldehyde from the Peroxidase-Catalyzed Aerobic Oxidation of Indole-3-Acetic Acid. Reaction with and Energy Transfer to Transfer Ribonucleic Acid. *Biochemistry.* 1980;19(23):5270-5275. doi:10.1021/bi00564a019
54. Jensen MT, Cox RP, Jensen BB. 3-Methylindole (skatole) and indole production by mixed populations of pig fecal bacteria. *Appl Environ Microbiol.* 1995;61(8):3180-3184. doi:10.1128/aem.61.8.3180-3184.1995
55. Yokoyama MT, Carlson JR. Microbial metabolites of tryptophan in the intestinal tract with special reference to skatole. *Am J Clin Nutr.* 1979;32(1):173-178. doi:10.1093/ajcn/32.1.173
56. Xue H, Chen X, Yu C, et al. Gut Microbially Produced Indole-3-Propionic Acid Inhibits Atherosclerosis by Promoting Reverse Cholesterol Transport and Its Deficiency Is Causally Related to Atherosclerotic Cardiovascular Disease. *Circ Res.* 2022;131(5):404-420. doi:10.1161/CIRCRESAHA.122.321253
57. Facchini PJ., Huber-Allanach KL., Leslie WT. Plant aromatic L-amino acid decarboxylases: evolution, biochemistry, regulation, and metabolic engineering

- applications. *Phytochemistry*. 2000;54:121-138. doi:10.1016/s0031-9422(00)00050-9
58. Koper JE, Troise AD, Loonen LM, et al. Tryptophan Supplementation Increases the Production of Microbial-Derived AhR Agonists in an In Vitro Simulator of Intestinal Microbial Ecosystem. *J Agric Food Chem*. 2022;70(13):3958-3968. doi:10.1021/acs.jafc.1c04145
59. Huang Z, Boekhorst J, Fogliano V, Capuano E, Wells JM. Distinct effects of fiber and colon segment on microbiota-derived indoles and short-chain fatty acids. *Food Chem*. 2023;398:133801. doi:10.1016/j.foodchem.2022.133801
60. Kurnasov O, Goral V, Colabroy K, et al. NAD Biosynthesis. *Chem Biol*. 2003;10(12):1195-1204. doi:10.1016/j.chembiol.2003.11.011
61. Tsavkelova EA, Klimova SI, Cherdyntseva TA, Netrusov AI. Hormones and hormone-like substances of microorganisms: a review. *Prikl biokhimiia i Mikrobiol*. 2006;42(3):261-268.
62. Nash AK, Auchtung TA, Wong MC, et al. The gut mycobiome of the Human Microbiome Project healthy cohort. *Microbiome*. 2017;5(1):153. doi:10.1186/s40168-017-0373-4
63. Zelante T, Choera T, Beauvais A, et al. *Aspergillus fumigatus* tryptophan metabolic route differently affects host immunity. *Cell Rep*. 2021;34(4):108673. doi:10.1016/j.celrep.2020.108673
64. Jain VK, Divol B, Prior BA, Bauer FF. Effect of alternative NAD<sup>+</sup>-regenerating pathways on the formation of primary and secondary aroma compounds in a *Saccharomyces cerevisiae* glycerol-defective mutant. *Appl Microbiol Biotechnol*. 2012;93(1):131-141. doi:10.1007/s00253-011-3431-z
65. Rothhammer V, Quintana FJ. The aryl hydrocarbon receptor: an environmental sensor integrating immune responses in health and disease. *Nat Rev Immunol*. 2019;19(3):184-197. doi:10.1038/s41577-019-0125-8
66. Lamas B, Natividad JM, Sokol H. Aryl hydrocarbon receptor and intestinal immunity. *Mucosal Immunol*. 2018;11(4):1024-1038. doi:10.1038/s41385-018-0019-2
67. Ekins S, Schuetz E. The PXR crystal structure: the end of the beginning. *Trends Pharmacol Sci*. 2002;23(2):49-50. doi:10.1016/S0165-6147(02)01977-6
68. Opitz CA, Litzenburger UM, Sahm F, et al. An endogenous tumour-promoting ligand of the human aryl hydrocarbon receptor. *Nature*. 2011;478(7368):197-203. doi:10.1038/nature10491
69. Novotna A, Pavek P, Dvorak Z. Novel stably transfected gene reporter human

- hepatoma cell line for assessment of aryl hydrocarbon receptor transcriptional activity: Construction and characterization. *Environ Sci Technol.* 2011;45(23):10133-10139. doi:10.1021/es2029334
70. Vyhřídálová B, Krasulová K, Pečínková P, et al. Gut microbial catabolites of tryptophan are ligands and agonists of the aryl hydrocarbon receptor: A detailed characterization. *Int J Mol Sci.* 2020;21(7):1-17. doi:10.3390/ijms21072614
  71. Hubbard TD, Murray IA, Bisson WH, et al. Adaptation of the human aryl hydrocarbon receptor to sense microbiota-derived indoles. *Sci Rep.* 2015;5(1):12689. doi:10.1038/srep12689
  72. Denison MS, Nagy SR. Activation of the Aryl Hydrocarbon Receptor by Structurally Diverse Exogenous and Endogenous Chemicals. *Annu Rev Pharmacol Toxicol.* 2003;43(1):309-334. doi:10.1146/annurev.pharmtox.43.100901.135828
  73. Manzella C, Singhal M, Alrefai WA, Saksena S, Dudeja PK, Gill RK. Serotonin is an endogenous regulator of intestinal CYP1A1 via AhR. *Sci Rep.* 2018;8(1):6103. doi:10.1038/s41598-018-24213-5
  74. Manzella CR, Ackerman M, Singhal M, et al. Serotonin modulates AhR activation by interfering with CYP1A1-mediated clearance of AhR ligands. *Cell Physiol Biochem.* 2020;54(1):126-141. doi:10.33594/000000209
  75. Murray IA, Perdew GH. Ligand activation of the Ah receptor contributes to gastrointestinal homeostasis. *Curr Opin Toxicol.* 2017;2:15-23. doi:10.1016/j.cotox.2017.01.003
  76. Meng D, Sommella E, Salvati E, et al. Indole-3-lactic acid, a metabolite of tryptophan, secreted by *Bifidobacterium longum* subspecies *infantis* is anti-inflammatory in the immature intestine. *Pediatr Res.* 2020;88(2):209-217. doi:10.1038/s41390-019-0740-x
  77. Ehrlich AM, Pacheco AR, Henrick BM, et al. Indole-3-lactic acid associated with *Bifidobacterium*-dominated microbiota significantly decreases inflammation in intestinal epithelial cells. *BMC Microbiol.* 2020;20(1):357. doi:10.1186/s12866-020-02023-y
  78. Hendrikx T, Duan Y, Wang Y, et al. Bacteria engineered to produce IL-22 in intestine induce expression of REG3G to reduce ethanol-induced liver disease in mice. *Gut.* 2019;68(8):1504-1515. doi:10.1136/gutjnl-2018-317232
  79. Monteleone I, Rizzo A, Sarra M, et al. Aryl Hydrocarbon Receptor-Induced Signals Up-regulate IL-22 Production and Inhibit Inflammation in the Gastrointestinal Tract. *Gastroenterology.* 2011;141(1):237-248. doi:10.1053/j.gastro.2011.04.007



80. Ouyang W, O'Garra A. IL-10 Family Cytokines IL-10 and IL-22: from Basic Science to Clinical Translation. *Immunity*. 2019;50(4):871-891. doi:10.1016/j.immuni.2019.03.020
81. Sovran B, Loonen LMP, Lu P, et al. IL-22-STAT3 pathway plays a key role in the maintenance of ileal homeostasis in mice lacking secreted mucus barrier. *Inflamm Bowel Dis*. 2015;21(3):531-542. doi:10.1097/MIB.0000000000000319
82. Dopkins N, Becker W, Miranda K, Walla M, Nagarkatti P, Nagarkatti M. Tryptamine Attenuates Experimental Multiple Sclerosis Through Activation of Aryl Hydrocarbon Receptor. *Front Pharmacol*. 2021;11. doi:10.3389/fphar.2020.619265
83. Powell DN, Swimm A, Sonowal R, et al. Indoles from the commensal microbiota act via the AHR and IL-10 to tune the cellular composition of the colonic epithelium during aging. *Proc Natl Acad Sci*. Published online 2020:202003004. doi:10.1073/pnas.2003004117
84. Hezaveh K, Shinde RS, Klötgen A, et al. Tryptophan-derived microbial metabolites activate the aryl hydrocarbon receptor in tumor-associated macrophages to suppress anti-tumor immunity. *Immunity*. 2022;55(2):324-340.e8. doi:10.1016/j.immuni.2022.01.006
85. Kliewer SA. The nuclear pregnane X receptor regulates xenobiotic detoxification. In: *Journal of Nutrition*. Vol 133. ; 2003:2444S-2447S. doi:10.1093/jn/133.7.2444s
86. Moreau A, Vilarem MJ, Maurel P, Pascussi JM. Xenoreceptors CAR and PXR activation and consequences on lipid metabolism, glucose homeostasis, and inflammatory response. *Mol Pharm*. 2008;5(1):35-41. doi:10.1021/mp700103m
87. Kliewer SA, Willson TM. Regulation of xenobiotic and bile acid metabolism by the nuclear pregnane X receptor. *J Lipid Res*. 2002;43(3):359-364. doi:10.1016/s0022-2275(20)30141-3
88. Cheng J, Shah YM, Gonzalez FJ. Pregnane X receptor as a target for treatment of inflammatory bowel disorders. *Trends Pharmacol Sci*. 2012;33(6):323-330. doi:10.1016/j.tips.2012.03.003
89. Shukla SJ, Sakamuru S, Huang R, et al. Identification of Clinically Used Drugs That Activate Pregnane X Receptors. *Drug Metab Dispos*. 2011;39(1):151-159. doi:10.1124/dmd.110.035105
90. Illés P, Krasulová K, Vyhlídalová B, et al. Indole microbial intestinal metabolites expand the repertoire of ligands and agonists of the human pregnane X receptor. *Toxicol Lett*. 2020;334:87-93. doi:10.1016/j.toxlet.2020.09.015

91. Huang K, Mukherjee S, DesMarais V, et al. Targeting the PXR–TLR4 signaling pathway to reduce intestinal inflammation in an experimental model of necrotizing enterocolitis. *Pediatr Res*. 2018;83(5):1031-1040. doi:10.1038/pr.2018.14
92. Dou W, Mukherjee S, Li H, et al. Alleviation of Gut Inflammation by Cdx2/Pxr Pathway in a Mouse Model of Chemical Colitis. Basu S, ed. *PLoS One*. 2012;7(7):e36075. doi:10.1371/journal.pone.0036075
93. Garg A, Zhao A, Erickson SL, et al. Pregnane x receptor activation attenuates inflammation-associated intestinal epithelial barrier dysfunction by inhibiting cytokine-induced myosin light-chain kinase expression and c-jun n-terminal kinase 1/2 activation. *J Pharmacol Exp Ther*. 2016;359(1):91-101. doi:10.1124/jpet.116.234096
94. Xiao HW, Cui M, Li Y, et al. Gut microbiota-derived indole 3-propionic acid protects against radiation toxicity via retaining acyl-CoA-binding protein. *Microbiome*. 2020;8(1):69. doi:10.1186/s40168-020-00845-6
95. Deslandes B, Gariépy C, Houde A. Review of microbiological and biochemical effects of skatole on animal production. *Livest Prod Sci*. 2001;71(2-3):193-200. doi:10.1016/S0301-6226(01)00189-0
96. Yokoyama MT, Carlson JR. Microbial metabolites of tryptophan in the intestinal tract with special reference to skatole. *Am J Clin Nutr*. 1979;32(1):173-178. doi:10.1093/ajcn/32.1.173
97. Honoré AH, Aunsbjerg SD, Ebrahimi P, et al. Metabolic footprinting for investigation of antifungal properties of *Lactobacillus paracasei*. *Anal Bioanal Chem*. 2016;408(1):83-96. doi:10.1007/s00216-015-9103-6
98. Narayanan TK, Ramananda Rao G. Beta indoleethanol and beta indolelactic acid production by *Candida* species: their antibacterial and autoantibiotic action. *Antimicrob Agents Chemother*. 1976;9(3):375-380. doi:10.1128/AAC.9.3.375
99. Bhattarai Y, Williams BB, Battaglioli EJ, et al. Gut Microbiota-Produced Tryptamine Activates an Epithelial G-Protein-Coupled Receptor to Increase Colonic Secretion. *Cell Host Microbe*. 2018;23(6):775-785.e5. doi:10.1016/j.chom.2018.05.004
100. Dvořák Z, Sokol H, Mani S. Drug Mimicry: Promiscuous Receptors PXR and AhR, and Microbial Metabolite Interactions in the Intestine. *Trends Pharmacol Sci*. 2020;41(12):900-908. doi:10.1016/j.tips.2020.09.013
101. Liang H, Dai Z, Liu N, et al. Dietary L-tryptophan modulates the structural and functional composition of the intestinal microbiome in weaned piglets. *Front Microbiol*. 2018;9(AUG). doi:10.3389/fmicb.2018.01736

102. Yin J, Zhang B, Yu Z, et al. Ameliorative Effect of Dietary Tryptophan on Neurodegeneration and Inflammation in  $\alpha$ -Galactose-Induced Aging Mice with the Potential Mechanism Relying on AMPK/SIRT1/PGC-1 $\alpha$  Pathway and Gut Microbiota. *J Agric Food Chem*. 2021;69(16):4732-4744. doi:10.1021/acs.jafc.1c00706
103. Capuano E. The behavior of dietary fiber in the gastrointestinal tract determines its physiological effect. *Crit Rev Food Sci Nutr*. 2017;57(16):3543-3564. doi:10.1080/10408398.2016.1180501
104. Sender R, Fuchs S, Milo R. Revised Estimates for the Number of Human and Bacteria Cells in the Body. *PLOS Biol*. 2016;14(8):e1002533. doi:10.1371/journal.pbio.1002533
105. Savage DC. Gastrointestinal Microflora in Mammalian Nutrition. *Annu Rev Nutr*. 1986;6(1):155-178. doi:10.1146/annurev.nu.06.070186.001103
106. Xiong W, Devkota L, Zhang B, Muir J, Dhital S. Intact cells: “Nutritional capsules” in plant foods. *Compr Rev Food Sci Food Saf*. 2022;21(2):1198-1217. doi:10.1111/1541-4337.12904
107. Korpela K. Diet, microbiota, and metabolic health: trade-off between saccharolytic and proteolytic fermentation. *Annu Rev Food Sci Technol*. 2018;9(1):65-84. doi:10.1146/annurev-food-030117-012830
108. Li Y, Xu W, Zhang F, et al. The Gut Microbiota-Produced Indole-3-Propionic Acid Confers the Antihyperlipidemic Effect of Mulberry-Derived 1-Deoxynojirimycin. Manichanh C, ed. *mSystems*. 2020;5(5):e00313-20. doi:10.1128/msystems.00313-20
109. Yang W, Ren D, Zhao Y, Liu L, Yang X. Fuzhuan Brick Tea Polysaccharide Improved Ulcerative Colitis in Association with Gut Microbiota-Derived Tryptophan Metabolism. *J Agric Food Chem*. Published online July 27, 2021:acs.jafc.1c02774. doi:10.1021/acs.jafc.1c02774
110. Yang C, Du Y, Ren D, Yang X, Zhao Y. Gut microbiota-dependent catabolites of tryptophan play a predominant role in the protective effects of turmeric polysaccharides against DSS-induced ulcerative colitis. *Food Funct*. 2021;12(20):9793-9807. doi:10.1039/d1fo01468d
111. Zhang Z, Liu H, Yu B, et al. Lycium barbarum polysaccharide attenuates myocardial injury in high-fat diet-fed mice through manipulating the gut microbiome and fecal metabolome. *Food Res Int*. 2020;138:109778. doi:10.1016/j.foodres.2020.109778
112. Sánchez B, Delgado S, Blanco-Míguez A, Lourenço A, Gueimonde M, Margolles A.

- Probiotics, gut microbiota, and their influence on host health and disease. *Mol Nutr Food Res.* 2017;61(1):1600240. doi:10.1002/mnfr.201600240
113. Hara T, Mihara T, Ishibashi M, Kumagai T, Joh T. Heat-killed *Lactobacillus casei* subsp. *casei* 327 promotes colonic serotonin synthesis in mice. *J Funct Foods.* 2018;47:585-589. doi:10.1016/j.jff.2018.05.050
114. Cox AJ, Pyne DB, Saunders PU, Fricker PA. Oral administration of the probiotic *Lactobacillus fermentum* VRI-003 and mucosal immunity in endurance athletes. *Br J Sports Med.* 2010;44(4):222-226. doi:10.1136/bjsm.2007.044628
115. Rinninella, Cintoni, Raoul, et al. Food Components and Dietary Habits: Keys for a Healthy Gut Microbiota Composition. *Nutrients.* 2019;11(10):2393. doi:10.3390/nu11102393
116. Zhang X, Coker OO, Chu ES, et al. Dietary cholesterol drives fatty liver-associated liver cancer by modulating gut microbiota and metabolites. *Gut.* 2021;70(4):761-774. doi:10.1136/gutjnl-2019-319664
117. Krishnan S, Ding Y, Saedi N, et al. Gut Microbiota-Derived Tryptophan Metabolites Modulate Inflammatory Response in Hepatocytes and Macrophages. *Cell Rep.* 2018;23(4):1099-1111. doi:10.1016/j.celrep.2018.03.109
118. Peron G, Meroño T, Gargari G, et al. A Polyphenol-Rich Diet Increases the Gut Microbiota Metabolite Indole 3-Propionic Acid in Older Adults with Preserved Kidney Function. *Mol Nutr Food Res.* Published online April 6, 2022:2100349. doi:10.1002/mnfr.202100349
119. Knarreborg A, Beck J, Jensen MT, Laue A, Agergaard N, Jensen BB. Effect of non-starch polysaccharides on production and absorption of indolic compounds in entire male pigs. *Anim Sci.* 2002;74(3):445-453. doi:10.1017/S1357729800052590
120. Zhu C, Sawrey-Kubicek L, Beals E, et al. Human gut microbiome composition and tryptophan metabolites were changed differently by fast food and Mediterranean diet in 4 days: a pilot study. *Nutr Res.* 2020;77:62-72. doi:10.1016/j.nutres.2020.03.005
121. Shi J, Zhao D, Zhao F, Wang C, Zamaratskaia G, Li C. Chicken-eaters and pork-eaters have different gut microbiota and tryptophan metabolites. *Sci Rep.* 2021;11(1):1-10. doi:10.1038/s41598-021-91429-3
122. Ziegler A, Gonzalez L, Blikslager A. Large Animal Models: The Key to Translational Discovery in Digestive Disease Research. *Cell Mol Gastroenterol Hepatol.* 2016;2(6):716-724. doi:10.1016/j.jcmgh.2016.09.003
123. Pérez-Burillo S, Molino S, Navajas-Porras B, et al. An in vitro batch fermentation

- protocol for studying the contribution of food to gut microbiota composition and functionality. *Nat Protoc.* 2021;16(7):3186-3209. doi:10.1038/s41596-021-00537-x
124. Van de Wiele T, Van den Abbeele P, Ossieur W, Possemiers S, Marzorati M. The Simulator of the Human Intestinal Microbial Ecosystem (SHIME®). In: *The Impact of Food Bioactives on Health*. Springer International Publishing; 2015:305-317. doi:10.1007/978-3-319-16104-4\_27



## CHAPTER 2

2





# Whole food modulates tryptophan-derived aryl hydrocarbon receptor ligands production in the intestine: a study in growing pigs

**Zhan Huang<sup>1,2,\*</sup>, Sonja de Vries<sup>3</sup>, Vincenzo Fogliano<sup>1</sup>, Jerry M. Wells<sup>2</sup>, Nikkie van der Wielen<sup>3,4</sup>, Edoardo Capuano<sup>1</sup>**

<sup>1</sup>Food Quality and Design Group, Department of Agrotechnology and Food Sciences, Wageningen University & Research, P.O. Box 17, 6700 AA, Wageningen, the Netherlands

<sup>2</sup>Host-Microbe Interactomics Group, Department of Animal Sciences, Wageningen University & Research, P.O. Box 17, 6700 AA, Wageningen, the Netherlands

<sup>3</sup>Animal Nutrition Group, Department of Animal Sciences, Wageningen University & Research, P.O. Box 17, 6700 AA, Wageningen, the Netherlands

<sup>4</sup>Human Nutrition and Health Group, Department of Agrotechnology and Food Sciences, Wageningen University & Research, P.O. Box 17, 6700 AA, Wageningen, the Netherlands



## Abstract

Effects of various whole foods on the production of tryptophan-derived aryl hydrocarbon receptor (AhR) ligands in the intestine were investigated in a pig model. Ileal digesta and faeces of pigs after feeding of eighteen different foods were analyzed. Indole, indole-3-propionic acid, indole-3-acetic acid, indole-3-lactic acid, kynurenine, tryptamine, and indole-3-aldehyde were identified in ileal digesta, which were also identified in faeces but at higher concentrations except indole-3-lactic acid, together with skatole, oxindole, serotonin, and indoleacrylic acid. The panel of tryptophan catabolites in ileal digesta and faeces varied across different foods. Eggs induced the highest overall concentration of catabolites in ileal digesta dominated by indole. Amaranth induced the highest overall concentration of catabolites in faeces dominated by skatole. Using a reporter cell line, we observed many faecal samples but not ileal samples retained AhR activity. Collectively, these findings contribute to food selection targeting AhR ligands production from dietary tryptophan in the intestine.

**Keywords:** food matrix; aryl hydrocarbon receptor; small intestine; colon; tryptophan; indole derivatives

## 1 Introduction

Aryl hydrocarbon receptor (AhR) is a well-known ligand-activated transcription factor,<sup>1</sup> which plays important physiological and homeostatic roles in many tissues and organs, as evidenced by AhR-deficient mice that suffer from developmental abnormalities.<sup>2,3</sup> In the intestine, AhR is expressed by intestinal epithelial cells and immune cells.<sup>4</sup> AhR activation protects the gut against pathogenic bacteria, maintains the epithelial barrier function, and regulates immune tolerance and inflammation.<sup>4,5</sup> Lack of AhR ligands in the intestine and particularly small intestine compromises the maintenance of intraepithelial lymphocytes and results in increased vulnerability to epithelial damage.<sup>6</sup> In a mouse colitis model, administration of a potent AhR agonist, 6-formylindolo[3,2-b]carbazole, attenuated the severity of symptoms by down-regulating pro-inflammatory cytokines and producing interleukin (IL)-22 to increase epithelial barrier defences.<sup>7</sup> IL-22 also aids in wound-healing by promoting tissue regeneration and producing antimicrobial peptides for innate defense.<sup>8</sup>

A number of microbiota-derived metabolites have been shown to be agonists of AhR of which tryptophan (Trp) catabolites are of particular interest.<sup>4</sup> Gut microbiota catabolizes Trp into the AhR agonists indole (Ind) and derivatives, such as tryptamine (TA), indole-3-aldehyde (I3A), indole-3-acetic acid (IAA), and indoleacrylic acid (IA).<sup>9</sup> Numerous studies have investigated the physiological functions of microbiota-derived Trp catabolites and their therapeutic effects in disease.<sup>10–13</sup> Nevertheless, no study has yet investigated the formation of these Trp catabolites along the intestine and very limited information on their presence in the small intestine exists. Previously, several Trp catabolites were reported in the ileal fluid samples of ileostomy patients, in which indole-3-lactic acid (ILA) was present at a relatively high concentration.<sup>14</sup> ILA has anti-inflammatory activity in the immature intestine by interacting with AhR and preventing the transcription of pro-inflammatory cytokine IL-8.<sup>15</sup> A recent study identified an AhR-dependent subset of eosinophils in the small intestine with an immunomodulatory profile.<sup>16</sup> Given the importance of the Trp catabolite-AhR axis to intestinal homeostasis, there is great interest in identifying microbiota-derived Trp catabolites produced in the small intestine, which may contribute to the design of dietary treatments to promote intestinal health.

The primary source of Trp in the intestine is from digestion of food, as Trp is an essential amino acid. The chemical composition of food varies greatly, as well as the structural organization of its components at macro-, meso-, and microscopic level.<sup>17</sup> We previously demonstrated that food matrix affects the *in vitro* microbial catabolism of Trp by influencing the microbial

community structure and the accessibility of Trp to microbiota.<sup>18</sup> To date, no study has yet investigated the microbial production of Trp-derived AhR ligands in the intestine using the whole food. This information is of particular importance for selecting foods in terms of AhR ligand production in the intestine.

In this study, we investigated the microbial catabolism of dietary Trp from various foods including algae, fungi, seeds, cereals, animal products, and potato protein along the intestine (i.e. small intestine and colon). We used growing pigs as a model given the high anatomical and physiological similarity between human and porcine intestinal tracts.<sup>19</sup> We collected samples from ileal digesta and faeces of pigs during the normal passage of whole foods along the intestine and quantified the Trp catabolites via LC-MS. We also characterized the AhR activation potential of ileal digesta and faeces of pigs using an AhR reporter cell line.

## 2 Experimental section

### 2.1 Ethical approval

The study was conducted at the research facilities of Wageningen University & Research (Wageningen, The Netherlands), and experimental procedures were approved by the Dutch Central Committee of Animal Experiments under the authorization number AVD104002015326.

### 2.2 Selection and preparation of foods

Eighteen foods were selected including algae (spirulina and seaweed), fungi (mushrooms, yeast, and quorn), seeds (kidney beans, linseed, buckwheat, and amaranth), cereals (wheat flour, oatmeal, millet, rice crackers, cornflakes), animal products (chicken, fish-tilapia, and eggs), and potato protein. They are food grade and were procured online or from local markets in Wageningen, The Netherlands (for details see Table S2.1). Each test food was used as the protein source in one test diet. The preparation of test foods was given in supplementary methods. In most cases, the test food was freshly prepared for each diet or stored frozen (-20 °C) and then mixed thoroughly with non-protein food ingredients, like purified maize starch, sucrose, vitamins and minerals, rapeseed oil, and purified cellulose, before being offered to pigs. The amount of test foods in the diet was adjusted to get a final protein concentration of 100 g/kg dry matter, except rice crackers and cornflakes because of their low protein content. Therefore, pigs fed with rice crackers and cornflakes were provided with additional amino acids on day 1 to 4 to meet the protein requirement. Basal and protein-free diets were also prepared. A basal diet was formulated to be structurally similar to a normal human diet and was fed to pigs during the period of acclimatization, recovery, and wash-out. A protein-free diet was used for correcting endogenous excretion of Trp catabolites. All diets were formulated to meet or exceed nutritional requirements for growing pigs, except protein, as prescribed by the National Research Council.<sup>20</sup> The ingredient composition basal diet, protein-free diet, and test diets were given in Table S2.2, together with the protein and Trp content in each diet.

### 2.3 Animals and experimental procedures

The experimental protocol followed the guidelines as previously described.<sup>21</sup> A total of eighteen health growing pigs (Topigs TN-70) with an initial body weight of  $19.7 \pm 1.4$  kg were used. Pigs were surgically fitted with a T-cannula (inner diameter 2.24 cm) in the distal ileum ( $\pm 10$ -

20 cm from cecum) according to the procedure described elsewhere.<sup>21</sup> This allows sampling at the end of small intestine and a normal passage towards the large intestine. Pigs then were moved into individual metabolism pens (minimum 1.2 × 1.5 m) with slatted floors covered by plastics. Room temperature was controlled to be 21-24 °C and a 12-h light/dark cycle was applied. Each pen had a single-space feeder and a low-pressure bowl drinker for free access to water. Pigs were given 8-11 days to recover from surgery prior to starting the assay phase. The experimental feed design consisted of a triple 6 × 6 latin square design, where each pig was assigned to six diets each in six weeks, with halfway one week protein free diet followed by one week wash-out. Eighteen diets were tested and each test cycle had a duration of seven days, in which the initial five days were the adaptation period to the test diet, and samples were collected in the last two days starting immediately after the first meal of the day. Pigs were weighed weekly prior to a diet change. The daily dietary ration for each pig was  $0.08 \times \text{bodyweight (kg)}^{0.75}$  calculated on a dry matter basis, which was adjusted according to the bodyweight of the pig. It was given in two equal meals at 08:00 and 17:00 of the day and fed as mash mixed with water in the feed trough. Feed refusals were recorded after each meal. Ileal digesta were collected from plastic bags attached to the T-cannula barrel using an elastic band. Bags were replaced whenever filled approximately 70% with digesta or at least once every 60 min from 08:00 to 17:00 of the day. Metabolism pens were cleaned every morning and faeces were collected from the floor if any from 15:00 to 16:00 of the day after the morning section of daily ration. Ileal digesta and faeces were pooled per pig within period and immediately frozen at -20 °C for further analysis. Pigs refused to eat yeast and sometimes showed clinical signs of sickness during the test week, resulting in some missing values. Therefore, samples from yeast diet were removed from the analysis.

## 2.4 Extraction and quantification of microbiota-derived Trp catabolites

Freeze-dried ileal digesta (~50 mg) were mixed with ice-cold 80% methanol at a ratio of 1 : 10 (w/v) and faeces (~100 mg) at 1 : 6 (w/v). The mixture was homogenized by vortexing at 2100 rpm for 30 min and then centrifuged at 22000 × g for 10 min at 4 °C. The supernatants were collected and referred to as extracts. For quantification, extracts were diluted 16-fold with Milli-Q water before being subjected to targeted analysis for Trp catabolites by a Shimadzu Nexera XR LC-20ADxr UPLC system coupled with a Shimadzu LCMS-8050 mass spectrometer (Kyoto, Japan) using a Phenomenex Kinetex 1.7 µm EVO C18 100 Å LC column (100 × 2.1 mm). The operation conditions, mobile phase, and elution program were described elsewhere.<sup>22</sup> Catabolites were identified by comparing the transitions (m/z) and retention time (RT) with

reference standards including TA ( $m/z$  161.1  $\rightarrow$  144.0; RT 2.08 min), Ind ( $m/z$  118.2  $\rightarrow$  91.1; RT 9.89 min), I3A ( $m/z$  146.0  $\rightarrow$  118.1; RT 9.36 min), IAA ( $m/z$  176.0  $\rightarrow$  130.1; RT 9.33 min), IA ( $m/z$  188.0  $\rightarrow$  115.1; RT 10.95 min), ILA ( $m/z$  205.9  $\rightarrow$  118.1; RT 9.05 min), indole-3-propionic acid (IPA,  $m/z$  190.1  $\rightarrow$  130.0; RT 9.88 min), oxindole (Oxi,  $m/z$  134.0  $\rightarrow$  77.1; RT 8.65 min), skatole (Ska,  $m/z$  132.0  $\rightarrow$  117.1; RT 11.52 min), kynurenine (Kyn,  $m/z$  209.0  $\rightarrow$  192.1; RT 1.91 min), and serotonin (5-HT,  $m/z$  177.0  $\rightarrow$  160.1; RT 1.63 min).

## 2.5 Recovery and matrix effect

Recovery of extraction and matrix effect on mass spectrometric response were determined as previously described.<sup>23</sup> Briefly, a known amount of analyte was spiked into the ileal digesta and faeces before and after extraction, and then applied to LC-MS measurement. Recovery was calculated as follows: (peak area of the spiked analyte before extraction – peak area of the endogenous analyte) / (peak area of the spiked analyte after extraction – peak area of the endogenous analyte). The matrix effect was calculated as follows: (peak area of the spiked analyte after extraction – peak area of the endogenous analyte) / peak area of the spiked analyte in Milli-Q water.

## 2.6 Cell culture

HepG2-Lucia<sup>TM</sup> AhR reporter cells (InvivoGen, San Diego, CA) were cultured in Gibco<sup>TM</sup> Eagle's minimal essential medium (No. 31095029, Thermo Fisher Scientific) supplemented with 10% (v/v) heat-inactivated fetal bovine serum (No. 10082147, Thermo Fisher Scientific), 1x non-essential amino acids (No. 11140050, Thermo Fisher Scientific), 100 U/mL penicillin-100 mg/mL streptomycin (No. P0781, Sigma-Aldrich), 100  $\mu$ g/mL Normocin<sup>TM</sup> (No. ant-nr-1, InvivoGen), and 100  $\mu$ g/mL Zeocin<sup>TM</sup> (No. ant-zn-05, InvivoGen). During the AhR induction, the cells were cultured in the test medium as above but without Normocin<sup>TM</sup> and Zeocin<sup>TM</sup>. Cell lines were cultured in a humidified incubator at 37 °C and 5% CO<sub>2</sub>.

## 2.7 Pre-treatment of samples for cellular assays

Extracts (100  $\mu$ L) of ileal digesta and faeces were evaporated by nitrogen to remove the organic solution and then redissolved in 200  $\mu$ L of the test medium of AhR reporter cells. After centrifugation at 11200 x g for 2 min at 4 °C, the supernatants were collected and used in the cellular assay.



## 2.8 Measurement of AhR activity

AhR activity of ileal digesta and faeces was measured using a luciferase reporter assay on HepG2-Lucia<sup>TM</sup> AhR reporter cells as previously described.<sup>14</sup> Briefly, AhR reporter cells were seeded into a 96-well plate with a volume of 180 µL per well containing about 20 000 cells and stimulated with tested samples (20 µL per well, in triplicate) for 48 h. Luciferase activity was quantified by QUANTI-Luc<sup>TM</sup> (No. rep-qlc2, InvivoGen) and measured via a Spectramax M5 (Molecular Devices, USA). Meanwhile, the cytotoxicity of test samples to AhR reporter cells was determined by the released lactate dehydrogenase (LDH) using the CytoTox 96 Non-Radioactive Cytotoxicity Assay (No. G1780, Promega) according to the manufacturer's instructions. The results of AhR activity were normalized on the basis of the luciferase activity of the vehicle. Cytotoxicity was expressed as the percentage of maximum LDH release achieved by adding 10X Lysis Solution in the kit.

## 2.9 Statistical analysis

Statistical analysis was performed in GraphPad Prism 9.1.0 (GraphPad Software, La Jolla, CA). Concentrations of Trp catabolites in ileal digesta and faeces of pigs fed with test foods were normalized by protein-free diet and corrected for recovery and matrix effect. AhR activity of ileal digesta and faeces was compared using Student's t test between treatment and control (test medium). Concentrations of Trp catabolites in ileal digesta and faeces of the same pig were compared using paired Student's t test. Data are expressed as mean  $\pm$  standard error of the mean (SEM). P value of  $< 0.05$  was considered significant.

### 3 Results

#### 3.1 Microbiota-derived Trp catabolites in ileal digesta and faeces of pigs

To understand the microbial catabolism of Trp along the intestine, we quantified the Trp catabolites in ileal digesta and faeces of pigs and reported the results from the first week of feeding experiments across all pigs and all food matrices based on wet matter in Figure 2.1. Most of Trp catabolites were more abundant in faeces than in ileal digesta with the exception of ILA (Figure 2.1a). Ska, Oxi, 5-HT, and IA were quantifiable in faeces but not in ileal digesta (Figure 2.1a). The overall concentration of Trp catabolites in the faeces was over 5-fold higher than that in ileal digesta (Figure 2.1b). Trp catabolites in ileal digesta were dominated by Ind (44.99%), ILA (25.86%), IPA (12.05%), and IAA (11.13%), whereas Trp catabolites in faeces were dominated by Ska (55.13%), Oxi (17.90%), and Ind (16.16%) (Figure 2.1c).

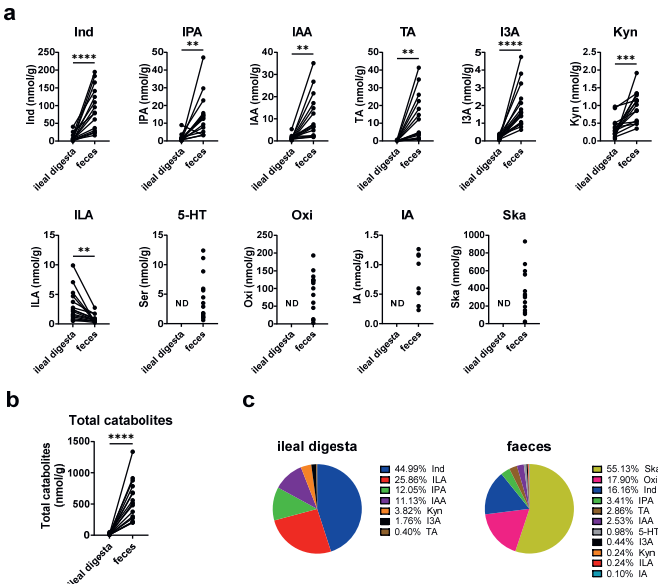


**Figure 2.1** Microbiota-derived Trp catabolites quantified in ileal digesta and faeces of pigs. a. Concentrations of individual catabolites. b. Concentrations of total examined catabolites. c. Average abundance of individual catabolites relative to the overall concentration of Trp catabolites. Data based on wet matter were from the first week of feeding experiments across all pigs and all food matrices. The lines connecting samples for same pig and analyzed by paired Student's t test. Significance is reported as \*\* $p < 0.01$ , \*\*\* $p < 0.001$ , and \*\*\*\* $p < 0.0001$ . ND: not detected. Ind: indole; IPA: indole-3-propionic acid; IAA: indole-3-acetic acid; TA: tryptamine; I3A: indole-3-aldehyde; Kyn: kynurenine; ILA: indole-3-lactic acid; 5-HT: serotonin; Oxi: oxindole; IA: indoleacrylic acid. Ska: skatole.

### 3.2 Food-derived Trp catabolites in ileal digesta and faeces of pigs

To explore the role of food matrix in microbial catabolism of Trp, we fed pigs with various foods and reported the concentration of food-derived Trp catabolites based on dry matter (DM) in Figure 2.2 for ileal digesta and in Figure 2.3 for faeces. In ileal digesta, feeding pigs with eggs resulted in the highest concentration of Ind (~300 nmol/g DM), cornflakes in the highest concentration of IPA (~85 nmol/g DM), amaranth in the highest concentration of IAA (~30 nmol/g DM), chicken in the highest concentration of ILA (~70 nmol/g DM), seaweed in the highest concentration of Kyn (~7 nmol/g DM), and linseed in the highest concentration of I3A (~4 nmol/g DM) and TA (~2 nmol/g DM) (Figure 2.2). In faeces, feeding pigs with amaranth resulted in the highest concentration of Ska (~1600 nmol/g DM), Ind (~600 nmol/g DM), IAA (~60 nmol/g DM), 5-HT (~28 nmol/g DM), and I3A (~10 nmol/g DM), millet in the highest concentration of Oxi (~500 nmol/g DM), buckwheat in the highest concentration of IPA (~110 nmol/g DM) and ILA (~6 nmol/g DM), mushrooms in the highest concentration of TA (~80 nmol/g DM), and kidney beans resulted in the highest concentration of Kyn (~5 nmol/g DM) and IA (~3 nmol/g DM) (Figure 2.3).

Overall, feeding pigs with eggs resulted in the highest concentration of total Trp catabolites in ileal digesta compared with other test foods, whereas feeding pigs with amaranth resulted in the highest concentration of total Trp catabolites in faeces (Figure 2.4). Spirulina, seaweed, mushrooms, and wheat flour induced a relatively low concentration of total Trp catabolites in both ileal digesta and faeces of pigs.

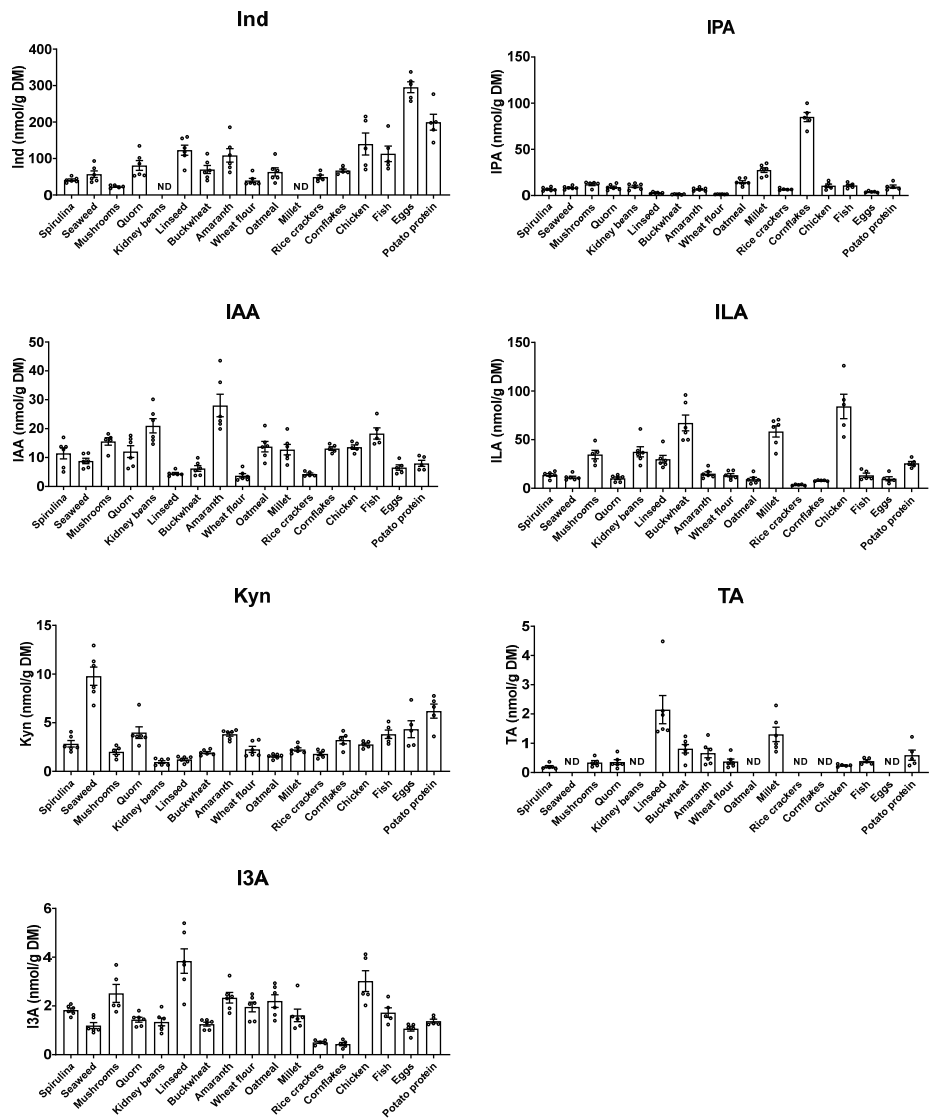


**Figure 2.2** Concentrations of microbiota-derived Trp catabolites produced from test foods in ileal digesta of pigs. Data are based on dry matter (DM) and presented as mean  $\pm$  SEM. ND: not detected. Ind: indole; IPA: indole-3-propionic acid; IAA: indole-3-acetic acid; ILA: indole-3-lactic acid; Kyn: kynurenine; TA: tryptamine; I3A: indole-3-aldehyde.

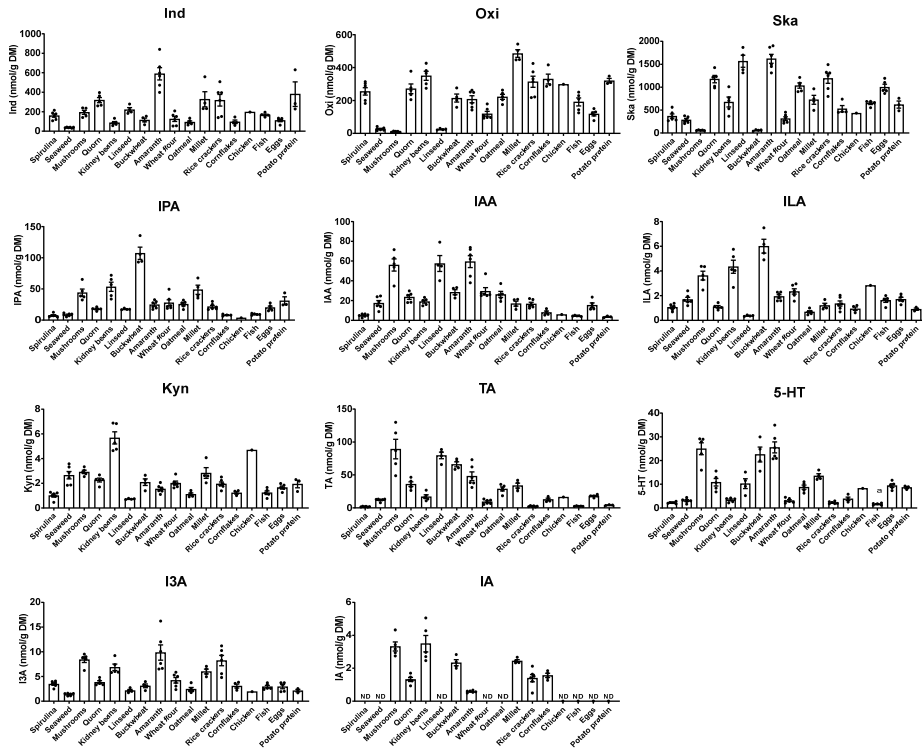


**Figure 2.3** Concentrations of microbiota-derived Trp catabolites produced from test foods in faeces of pigs. Data are based on dry matter (DM) and presented as mean  $\pm$  SEM. ND: not detected. Ind: indole; Oxi: oxindole; Ska: skatole; IPA: indole-3-propionic acid; IAA: indole-3-acetic acid; ILA: indole-3-lactic acid; Kyn: kynurenine; TA: tryptamine; 5-HT: serotonin; I3A: indole-3-aldehyde; IA: indoleacrylic acid.

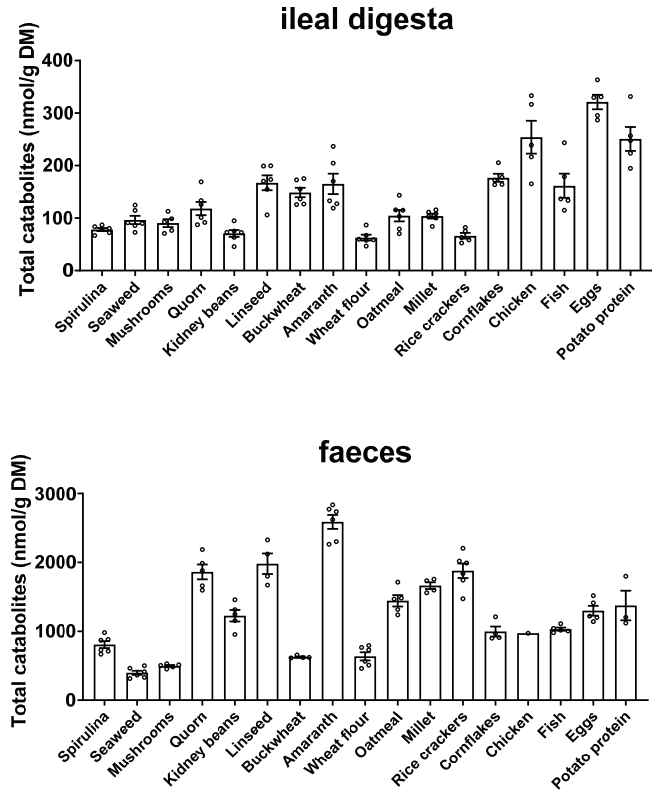


**Figure 2.4** Concentrations of total microbiota-derived Trp catabolites in ileal digesta and faeces of pigs. Data are based on dry matter (DM) and presented as mean  $\pm$  SEM.

### 3.3 Food matrix affects the microbial catabolism of Trp in the intestine

To compare the pattern of Trp catabolites driven by different food matrices, we calculated the percent abundance of each catabolite relative to the overall Trp catabolites concentration and reported the results in Figure 2.5. Trp catabolites in ileal digesta were dominated by Ind, especially in pigs fed with eggs, in which Ind represents more than 90% of the measured catabolites (Figure 2.5). However, feeding pigs with millet and kidney beans inhibited the microbial biosynthesis of Ind in the small intestine and drove the catabolism to IAA, IPA, and ILA biosynthesis (Figure 2.4 and 2.5). Decreases in the relative abundance of Ind were also observed in ileal digesta of pigs fed with mushrooms, which were dominated by ILA (37.97%) and cornflakes dominated by IPA (48.02%). Trp catabolites in faeces were dominated by Ska, but feeding pigs with mushrooms shifted the microbial catabolism of Trp in porcine colon to

Ind and TA biosynthesis and to Oxi, Ind, and IPA biosynthesis by feeding with buckwheat, which is reflected by the relative abundance of Trp catabolites in faeces (Figure 2.5). Collectively, different foods induced distinct profiles of microbiota-derived Trp catabolites in ileal digesta and faeces of pigs (Figure 2.5).

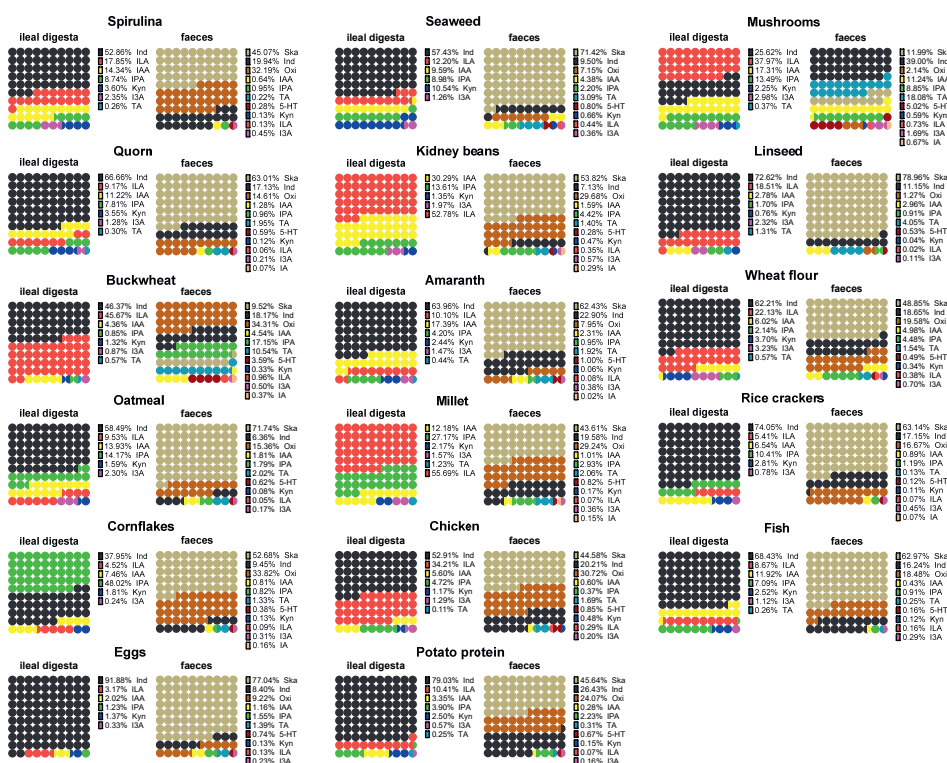


**Figure 2.5** Relative abundance of microbiota-derived Trp catabolites produced from test foods in ileal digesta and faeces of pigs. The dot plot only displays the major catabolites; the corresponding average abundances of all the pigs are indicated in the legend. Ind: indole; Oxi: oxindole; Ska: skatole; IPA: indole-3-propionic acid; IAA: indole-3-acetic acid; ILA: indole-3-lactic acid; Kyn: kynurenine; TA: tryptamine; 5-HT: serotonin; I3A: indole-3-aldehyde; IA: indoleacrylic acid.

### 3.4 AhR activation of ileal and faecal samples

The presence of AhR active Trp catabolites within the ileal digesta and faeces of pigs prompted us to examine their capacity to stimulate activity in an AhR reporter cell line. In the cellular assay, ileal and faecal samples were diluted 200 times to avoid cytotoxicity, but ileal samples from pigs fed with linseed still had a high cytotoxicity leading to cell inactivation (Figure S2.1). As shown in Figure 2.6, all ileal extracts failed to elicit a significant activation of AhR on the

reporter cell line, but many faecal extracts significantly activated the AhR, showing a more than two-fold activation over the negative control (test medium).

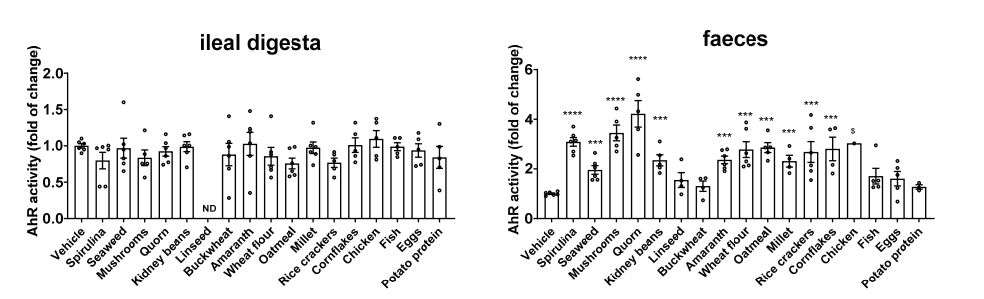


**Figure 2.6** AhR activity of ileal digesta and faeces of pigs. HepG2-Lucia™ cells were treated for 48 h with extracts from ileal digesta and fecal samples of pig after pre-treatment. Experiments were performed in two consecutive cell passages in triplicate. Results were expressed as luciferase fold change over cell test medium (vehicle). Data are presented as mean ± SEM. Statistical analysis was performed between treatment and vehicle, except chicken diet (\$) due to limited observations, using Student's t-test. Significance is reported as \*  $p < 0.05$ , \*\*  $p < 0.01$ , \*\*\*  $p < 0.001$ , and \*\*\*\*  $p < 0.0001$ . ND: not detected.



## 4 Discussion

Gut microbiota-derived metabolites are able to promote host health, especially those produced from Trp with the capability to activate the AhR signaling in the intestine.<sup>1,4</sup> Therefore, in this study, we used growing pigs as a model to investigate the concentration of Trp catabolites present in the ileum effluents and faeces upon different human dietary protein sources, and measured the AhR activity triggered by ileum effluents and faeces of pigs using a reporter cell line.

Small intestine is the most important site for nutrient digestion and absorption in the body, where Trp is released from hydrolysis of proteins by digestive enzymes.<sup>24</sup> Over 90% of released Trp is absorbed by intestinal epithelium for peptide synthesis and endogenous metabolism,<sup>25</sup> but this study shows that small bowel microbiota can compete with epithelial cells for Trp and generate several Trp catabolites, consistent with our previous findings in human ileal fluid samples.<sup>14</sup> Information on the presence of Trp-derived catabolites in foods is limited, only IAA has been identified in plants.<sup>26</sup> Bacterial genera commonly found in the small intestine of pigs include *Streptococcus*, *Clostridium*, and *Lactobacillus*.<sup>27</sup> Several species from *Clostridium* are able to convert Trp into Ind, IAA, ILA, IPA, and TA, and some *Lactobacillus* spp. have a capacity to produce I3A and ILA.<sup>9</sup> Since the microbial population in the small intestine is much smaller than the colon,<sup>28</sup> and the transit time of food in the small intestine is shorter than in the large intestine, it is not surprising to find lower concentrations of Trp catabolites in ileal digesta compared to faeces, except for ILA. This suggests that small intestine may be the main location for the microbial biosynthesis of ILA from Trp.

Given the extensive metabolic capacity of colonic microbiota,<sup>29</sup> a more diverse panel of Trp catabolites was observed in faeces compared to ileal digesta of pigs, in which Ska, Oxi, IA, and 5-HT were only identified in faeces. Different to human stool dominated by Ind,<sup>23</sup> Ska was the major Trp catabolite in the faeces of pigs, which is produced by a few species mainly from *Clostridium* and *Bacteroides* genera via decarboxylation of IAA.<sup>30</sup> Oxi can also be measured in human stool at a concentration of 2-800 nmol/g.<sup>23</sup> 5-HT together with Kyn are endogenous Trp metabolites, but recent studies suggest that they can also be produced by gut microbiota,<sup>31,32</sup> which is further supported by our data in pigs.

As expected, feeding pigs with different food matrices induced the different concentrations of microbiota-derived Trp catabolites in ileal digesta and faeces of pigs. We first speculated that

the overall concentration of Trp catabolites in the lumen of the small intestine would be proportional to the content of Trp released from proteins in the small intestinal lumen which is in turn proportional to the amount of Trp in the test foods and positively correlated to protein digestibility. We indeed found a significant positive correlation between the Trp content (%) of test foods and the overall concentration of Trp catabolites in ileal digesta of pigs ( $r = 0.49$ ,  $p = 0.0251$ ) (Figure S2.2). This hypothesis is further supported by the relatively higher content of Trp catabolites in ileal digesta of pigs fed with chicken and egg (both with expected high protein digestibility and Trp content) compared to most of the plant-based foods (Table S2.2) in which an intact plant cell wall and the presence of anti-nutritional compounds protect the intracellular protein against digestive enzymes in the small intestine.<sup>33</sup> However, no correlation was found between the Trp content and the overall concentration of Trp catabolites in faeces (Figure S2.2). This could be due to the fact that the Trp reaching the colon is inversely correlated to protein digestibility and this is lower in plant-based foods compared to animal foods. However, food processing can improve the digestibility of plant proteins,<sup>34</sup> and therefore increase the availability of Trp to small bowel microbiota. A good example was shown in pigs fed with potato protein. The capacity of small bowel microbiota to compete with epithelial cells for Trp may also influence the overall concentration of Trp catabolites in the small intestine, which is likely to be variable across different foods.

The low protein digestibility of unprocessed plant-based foods in the small intestine would suggest that they could be suitable vectors for delivering Trp to the colon. Colonic microbiota preferentially utilizes fermentable carbohydrates over proteins as the energy source,<sup>35</sup> which suggests that dietary fibers, especially fermentable fibers in plant-based foods may negatively affect the microbial production of Trp catabolites by reducing the protein fermentation in the colon. However, despite a range of commensal species can secrete carbohydrate-active enzymes to utilize polysaccharides in the plant cell wall,<sup>36</sup> we also proved that the level of integrity of a plant matrix (i.e. the level of integrity of a cell wall) may reduce the amount of microbial metabolites from dietary substrate.<sup>18</sup> This may have reduced the actual accessibility of colonic microbiota to dietary Trp in some of the plant-based foods tested here.

Apart from the effect of the food matrix on the amount of Trp available in the intestinal lumen, food components can modulate the gut microbiota composition, which may influence the microbial catabolism of Trp in the intestine. Although few studies have addressed how dietary shifts influence the microbiota composition and function in the small intestine, the distinct panel of Trp catabolites across different test foods in ileal digesta of pigs suggests that small bowel

microbiota is likely very responsive to dietary perturbations, which influences the microbial production of Trp-derived catabolites in the small intestine. A recent study showed that a peptide-rich diet can enrich *Lactobacillus* species in the porcine small intestine compared to a protein-rich diet.<sup>37</sup> A high-fat diet can increase the relative abundance of the family Clostridiaceae in the ileum of mice.<sup>38</sup> Dietary fiber resists digestion in the small intestine, but in the colon, it can be fermented by colonic microbiota and increases the populations of fiber-degrading bacteria,<sup>36</sup> some of which may have the capacity to catabolize Trp.<sup>9</sup> Previously, we demonstrated that fiber supplementation (i.e. pectin and inulin) can promote the microbial production of IPA, IAA, and ILA by human gut microbiota.<sup>22</sup> We also observed that pectin and inulin differently modulated the microbial catabolism of Trp, in which pectin specifically promoted the microbial production of I3A.<sup>22</sup> Collectively, these observations suggest a combined effect of food matrix and gut microbiota on the production of Trp catabolites in the intestine.

The most documented beneficial effect of Trp catabolites is their capacity to activate the AhR.<sup>4</sup> However, we failed to observe a significant activation of AhR when the reporter cell line was exposed to ileal extracts. One possible explanation is that the dilution of the ileal samples to avoid cytotoxicity reduced the concentration of Trp catabolites below the threshold concentration needed to activate AhR *in vitro*. Many faecal extracts were able to elicit a significant activation of AhR on the reporter cell line. We speculated that this could be due to the more abundant Trp catabolites in faecal extracts. However, the Spearman rank correlation analyses between the concentration of Trp catabolites and the AhR activity of faecal extracts appear to contradict this notion, in which we only found a positive correlation between I3A and AhR activity ( $r = 0.2991$ ,  $p = 0.007$ ) (Table S2.3). This suggests the presence of other molecules in faecal extracts that can modulate the AhR activation on the reporter cell line. We previously showed that propionate and butyrate can activate the AhR and have synergistic effects on the AhR activation.<sup>18</sup> Additionally, we cannot rule out the possibility that unknown inhibitors of AhR activity are similarly present in faecal extracts.

## 5 Conclusion

In conclusion, this study provides the first quantitative assessment of a panel of food-derived Trp catabolites in ileal digesta and faeces of pigs during the passage of whole foods along the intestine. The small intestine is known for nutrient digestion and absorption, but this study shows that, in pigs, the microbiota in this segment plays a role in the catabolism of dietary Trp to produce AhR active Trp catabolites and it is particularly sensitive to dietary pressures that modulate the Trp catabolism by small bowel microbiota. Food selection aiming to promote the production of Trp-derived AhR ligands in the intestine should consider the intestinal segments and dietary factors influencing the microbial catabolism of Trp, specifically the amount of Trp available in the intestinal lumen and microbiota composition and function. Together, this study has important implications in the design of dietary approaches targeting the Trp catabolism by gut microbiota to improve intestinal health.

## **CRedit authorship contribution statement**

Zhan Huang: Conceptualization, Methodology, Investigation, Formal analysis, Writing – original draft, Writing – review & editing.

Sonja de Vries: Formal analysis, Writing – review & editing.

Vincenzo Fogliano: Writing – review & editing, Supervision.

Jerry M. Wells: Writing – review & editing, Supervision.

Nikkie van der Wielen: Writing – review & editing.

Edoardo Capuano: Writing – review & editing, Supervision.

## **Declaration of Competing Interest**

The authors declare that they have no known competing financial interests or personal relationships that could have appeared to influence the work reported in this paper.

## **Acknowledgement**

The authors would like to thank the staff of the research facilities, technicians, and students, particularly Arjan van Dolderen, Sabine van Woudenberg, Huyen Nguyen, Roseanne Minderhoud, Wendy Izedonmwon, Saskia van Laar-Schuppen, Erika Beukers-van Laar, Niels Wever, Frans Lettink, and Erik Meulenbroeks of Wageningen University & Research, Wageningen, The Netherlands, for technical assistance during the experiment, and the China Scholarship Council for the financial support to the first author.

## Reference

1. Gutiérrez-Vázquez C, Quintana FJ. Regulation of the Immune Response by the Aryl Hydrocarbon Receptor. *Immunity*. 2018;48(1):19-33. doi:10.1016/j.immuni.2017.12.012
2. Lahvis GP, Lindell SL, Thomas RS, et al. Portosystemic shunting and persistent fetal vascular structures in aryl hydrocarbon receptor-deficient mice. *Proc Natl Acad Sci*. 2000;97(19):10442-10447. doi:10.1073/pnas.190256997
3. Fernandez-Salguero P, Pineau T, Hilbert DM, et al. Immune System Impairment and Hepatic Fibrosis in Mice Lacking the Dioxin-Binding Ah Receptor. *Science (80- )*. 1995;268(5211):722-726. doi:10.1126/science.7732381
4. Lamas B, Natividad JM, Sokol H. Aryl hydrocarbon receptor and intestinal immunity. *Mucosal Immunol*. 2018;11(4):1024-1038. doi:10.1038/s41385-018-0019-2
5. Moura-Alves P, Faé K, Houthuys E, et al. AhR sensing of bacterial pigments regulates antibacterial defence. *Nature*. 2014;512(7515):387-392. doi:10.1038/nature13684
6. Li Y, Innocentin S, Withers DR, et al. Exogenous Stimuli Maintain Intraepithelial Lymphocytes via Aryl Hydrocarbon Receptor Activation. *Cell*. 2011;147(3):629-640. doi:10.1016/j.cell.2011.09.025
7. Monteleone I, Rizzo A, Sarra M, et al. Aryl Hydrocarbon Receptor-Induced Signals Up-regulate IL-22 Production and Inhibit Inflammation in the Gastrointestinal Tract. *Gastroenterology*. 2011;141(1):237-248.e1. doi:10.1053/j.gastro.2011.04.007
8. Ouyang W, O'Garra A. IL-10 Family Cytokines IL-10 and IL-22: from Basic Science to Clinical Translation. *Immunity*. 2019;50(4):871-891. doi:10.1016/j.immuni.2019.03.020
9. Roager HM, Licht TR. Microbial tryptophan catabolites in health and disease. *Nat Commun*. 2018;9(1):1-10. doi:10.1038/s41467-018-05470-4
10. Bhattacharai Y, Williams BB, Battaglioli EJ, et al. Gut Microbiota-Produced Tryptamine Activates an Epithelial G-Protein-Coupled Receptor to Increase Colonic Secretion. *Cell Host Microbe*. 2018;23(6):775-785.e5. doi:10.1016/j.chom.2018.05.004
11. Wlodarska M, Luo C, Kolde R, et al. Indoleacrylic Acid Produced by Commensal *Peptostreptococcus* Species Suppresses Inflammation. *Cell Host Microbe*. 2017;22(1):25-37.e6. doi:10.1016/j.chom.2017.06.007
12. Cervantes-Barragan L, Chai JN, Tianero MD, et al. *Lactobacillus reuteri* induces gut intraepithelial CD4 + CD8αα + T cells. *Science (80- )*. 2017;357(6353):806-810.

doi:10.1126/science.aah5825

13. Natividad JM, Agus A, Planchais J, et al. Impaired Aryl Hydrocarbon Receptor Ligand Production by the Gut Microbiota Is a Key Factor in Metabolic Syndrome. *Cell Metab.* 2018;28(5):737-749.e4. doi:10.1016/j.cmet.2018.07.001
14. Koper JEB, Kortekaas M, Loonen LMP, et al. Aryl hydrocarbon Receptor activation during in vitro and in vivo digestion of raw and cooked broccoli ( *brassica oleracea* var. *Italica* ). *Food Funct.* 2020;11(5):4026-4037. doi:10.1039/D0FO00472C
15. Meng D, Sommella E, Salviati E, et al. Indole-3-lactic acid, a metabolite of tryptophan, secreted by *Bifidobacterium longum* subspecies *infantis* is anti-inflammatory in the immature intestine. *Pediatr Res.* 2020;88(2):209-217. doi:10.1038/s41390-019-0740-x
16. Wang W Le, Kasamatsu J, Joshita S, et al. The aryl hydrocarbon receptor instructs the immunomodulatory profile of a subset of Clec4a4<sup>+</sup> eosinophils unique to the small intestine. *Proc Natl Acad Sci U S A.* 2022;119(23). doi:10.1073/pnas.2204557119
17. Capuano E, Oliviero T, van Boekel MAJS. Modeling food matrix effects on chemical reactivity: Challenges and perspectives. *Crit Rev Food Sci Nutr.* 2018;58(16):2814-2828. doi:10.1080/10408398.2017.1342595
18. Huang Z, Schoones T, Wells JM, Fogliano V, Capuano E. Substrate-Driven Differences in Tryptophan Catabolism by Gut Microbiota and Aryl Hydrocarbon Receptor Activation. *Mol Nutr Food Res.* 2021;65(13):2100092. doi:10.1002/mnfr.202100092
19. Ziegler A, Gonzalez L, Blikslager A. Large Animal Models: The Key to Translational Discovery in Digestive Disease Research. *Cell Mol Gastroenterol Hepatol.* 2016;2(6):716-724. doi:10.1016/j.jcmgh.2016.09.003
20. National Research Council. *Nutrient Requirements of Swine*. National Academies Press; 2012. doi:10.17226/13298
21. Hodgkinson SM, Stein HH, de Vries S, Hendriks WH, Moughan PJ. Determination of True Ileal Amino Acid Digestibility in the Growing Pig for Calculation of Digestible Indispensable Amino Acid Score (DIAAS). *J Nutr.* 2020;150(10):2621-2623. doi:10.1093/jn/nxaa210
22. Huang Z, Boekhorst J, Fogliano V, Capuano E, Wells JM. Distinct effects of fiber and colon segment on microbiota-derived indoles and short-chain fatty acids. *Food Chem.* 2023;398:133801. doi:10.1016/j.foodchem.2022.133801
23. Dong F, Hao F, Murray IA, et al. Intestinal microbiota-derived tryptophan metabolites are predictive of Ah receptor activity. *Gut Microbes.* 2020;12(1):1788899.

- doi:10.1080/19490976.2020.1788899
24. Snook JT, Meyer JH. Response of digestive enzymes to dietary protein. *J Nutr.* 1964;82(4):409-414. doi:10.1093/jn/82.4.409
25. Gao J, Xu K, Liu H, et al. Impact of the gut microbiota on intestinal immunity mediated by tryptophan metabolism. *Front Cell Infect Microbiol.* 2018;8(13):1-22. doi:10.3389/fcimb.2018.00013
26. Fu SF, Wei JY, Chen HW, Liu YY, Lu HY, Chou JY. Indole-3-acetic acid: A widespread physiological code in interactions of fungi with other organisms. *Plant Signal Behav.* 2015;10(8):e1048052. doi:10.1080/15592324.2015.1048052
27. Crespo-Piazuelo D, Estellé J, Revilla M, et al. Characterization of bacterial microbiota compositions along the intestinal tract in pigs and their interactions and functions. *Sci Rep.* 2018;8(1):12727. doi:10.1038/s41598-018-30932-6
28. Sender R, Fuchs S, Milo R. Revised Estimates for the Number of Human and Bacteria Cells in the Body. *PLOS Biol.* 2016;14(8):e1002533. doi:10.1371/journal.pbio.1002533
29. Martinez-Guryn K, Leone V, Chang EB. Regional diversity of the gastrointestinal microbiome. *Cell Host Microbe.* 2019;26(3):314-324. doi:10.1016/j.chom.2019.08.011
30. Zamaratskaia G, Squires EJ. Biochemical, nutritional and genetic effects on boar taint in entire male pigs. *Animal.* 2009;3(11):1508-1521. doi:10.1017/S1751731108003674
31. Krautkramer KA, Fan J, Bäckhed F. Gut microbial metabolites as multi-kingdom intermediates. *Nat Rev Microbiol.* 2021;19(2):77-94. doi:10.1038/s41579-020-0438-4
32. Valles-Colomer M, Falony G, Darzi Y, et al. The neuroactive potential of the human gut microbiota in quality of life and depression. *Nat Microbiol.* 2019;4(4):623-632. doi:10.1038/s41564-018-0337-x
33. Capuano E, Pellegrini N. An integrated look at the effect of structure on nutrient bioavailability in plant foods. *J Sci Food Agric.* 2019;99(2):493-498. doi:10.1002/jsfa.9298
34. Sá AGA, Moreno YMF, Carciofi BAM. Food processing for the improvement of plant proteins digestibility. *Crit Rev Food Sci Nutr.* 2020;60(20):3367-3386. doi:10.1080/10408398.2019.1688249
35. Oliphant K, Allen-Vercoe E. Macronutrient metabolism by the human gut microbiome: major fermentation by-products and their impact on host health. *Microbiome.* 2019;7(1):91. doi:10.1186/s40168-019-0704-8
36. Flint HJ, Scott KP, Duncan SH, Louis P, Forano E. Microbial degradation of complex



- carbohydrates in the gut. *Gut Microbes*. 2012;3(4). doi:10.4161/gmic.19897
37. Jing Y, Mu C, Wang H, Shen J, Zoetendal EG, Zhu W. Amino acid utilization allows intestinal dominance of *Lactobacillus amylovorus*. *ISME J*. 2022;16(11):2491-2502. doi:10.1038/s41396-022-01287-8
  38. Martinez-Guryn K, Hubert N, Frazier K, et al. Small Intestine Microbiota Regulate Host Digestive and Absorptive Adaptive Responses to Dietary Lipids. *Cell Host Microbe*. 2018;23(4):458-469.e5. doi:10.1016/j.chom.2018.03.011

## Supporting information

### Supplementary Methods: Preparation of test foods

Spirulina, yeast, linseed (broken), wheat flour, potato protein were stored in serving bins at room temperature and they required neither cooking nor processing before feeding.

Seaweed was cut into ~0.5 cm and kidney beans, rice crackers, and cornflakes were cut into ~0.2 cm using cutter (Mado Supra 50). After processing, seaweed, rice crackers, and cornflakes were stored in serving bins at room temperature and kidney beans were stored in serving bins in the fridge.

Mushrooms were cut in slices and steamed for 6 min in the oven, and then cut into ~0.2 cm. Buckwheat was simmered with water at a ratio of 7:20 (g/mL) for 25 min in the oven, amaranth and millet were simmered with water at a ratio of 1:2 (g/mL) for 25 min in the oven, and oatmeal was simmered with water at a ratio of 4:25 (g/mL) for 15 min in the oven. After cooling down, they were stored in closed bags in the freezer if not consumed within 2-3 days or used directly.

Quorn, chicken, and fish-tilapia were mixed with water at a ratio of 3:5 (g/mL) and cooked in the oven. After boiling, the oven heat was reduced to low for quorn and fish to simmer for 9-10 min, and was reduced to medium for chicken to simmer for 20-25 min until it is cooked through. Eggs were placed in the oven tray with holes and cooked by setting the program in oven to 'eieren stomen'. After cooling down and peeling the eggs, they were cut into ~0.2 cm and stored in closed bags in the freezer if not consumed within 2-3 days or used directly

**Table S2.1** Product information of the test foods.

Food	Brand
Spirulina	Bio Spirulina, Eco Mundo, The Netherlands
Seaweed	Yakisushinori A grade, Yama, Japan
Mushrooms	White Mushrooms ( <i>Agaricus bisporus</i> ), Local green grocer
Yeast	Bruggeman Yeast, Algist Bruggeman, Belgium
Quorn	Quorn Pieces, Quorn Foods, UK
Kidney beans	Kidneybonen, Albert Heijn, The Netherlands
Linseed	Biologic Linseed Broken, Albert Heijn, The Netherlands
Buckwheat	Buckwheat, Smaakt bio, The Netherlands
Amaranth	Biologic amaranth, Ekoplaza, The Netherlands
Wheat flour	Patent wheat flour, Albert Heijn, The Netherlands
Oatmeal	Quaker Oatmeal, Pepsico, USA
Millet	Millet, Smaakt bio, The Netherlands
Rice crackers	Ricetoast natural, Van der Meulen, The Netherlands
Cornflakes	Kellogg's Cornflakes, Kellogg's, USA
Chicken	Chicken breast, Local butcher
Fish	Tilapia filet, Albert Heijn, The Netherlands
Eggs	Free range eggs medium, Albert Heijn, The Netherlands
Coagulated potato protein	Avebe

**Table S2.2** Composition of experimental diets (g/kg dry matter) for growing pigs.

Item	Basal diet	Protein free diet	Chicken	Spirulina	Seaweed	Mushrooms	Quorn	Kidney beans	Cornflakes
<b>Ingredient</b>									
Tested food	0	0	107	140	191	253	181	381	947
Purified maize starch	0	763	656	623	587	517	582	392	0
Purified cellulose	0	30	30	30	30	30	30	30	0
Rapeseed oil	50	50	50	50	50	50	50	50	0
Sucrose	0	100	100	100	100	100	100	100	0
Premix <sup>1</sup>	10	5	5	5	5	5	5	5	5
Dicalcium phosphate	17	25	25	25	25	25	25	25	25
Magnesium oxide	0	1	1	1	0	1	1	1	1
CaCO <sub>3</sub>	5	3	3	3	3	3	3	3	3
K <sub>2</sub> CO <sub>3</sub>	3	7	7	7	0	0	7	0	7
NaHCO <sub>3</sub>	5	3	3	3	0	3	3	0	3
NaCl	0	4	4	4	0	4	4	4	0
Bread meal	688	0	0	0	0	0	0	0	0
Casein	70	0	0	0	0	0	0	0	0
Wheat gluten meal	50	0	0	0	0	0	0	0	0
Whey powder	50	0	0	0	0	0	0	0	0
Potato protein	30	0	0	0	0	0	0	0	0
Skimmed milk powder	20	0	0	0	0	0	0	0	0
L-Lysine HCl	2	0	0	0	0	0	0		
Titanium dioxide	0	4	4	4	4	4	4	4	4
PEG8000 <sup>2</sup>	0	5	5	5	5	5	5	5	5
<b>Chemical composition</b>									
Protein <sup>3</sup>	243	0	100	100	100	100	100	100	69
Trp <sup>4</sup>	2.5	0.04	11.35	1.43	1.33	5.06	7.62	2.71	0.36

1 Vitamin and mineral premix in final diet (per kg DM): Cu 10 mg; I 1.3 mg; Fe 125 mg; Mn 60 mg; Se 0.3 mg; Zn 100 mg; niacin 44 mg; cobalamin 0.03 µg; pantothenic acid 24 mg; riboflavin 6.6 mg; phytonadione 1.4 mg; biotin 0.44 mg; retinol 11 IU; cholecalciferol 2.2 IU; d,l- $\alpha$ -tocopherol 66 IU; pyridoxine 0.24 mg; folate 1.6 mg; thiamin 0.24 mg.

2 PEG8000: Polyethylene glycol 8000

3 Protein content was measured by DUMAS (FlashSmart N/PROTEIN, Thermo Fisher Scientific)

4 Trp content was measured according to ISO 13904:2005: *Animal feeding stuffs-Determination of tryptophan content*

**Table S2.2** Composition of experimental diets (g/kg dry matter) for growing pigs (continued).

Ingredient	Rice Cracker	Potato protein	Wheat flour	Eggs	Buckwheat	Linseed	Fish	Amaranth	Oatmeal	Millet
<i>Ingredient</i>										
Tested food	947	115	812	181	675	459	113	592	760.5	881
Purified maize starch	0	648	0	582	0	305	650	172	0	0
Purified cellulose	0	30	65	30	134	30	30	30	91.75	31
Rapeseed oil	0	50	65	50	134	50	50	50	91.75	31
Sucrose	0	100	0	100	0	100	100	100	0	0
Premix	5	5	5	5	5	5	5	5	5	5
Dicalcium phosphate	25	25	25	25	25	25	25	25	25	25
Magnesium oxide	1	1	1	1	1	0	1	0	0	1
CaCO <sub>3</sub>	3	3	3	3	3	3	3	3	3	3
K <sub>2</sub> CO <sub>3</sub>	7	7	7	7	7	7	7	7	7	7
NaHCO <sub>3</sub>	3	3	3	3	3	3	3	3	3	3
Salt extra	0	4	4	4	4	4	4	4	4	4
Titanium dioxide	4	4	4	4	4	4	4	4	4	4
PEG8000	5	5	5	5	5	5	5	5	5	5
<i>Chemical composition</i>										
Protein	62	100	100	100	100	100	100	100	100	100
Trp	0.87	1.48	0.91	7.71	2.15	3.46	10.93	2.20	1.77	1.42

**Table S2.3** Spearman rank correlation between Trp catabolites and AhR activity of fecal samples. Quantifiable Trp catabolites in the faeces of pigs were correlated with the corresponding AhR activity through non-parametric Spearman rank analysis.

Catabolite	Spearman r	Significance <i>p</i> (two-tailed)
kynurenine	0.0431	0.7048
serotonin	-0.0277	0.8073
indole	0.0918	0.4179
indole-3-acetic acid	0.1237	0.2741
indole-3-lactic acid	-0.0868	0.4439
oxindole	0.1226	0.2785
indole-3-propionic acid	-0.0841	0.4584
indole-3-aldehyde	0.2991	0.0070
skatole	-0.0325	0.7745
tryptamine	0.0206	0.8560
indoleacrylic acid	-0.0202	0.9026
Total catabolites	0.0069	0.9509

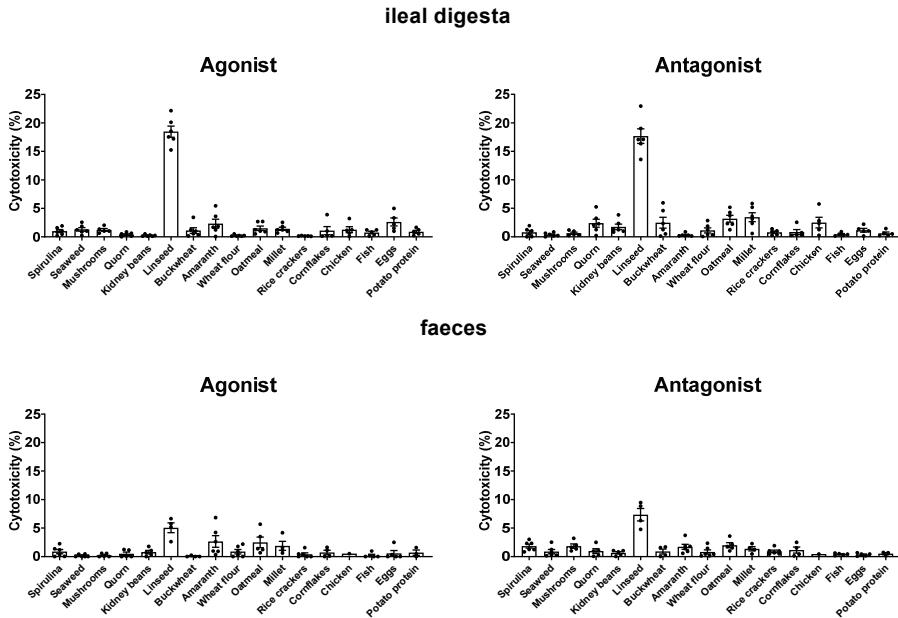


**Figure S2.1** Cytotoxicity of tested samples from ileal digesta and faeces of pigs to HepG2-Lucia™ AhR reporter cells after 48 h incubation. Cytotoxicity was measured by the released lactate dehydrogenase (LDH) using CytoTox 96 Non-Radioactive Cytotoxicity Assay and normalized by the vehicle. Results are expressed as the percentage of the maximum LDH release achieved by adding 10X Lysis Solution. Data are presented as mean  $\pm$  SEM.

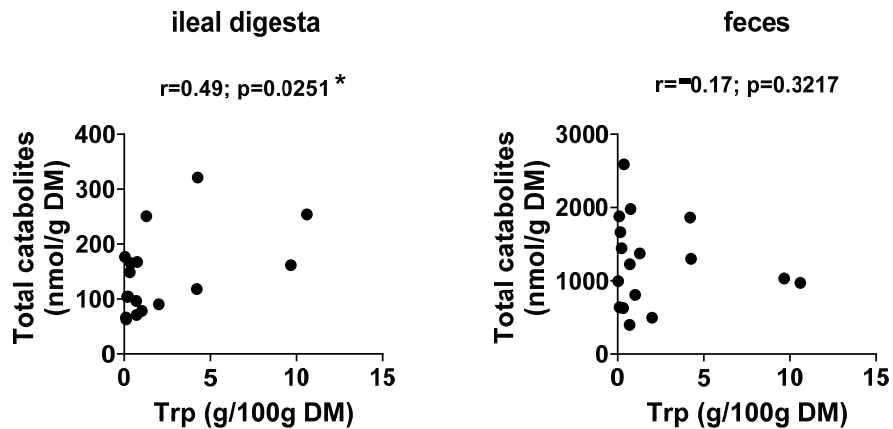


**Figure S2.2** Pearson correlation between Trp content (%) in the dry matter of test foods and total Trp catabolites in the dry matter (DM) of ileal digesta and faeces of pigs. Each dot represents an individual observation. Every plot contains the Pearson  $r$  value and two-tailed  $p$  value marked with \* to indicate significance.



## CHAPTER 3

# 3



# Substrate-driven differences in tryptophan catabolism by gut microbiota and Aryl hydrocarbon Receptor activation

**Zhan Huang<sup>1,2</sup>, Tessa Schoones<sup>1</sup>, Jerry M. Wells<sup>2</sup>, Vincenzo Fogliano<sup>1</sup>, Edoardo Capuano<sup>1,\*</sup>**

<sup>1</sup>Food Quality and Design Group, Department of Agrotechnology and Food Sciences, Wageningen University, P.O. Box 17, 6700 AA, Wageningen, the Netherlands

<sup>2</sup>Host-Microbe Interactomics Group, Department of Animal Sciences, Wageningen University, P.O. Box 17, 6700 AA, Wageningen, the Netherlands



## Abstract

This study aimed to investigate the effect of tryptophan sources on tryptophan catabolism by gut microbiota and the Aryl hydrocarbon Receptor (AhR) activation. Four substrates (free tryptophan, soybean protein, single and clustered soybean cells) containing an equimolar amount of tryptophan, but with a different bioaccessibility were studied using *in vitro* batch fermentation. Tryptophan catabolites were identified by LC-MS/MS. AhR activity was measured by HepG2-Lucia<sup>TM</sup> AhR reporter cells. The total amount of tryptophan-derived catabolites increased with decreasing level of substrate complexity. Indole was the major catabolite produced from tryptophan and it was the most abundant in the free tryptophan fermentation. Indole-3-acetic acid and indole-3-aldehyde were abundantly generated in the soybean protein fermentation. The soybean cell fermentation produced high concentrations of tryptamine. Interestingly, we also found large amounts of short-chain fatty acids (SCFAs) in the soybean cell and protein fermentation. Both tryptophan-derived catabolites and SCFAs were able to increase AhR reporter activity over time in all four groups. This study illustrated that bacterial catabolism of tryptophan and resulting AhR activation in the gut is modulated by the food matrix, suggesting a role for food design to improve gut health.

**Keywords:** colonic fermentation; food matrix; tryptophan catabolites; short-chain fatty acids; aryl hydrocarbon receptor

## 1 Introduction

Tryptophan is an essential amino acid and its average daily intake in the western diet is approximately 800 mg.<sup>1</sup> After digestion and absorption in the small intestine, about 4-6% of the total available tryptophan pass into the colon for microbial fermentation.<sup>2</sup> Recently, this fraction of tryptophan catabolized by intestinal microorganisms in the colon has gained much interest due to microbial metabolism and formation of Aryl hydrocarbon Receptor (AhR) agonists, like tryptamine, indoleacrylic acid, skatole and indole-3-aldehyde.<sup>3-5</sup>

AhR is a ligand-activated regulator of intestinal immunity and it plays a pivotal role in maintaining the balance between intestinal health and disease.<sup>6</sup> The specific deletion of AhR in intestinal epithelial cells was shown to significantly induce the development of premalignant lesions.<sup>7,8</sup> AhR ligands derived from bacterial catabolism of tryptophan profoundly affect intestinal homeostasis and immune system by promoting gut barrier functions and immune tolerance.<sup>9-11</sup> Reduced tryptophan metabolism and lower levels of microbial tryptophan catabolites have been measured in patients with various diseases.<sup>2,12,13</sup> Available data from both mammalian cell lines and animal models suggest the considerable potential of bacterial tryptophan catabolites activating AhR for prevention and treatment of inflammatory diseases affecting the intestine.<sup>12-15</sup>

Tryptophan is most abundant in protein-rich foods, like meat, fish, cheese; however, it is also present in plant foods like beans and nuts. Plant proteins have lower digestibility than animal proteins in the upper gastrointestinal tract, due to the presence of antinutritional factors and cell walls.<sup>16,17</sup> Therefore a relatively higher fraction of plant proteins than animal proteins, reach the colon. Soybean is one of the most important sources of plant proteins in our diets and it is relatively high in tryptophan content. Recent studies have shown that soybean cell walls can impede access of digestive enzymes to the intracellular proteins resulting in the passage of soybean proteins into the colon.<sup>18</sup> Therefore soybean would be a suitable vector for delivering tryptophan to the intestinal microorganisms, occurring as particles of varying size, proteins, peptides, or free amino acids.<sup>17,19,20</sup>

Here we investigated the effect of the food matrix on the production of tryptophan catabolites by human fecal bacteria using a batch fermentation model, as the food matrix is expected to affect the release and availability of substrates to microbiota.<sup>21</sup> We used soybean as fermentation substrate and modified the degree of processing of soybean to prepare intact single

or clustered soybean cells that were compared with soy protein isolate and free tryptophan, representing different forms in which tryptophan can be delivered to the intestinal microorganisms. However, soybean cells also contain large amounts of polysaccharides within the cell wall. Colonic fermentation of these polysaccharides results in the production of short-chain fatty acids (SCFAs). In addition, SCFAs were reported to have a synergistic effect on the AhR activation,<sup>22,23</sup> and butyrate is an AhR agonist in intestinal epithelial cells based on the finding that AhR antagonists and siRNA targeting AhR diminished the expression of AhR regulated genes in presence of butyrate.<sup>24</sup> Therefore we also studied the SCFA production during fermentation. The activation of AhR by tryptophan catabolites and SCFAs was performed on HepG2-Lucia™ AhR reporter cells.

## 2 Experimental Section

### 2.1 Materials and chemicals

Dried soybean supplied by De Molukken B.V. (batchcode: 3005193871) were purchased from a local supermarket (Wageningen, The Netherlands) and stored at room temperature. Soy protein isolate (91% protein) containing 1.2g tryptophan per 100g was purchased from Bulk Powders (Colchester, UK). All chemicals used were purchased from Sigma Aldrich (St. Louis MO, USA), unless stated otherwise.

### 2.2 Sample preparation

The single and clustered soybean cells were isolated as previously described.<sup>18</sup> In brief, soybean was dehulled and autoclaved at 121°C for 10 min and mashed by Stomacher® 400 Circulator (Seward, UK). Soybean cells were isolated using a wet sieve shaker. Particles retained in a sieve with a mesh size between 425 and 250 µm were referred to as clustered cells, and those retained in a sieve between 125 and 71 µm were referred to as single cells. Collected samples were freeze-dried. The chemical composition of single and clustered cells, as well as soy protein isolate, was determined and presented in Table S3.1. The tryptophan content of single and clustered cells was calculated based on their protein content (Table S3.1) and assuming a content of 1.311 g tryptophan/100 g soybean protein.<sup>25</sup>

### 2.3 *In vitro* colonic fermentation

Fresh fecal samples were collected from three Dutch adults, 22-25 years old, with a body mass index (BMI) between 18.5 and 25. All donors were in good health and with no history of gastrointestinal disorders or antibiotic treatment for at least 6 months before this study. Faecal slurries were processed within 2 h after defecation following the method described by Koper et al.<sup>26</sup> Batch-culture fermentation vessels (70 mL working volume) were sterilized and filled with 43 mL autoclaved basal nutrient medium, consisting of 5.22 g/L K<sub>2</sub>HPO<sub>4</sub>, 16.32 g/L KH<sub>2</sub>PO<sub>4</sub>, 2.0 g/L NaHCO<sub>3</sub>, 2.0 g/L yeast extract, 2.0 g/L special peptone, 1.0 g/L mucin, 0.5 g/L L-cysteine HCl, and 2.0 mL/L tween 80. Before addition of 7 mL faecal slurries, vessels were flushed with N<sub>2</sub>/CO<sub>2</sub> (80/20, v/v) gas mixture to create an anaerobic condition. Substrates, containing 10 mg tryptophan, were inoculated with faecal slurries at 37 °C with mild shaking. Fermentation with free tryptophan is referred to here as Trp, with isolated soybean protein as SP, with single soybean cells as SC, and with clustered soybean cells as CC. Fermentor samples



were taken at 0, 2, 4, 8, 24 and 48 h after inoculation, and then immediately centrifuged (12000 g, 5 min) and filtered (0.20  $\mu$ m regenerated cellulose filter). The supernatant and residue were separately collected and frozen at -20 °C before analysis.

## 2.4 Light microscopy

Residues of SC or CC samples from three independent fermentation experiments were defrosted at 4 °C and then combined. The upper layer of sediments, containing mainly products of faecal slurries and some bacteria, were gently scraped. The lower part was diluted with water and covered with a glass coverslip. Microscopy images (5 x magnification) were taken with a camera (AxioCam HRc, Carl Zeiss AG, Oberkochen, Germany).

## 2.5 Particle size distribution

The size distribution of SC or CC samples from three independent replicates during fermentation was separately measured by MasterSizer 2000 with laser diffraction (Malvern Instruments, UK). The refractive index of samples was set at 1.473 and that of the dispersant (water) at 1.330. Pump speed was 1200 rpm. Before each test, samples were equilibrated in water for 2 min. All experiments were performed at 25 °C, and each recorded measurement was determined as the average of three scans. The results are expressed as the average of three samples.

## 2.6 Tryptophan and its derived catabolites

Tryptophan-derived catabolites in supernatants were quantified via a Shimadzu Nexera XR LC-20ADxr UPLC system coupled with a Shimadzu LCMS-8050 mass spectrometer (Kyoto, Japan). Chromatographic separations were accomplished on a Phenomenex Kinetex 1.7  $\mu$ m EVO C18 100 Å LC column (100 × 2.1 mm) maintained at 45 °C. Mobile phase A was 0.1% (v/v) formic acid in water and mobile phase B was 0.1% (v/v) formic acid in methanol. The elution program was as follows: 0-2 min, 0.1% B; 2-6 min 0.1-25% B; 6-10 min, 25-80% B; 10-12 min 80-90% B; 12-15 min 90% B; 15-16 min 90-0.1% B; then re-equilibration for 8 min. Flow rate was maintained at 0.3 mL/min throughout the run. Ten microliters of sample supernatants were applied to LC/MS/MS analysis. Mass spectrometer was operated using an electrospray ionization source under the positive mode in the multiple reaction monitoring (MRM) mode with a spray voltage of 4.5 kV. Compounds were identified by comparing with transitions (m/z) and retention time (RT) of reference standards: tryptophan (m/z 205.2 → 188.2;

RT 2.97 min), tryptamine ( $m/z$  161.1  $\rightarrow$  144.0; RT 2.11 min), indole ( $m/z$  118.0  $\rightarrow$  91.1; RT 9.77 min), indole-3-aldehyde (IAA;  $m/z$  146.1  $\rightarrow$  91; RT 9.31 min), indole-3-acetic acid (IAA;  $m/z$  176.1  $\rightarrow$  130.0; RT 9.48 min), 3-indolepropionic acid (IPA;  $m/z$  190.1  $\rightarrow$  130.0; RT 10.35 min), and indole-3-lactic acid (ILA;  $m/z$  206.1  $\rightarrow$  118.1; RT 9.01 min). Skatole ( $m/z$  132.1  $\rightarrow$  117.1; RT 11.36 min) and indoleacrylic acid ( $m/z$  187.9  $\rightarrow$  115.1; RT 10.75 min) were also included in the reference, but not found in the fermentor supernatant. Data analysis was performed on LabSolutions LCMS 5.6 (Shimadzu Corporation, Japan). The content of tryptophan catabolites in each group has been normalized by that in the control samples fermented without supplied substrates.

## 2.7 Short-chain fatty acid (SCFA) and branched-chain fatty acids (BCFA)

SCFA and BCFA measurements were performed using a Shimadzu GC-2014 (Kyoto, Japan) equipped with a Flame-ionization detector (FID), a capillary fatty acid-free Stabil wax-DA column (1  $\mu\text{m} \times 0.32 \text{ mm} \times 30 \text{ m}$ ) (Restek, Bellefonte, PA, USA) and a split injector. Supernatants were thawed and combined with the internal standard (0.45 mg/mL 2-ethylbutyric acid in 0.3 mol/L HCl and 0.9 mol/L oxalic acid) for quantification. The injection volume was 0.5  $\mu\text{L}$  and the carrier gas was nitrogen. Temperatures of the injector and detector were 100 and 250  $^{\circ}\text{C}$ , respectively. The temperature profile started at 100  $^{\circ}\text{C}$ , increased to 172  $^{\circ}\text{C}$  by 10.8  $^{\circ}\text{C}/\text{min}$ , then to 200  $^{\circ}\text{C}$  by 50  $^{\circ}\text{C}/\text{min}$ , and was held at this temperature for 1 min. Standard solutions (acetate, propionate, butyrate, valerate, isobutyrate, and isovalerate) were prepared and used for identification and quantification. The results were processed using Chromeleon 7.2.10 (Thermo Fisher Scientific, San Jose, CA) and normalized by control samples fermented without supplied substrates.

## 2.8 AhR activation

The AhR activity was measured using a luciferase reporter assay method as described previously.<sup>27</sup> In brief, HepG2-Lucia<sup>TM</sup> AhR reporter cells (InvivoGen, San Diego, CA) were grown and maintained according to the manufactures instructions. To induce AhR, 20  $\mu\text{L}$  samples separately from three independent replicates and 180  $\mu\text{L}$  cell suspension containing about 20 000 cells were added per well in triplicate to a flat-bottom 96-well plate (Corning, USA), which diluted samples by ten times. The plate was placed at 37  $^{\circ}\text{C}$  in a  $\text{CO}_2$  incubator for 48 h, and then 20  $\mu\text{L}$  of stimulated cells supernatant was transferred into a white walled clear bottom 96-wells plate (Corning, USA), followed by addition of 50  $\mu\text{L}$  QUANTI-Luc<sup>TM</sup>

(InvivoGen). The luminescence was immediately measured by a Spectramax M5 (Molecular Devices, USA). The results are expressed as the percentage of AhR activity of positive control (5  $\mu$ M  $\beta$ -naphthoflavone or  $\beta$ -NAPH in DMSO) and normalized by either DMSO, cell growth medium or control samples fermented without substrates.

## 2.9 Statistical analysis

Data were expressed as mean  $\pm$  standard error of the mean (SEM). Statistical analysis was performed by GraphPad Prism 9.1.0 (GraphPad Software, La Jolla, CA). Differences were evaluated using the analysis of variance (ANOVA) indicated in the figure caption. A value of  $p < 0.05$  was considered as statistically significant.

## 3 Results

### 3.1 Light microscopy and particle size distribution

The structure of single and clustered soybean cells changed during fermentation (Figure 3.1). The cell wall limited bacterial degradation in the first 4 h incubation and most cells remained physically intact in the SC group, while clustered soybean cells started to dissociate into smaller particles and single cells (Figure 3.1A). With longer incubation, the cell particle size decreased reflecting the breakdown of cell structures (Figure 3.1B and 3.1C). Several ruptured cells and possible cell fragments were observed in both groups (Figure 3.1A), as well as a floating lipid-like layer due to hydrophobic components that escaped from the cell (data not shown). The breakdown of single cell structure started after 4 h incubation and was almost complete after 24 h, as there were no obvious differences on the average particle size between 0 and 4 h incubation or between 24 and 48 h incubation (Figure 3.1C). The degradation of clustered cells took longer than single cells and the decrease in the average particle size in the CC group was observed throughout the 48 h incubation (Figure 3.1C). Even at the end of fermentation, some intact soybean cells were still present (Figure 3.1A).

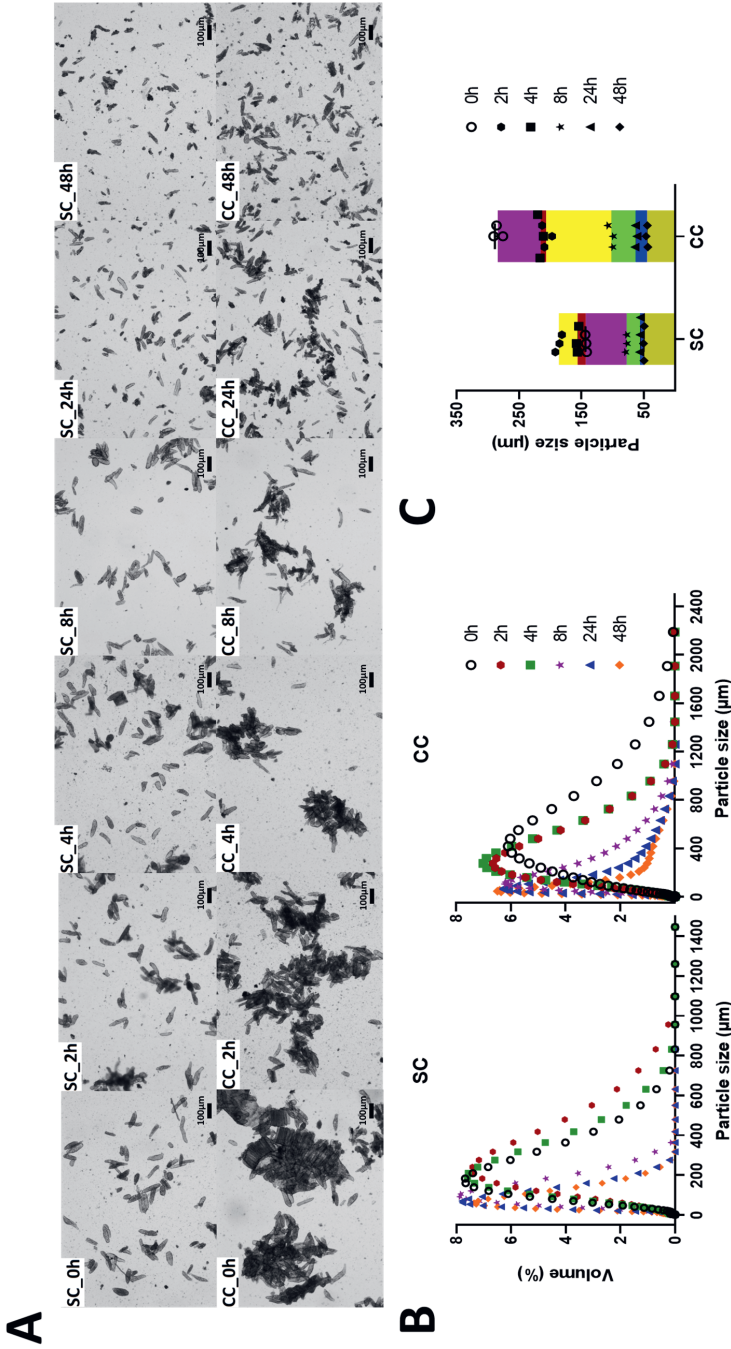


**Figure 3.1** Representative light microscopy images (A), size distribution (B), and average particle size (C) of soybean-based samples collected during fermentation. SC: fermentation with single soybean cells; CC: fermentation with clustered soybean cells.



### 3.2 Tryptophan and its derived catabolites

Figure 3.2 shows changes in the concentration of tryptophan and total catabolites during fermentation. In the Trp group, tryptophan was directly accessible for microbes and its concentration decreased with incubation time (Figure 3.2A). Conversely, the concentration of tryptophan in the SP group firstly increased, and then rapidly decreased after 4 h incubation (Figure 3.2B), due to hydrolysis of proteins and subsequent metabolism by gut bacteria. Similar fluctuations in the tryptophan concentration were observed in the SC and CC groups during the first 8 h incubation (Figure 3.2C and 3.2D). Most tryptophan was catabolized by fecal microbes after 24 h incubation and the catabolites accumulated in the medium. The degradation of tryptophan followed a typical sigmoid kinetics, reflecting a slower rate of formation at the beginning of fermentation and possibly reaching a plateau at longer fermentation times. The concentration of total catabolites, and at the end of fermentation, was the highest in the Trp group, followed by the SP, SC, and CC groups (Figure 3.2).

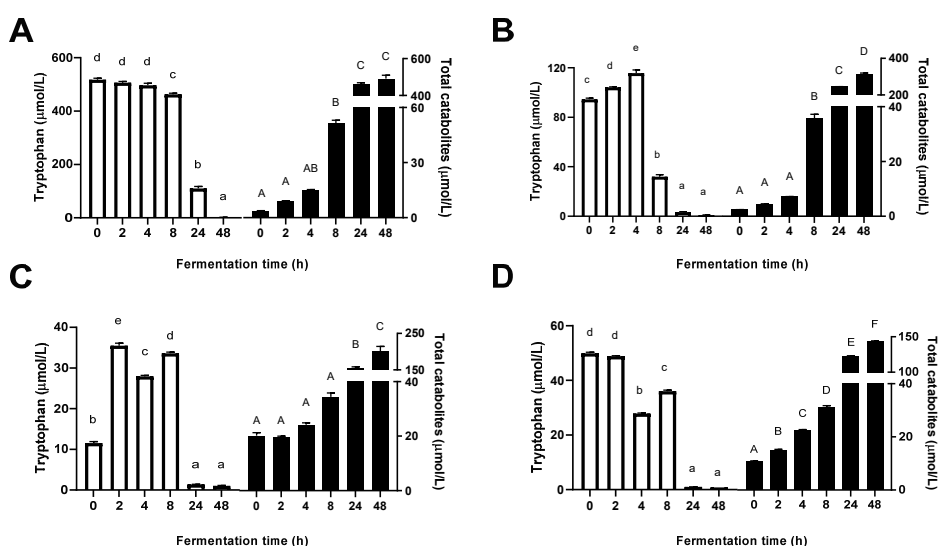


**Figure 3.2** Concentrations of tryptophan (white bars) and total catabolites (black bars) in supernatants collected during fermentation. A: fermentation with tryptophan; B: fermentation with isolated soybean protein; C: fermentation with single soybean cells; D: fermentation with clustered soybean cells. Results are normalized by control samples fermented without supplied substrates and expressed as mean  $\pm$  SEM ( $n = 3$ ). Different lowercase

or uppercase letters above bars indicate significant differences over time ( $p < 0.05$ , one-way ANOVA followed by a Tukey post-hoc test).

Interestingly the concentration of tryptophan-derived catabolites in the four groups showed different trends (Figure 3.3). Indole was the major catabolite produced from tryptophan and its concentration followed the same trend as total catabolites. Large amounts of IPA and IAA were also found in all groups at the end of fermentation. Relatively small amounts of tryptamine and I3A were produced compared to the other tryptophan catabolite. The Trp group had the highest concentration of indole and IPA after 24 h and 48 h incubation. Although less total catabolites were produced in the SP, SC, and CC groups at the end of fermentation, IAA and I3A were most abundant in the SP group ( $p < 0.05$ ), and the SC and CC groups contained significantly higher concentrations of tryptamine than the Trp and SP groups ( $p < 0.05$ ). ILA was rapidly generated during the first 8 h incubation, and then further metabolized by microbes, as very limited amounts were found in all groups at the end of fermentation.



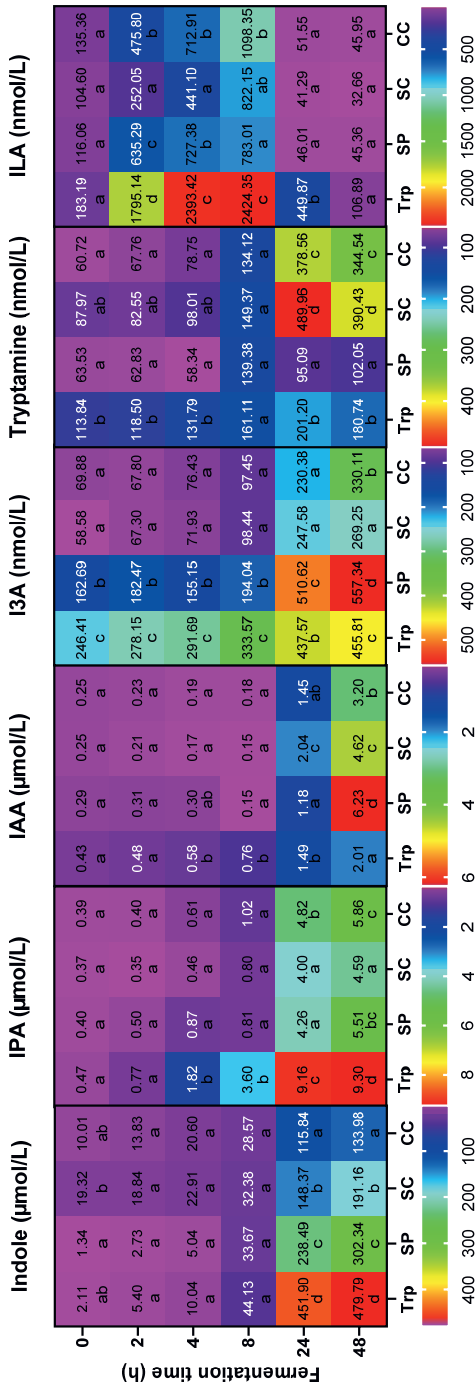


**Figure 3.3** Heatmap of tryptophan-derived catabolites in supernatants collected during fermentation. Trp: fermentation with tryptophan; SP: fermentation with isolated soybean protein; SC: fermentation with single soybean cells; CC: fermentation with clustered soybean cells. Each catabolite has its own legend and corresponding concentrations are normalized by control samples fermented without supplied substrates and presented as the average of 3 independent replicates. Blocks with different lowercase letters in a row indicate treatments that are significantly different ( $p < 0.05$ , two-way ANOVA followed by a Tukey post-hoc test).



### 3.3 SCFAs and BCFAs

Acetate and propionate were the two major fatty acids produced during fermentation, followed by butyrate, isovalerate, valerate, and isobutyrate (Figure 3.4). Considerable substrate-driven changes in the SCFA production were observed in the SP, SC, and CC groups, which all induced high concentrations of SCFAs and BCFAs. Acetate, propionate, and butyrate were significantly produced in the SC and CC groups than that in the SP group after 24 h incubation ( $p < 0.05$ ) (Figure 3.4A-C). The concentration of valerate in the SP, SC, and CC groups was similar at the end of fermentation (Figure 3.4D). The SP group yielded the highest concentrations of isobutyrate and isovalerate after 48 h incubation, in comparison to other groups ( $p < 0.05$ ) (Figure 3.4E and 3.4F). Fermentation with single and clustered cells induced similar effects on the SCFA and BCFA production, but the CC group had significantly higher concentrations of acetate and propionate than the SC group after 24 h incubation ( $p < 0.05$ ) (Figure 3.4A and 3.4B), and significantly higher concentration of isobutyrate at the end of fermentation ( $p < 0.05$ ) (Figure 3.4E).

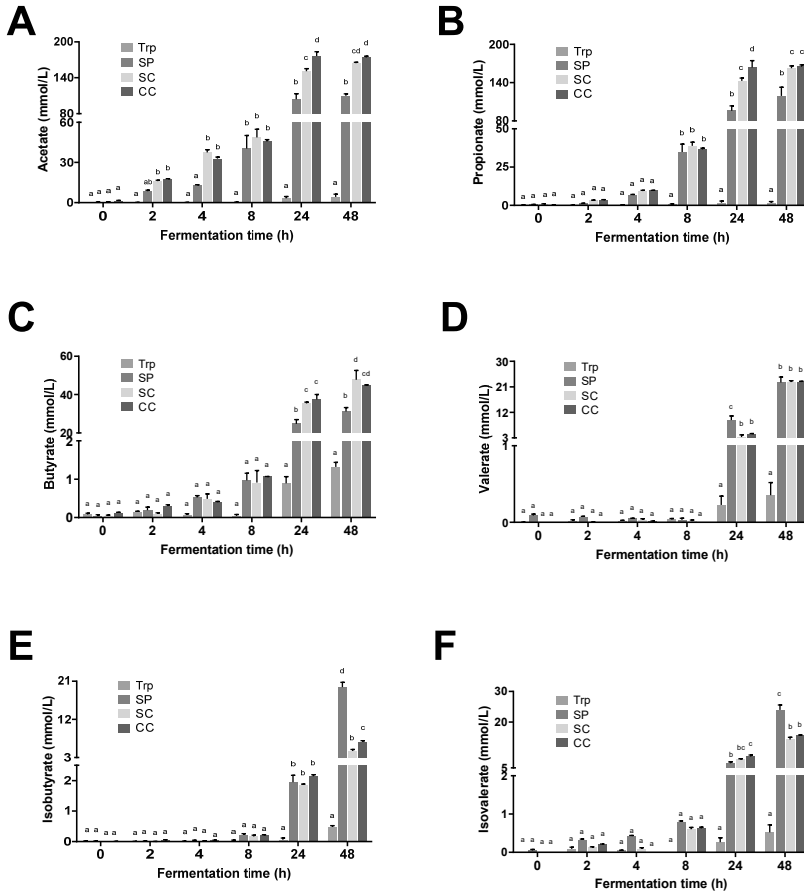


**Figure 3.4** Concentration of SCFAs and BCFAs in supernatants collected during fermentation. A: acetate; B: propionate; C: butyrate; D: valerate; E: isobutyrate; F: isovalerate. Trp: fermentation with tryptophan; SP: fermentation with isolated soybean protein; SC: fermentation with single soybean cells; CC: fermentation with clustered soybean cells. Results are normalized by control samples fermented without supplied substrates and expressed as mean  $\pm$  SEM ( $n = 3$ ). Bars with different lowercase letters indicate treatments that are significantly different ( $p < 0.05$ , two-way ANOVA followed by a Tukey post-hoc test).

### 3.4 AhR activity

The AhR activity in the four groups increased with incubation time (Figure 3.5). The Trp group had the lowest AhR activity and this value gradually increased over time. The SC and CC groups exhibited a rapid increase in AhR activity and showed higher AhR activity compared to the SP and Trp groups. After 24 h incubation, AhR activity in the SP group was significantly

higher than that of the Trp group ( $p < 0.05$ ), but markedly lower than that of the SC and CC groups ( $p < 0.05$ ). Interestingly a decrease in AhR activity was observed in the SP group after 48 h incubation. AhR activity in the SC group was higher than that in the CC group except for 48 h, when the CC group gave significantly higher AhR activity compared to the SC group ( $p < 0.05$ ).

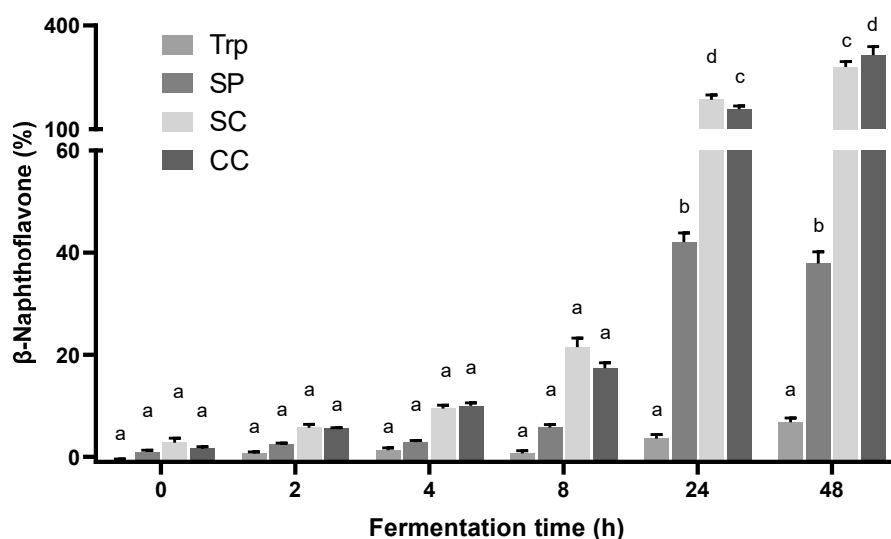


**Figure 3.5** Quantification of the AhR activity of supernatants collected during fermentation using the cell reporter assay. HepG2-Lucia™ AhR reporter cells were incubated for 48 h with vehicle (medium or 1% v/v DMSO) and fermented samples. Trp: fermentation with tryptophan; SP: fermentation with isolated soybean protein; SC: fermentation with single soybean cells; CC: fermentation with clustered soybean cells. Results are normalized by control samples fermented without supplied substrates and expressed as mean  $\pm$  SEM ( $n = 3$ ). Bars with different lowercase letters indicate treatments that are significantly different ( $p < 0.05$ , two-way ANOVA followed by a Tukey post-hoc test).

To better understand the above results, we further tested the AhR activation induced by individual tryptophan-derived catabolites, SCFAs, and BCFAs (Figure 3.6). All detected tryptophan catabolites displayed AhR activation, even at concentrations as low as 10 nmol/L, showing they are potent activators of the AhR. In general, AhR activities increased with

increasing concentrations of the tryptophan-derived catabolites. Propionate and butyrate increased AhR reporter activity at concentrations above 10 and 5 mmol/L respectively. However, we also cannot rule out the cytotoxicity of butyrate at high concentrations (above 5 mmol/L) (Figure 3.2S), as it accumulates in cancer cells growing in glucose.<sup>28</sup> The AhR activity induced by acetate, valerate, and isovalerate was found at high concentrations (50, 5, and 5 mmol/L respectively), whereas isobutyrate did not activate AhR.  $\beta$ -NAPH is a potent AhR agonist and was used as the positive control. The  $\beta$ -NAPH-induced AhR activation was greatly strengthened in combination with propionate and butyrate, and slightly increased in combination with IPA, I3A, tryptamine, and ILA at high concentrations. Acetate, valerate, and isovalerate at low concentrations partially antagonized the AhR activity of  $\beta$ -NAPH and was similar for IAA at high concentrations. Isobutyrate and indole showed decreasing AhR activation with increasing concentrations, when they were in combination with  $\beta$ -NAPH.

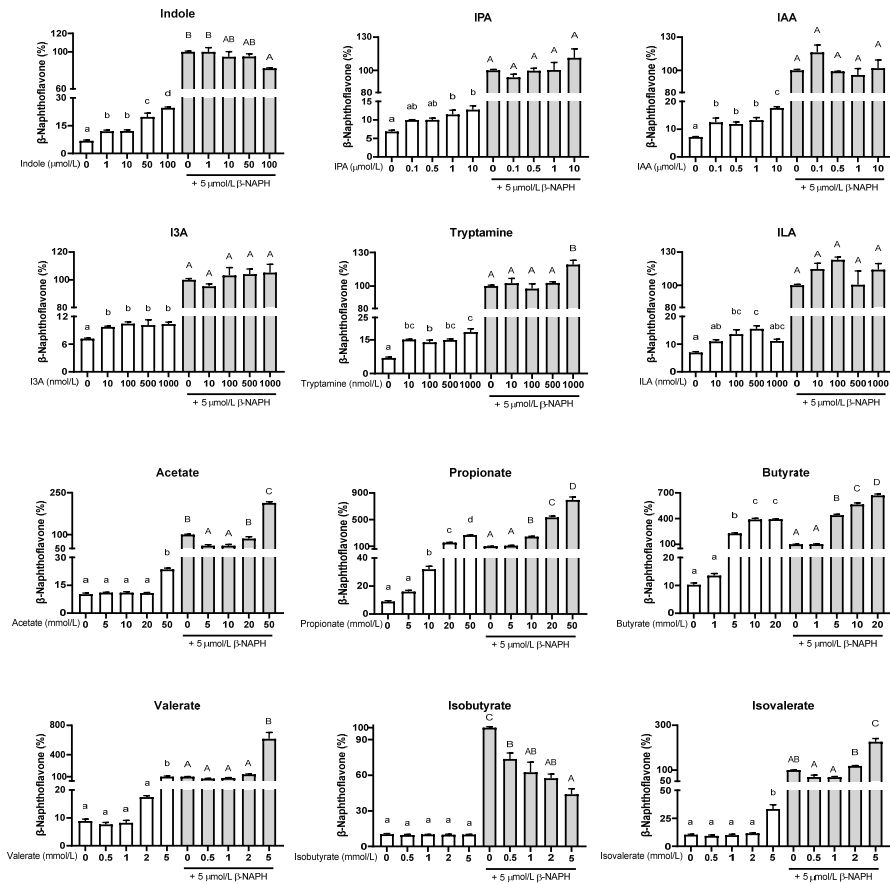


**Figure 3.6** Quantification of the AhR activation of tryptophan-derived catabolites, SCFAs, and BCFAs using the cell reporter assay. HepG2-Lucia™ AhR reporter cells were incubated for 48 h with vehicle (medium or 1% v/v DMSO) and increasing concentrations of tryptophan-derived catabolites, SCFAs, or BCFAs in the absence (white bars) or the presence (grey bars) of  $\beta$ -NAPH ( $\beta$ -naphthoflavone; 5  $\mu\text{mol/L}$ ). Results are expressed as mean  $\pm$  SEM ( $n = 3$ ). Bars with different lowercase or uppercase letters indicate treatments that are significantly different ( $p < 0.05$ , one-way ANOVA followed by a Tukey post-hoc test).

## 4 Discussion

To date several studies have been performed to investigate the relationship between tryptophan catabolites and intestinal health,<sup>12,14,29</sup> but the dietary factors affecting bacterial catabolism of tryptophan remain largely unknown. This is the first study that investigated the changes in bacterial tryptophan catabolism by *ex vivo* human gut microbiota using the static batch fermentation model when tryptophan was provided in different forms.

We provided evidence that the incorporation of tryptophan in increasingly complex structure, i.e. in proteins, single cells or clustered cells, modulates tryptophan utilization which can be related to microbial accessibility to tryptophan. As compared to directly available free tryptophan, the intestinal microorganisms needed to secrete enzymes to breakdown soybean cell complexes, degrade the cell wall and gain access to the intracellular space to break down the protein into amino acids via bacterial proteases and peptidases.<sup>30</sup> Therefore, the more complex the structure, the less tryptophan was catabolized, and then the less total catabolites were generated during 48 h fermentation (Figure 3.2). In addition, the structure of soybean cells also played a role during the early stage of batch fermentation (24 h), in which clustered soybean cells were more rapidly and continuously fermented than single soybean cells. This is possibly due to the junctions between cells providing a microenvironment that was more conducive to the bacterial growth.<sup>31</sup> However, this difference in fermentation rate was no longer evident after longer incubation (48 h).

We also found that different substrates alter the type of colonic fermentation and affect the generation of tryptophan-derived catabolites, likely due to compositional differences among samples. In addition to tryptophan, soybean proteins contain various other amino acids and soybean cell wall contains large amounts of polysaccharides, including pectin, hemicellulose, and cellulose. This means that gut microbiota has a different set of available substrates to grow. In the SP, bacteria actively fermented proteins as energy source which resulted in a pH value above 7 after 48 h fermentation (Figure S3.1). In the SC and CC groups, bacteria tend to utilize carbohydrates as energy source rather than proteins, which produces, and is favored by, the significantly lower pH values compared to the control fermentation without supplied substrates ( $p < 0.05$ ) (Figure S3.1). The modulation of colonic microbiome induced by shifts toward proteolytic and saccharolytic fermentation altered the bacterial tryptophan catabolism, showing different trends between total catabolites and single catabolites in the four groups.



We further studied the *in vitro* activation of the AhR during fermentation to gain insight into the outcome of colonic fermentation. In the intestine, several AhR ligands are derived from commensal bacteria, of which the most reported ones are bacterial tryptophan catabolites, such as indole, tryptamine, I3A, IAA, and ILA.<sup>2,9</sup> The generation of indole is mediated by tryptophanase that is expressed in many bacterial species, which makes indole the major catabolite derived from tryptophan. ILA can be further converted to IPA by phenyllactate dehydratase and acyl-CoA dehydrogenase.<sup>10</sup> The bacterial tryptophan catabolites activated the AhR, but had varying levels of affinity and reactivity (Figure 3.6). Tryptamine was found to be a more active AhR activator than IPA, I3A, and ILA. The AhR activation induced by indole was concentration dependent, while indole exhibited an antagonistic effect on the AhR activation in the combination with  $\beta$ -NAPH. These findings suggest the tryptophan-derived catabolites contributed to the total AhR activation of fermentor supernatants, but the marked difference in the AhR activation over the time led us to consider other potent ligands affecting AhR activation.

It has been recently shown that SCFAs are able to enhance the activity of other AhR-active ligands.<sup>22,23,32</sup> Consistently, we found large amounts of SCFAs in fermentor supernatants after 24 h incubation in the SC and CC groups, mainly due to the fermentation of polysaccharides within the soybean cell wall by gut microbiota, and in the SP group via the reductive deamination of amino acids (Figure 3.4).<sup>33</sup> In the assay of AhR activation, we confirmed that SCFAs displayed AhR activity especially at high concentrations and they had an synergistic effect on the AhR activation (Figure 3.6). Isobutyrate had no AhR activity and antagonizes the AhR activation induced by  $\beta$ -NAPH. The high concentrations of butyrate and propionate inside the fermentor supernatant largely contributed to the significantly high AhR activity of the SC and CC groups after 24 h incubation. As a low concentration of SCFA was found in the Trp group, its AhR activity was mainly induced by tryptophan-derived catabolites. These results suggest that SCFAs with high concentrations played a more significant role in the total AhR activity of our fermentor supernatants than the tryptophan-derived catabolites. It is also important to notice that the coverage of AhR activators in this study may not have included all the possible ligands. Some other tryptophan catabolites potentially activating AhR, such as the recently reported indole-3-ethanol and indole-3-pyruvate,<sup>11</sup> were not measured in the present study. It cannot be ruled out that other compounds in the fermentor supernatant might exert agonistic or antagonistic effects on the AhR activation. For a proper interpretation of the AhR activation, it should be considered that the type of cell line used in the assay has an effect on

the ligand-activated AhR activation. Compared with previously reported studies,<sup>23,34,35</sup> we observed that the affinity of tryptophan-derived catabolites and SCFAs for the AhR differ between mice and human cells, as well as in cells from different tissues. This could be due to the sensitivity and transport of tryptophan-derived catabolites and SCFAs differ in different cell lines. Indole exhibited AhR activation in HepG2 cells, but it was inactive in young adult mouse colonocyte cells.<sup>35</sup> Treatment of HepG2 cells with 20 mmol/L propionate and 5 mmol/L butyrate gave induction responses similar to  $\beta$ -NAPH (5  $\mu$ mol/L), whereas in Caco-2 cells they induced CYP1A1 mRNA levels less than 5% of 2,3,7,8-tetrachlorodibenzodioxin (10 nmol/L).<sup>23</sup> In addition, the synergistic effect of acetate, propionate, and butyrate as histone deacetylase inhibitors on AhR responsiveness is also gene- and cell context-dependent.<sup>23</sup> Taken together, these results suggest cell context and reporter gene differences in the AhR activity induced by tryptophan-derived catabolites and SCFAs.

In summary, our study shows how the form in which a fermented food substrate is provided, and specifically the structural and compositional elements of the food matrix can affect the concentration and type of bioactive microbial metabolites. Importantly, our results may be useful to understand the *in vivo* fermentation and tryptophan catabolism by gut microbiota, in which the passage time, host metabolism, absorption and transport of produced metabolites also play a role in the evaluation of overall health effects to the intestine. This study also highlights the need for further studies on the combined effects of different intestinal microbial metabolites on the AhR activation.

## **Acknowledgement**

Z.H., T.S., J.W., V.F., and E.C. contributed to the design of this study. Z.H. and T.S. conducted the research. Z.H. wrote the original draft and all authors reviewed and edited the draft. The authors would like to thank Geert Meijer and Christos Fryganas for setting up the LC–MS/MS method, and the China Scholarship Council for the financial support to the first author.

## **Conflict of interest**

The authors declare no conflict of interest.

## References

1. Lieberman HR, Agarwal S, Fulgoni VL. Tryptophan intake in the us adult population is not related to liver or kidney function but is associated with depression and sleep outcomes. *J Nutr.* 2016;146(12):2609S-2615S. doi:10.3945/jn.115.226969
2. Gao J, Xu K, Liu H, et al. Impact of the gut microbiota on intestinal immunity mediated by tryptophan metabolism. *Front Cell Infect Microbiol.* 2018;8(13):1-22. doi:10.3389/fcimb.2018.00013
3. Hubbard TD, Murray IA, Perdew GH. Indole and tryptophan metabolism: Endogenous and dietary routes to ah receptor activation. *Drug Metab Dispos.* 2015;43(10):1522-1535. doi:10.1124/dmd.115.064246
4. Bhattacharai Y, Williams BB, Battaglioli EJ, et al. Gut Microbiota-Produced Tryptamine Activates an Epithelial G-Protein-Coupled Receptor to Increase Colonic Secretion. *Cell Host Microbe.* 2018;23(6):775-785.e5. doi:10.1016/j.chom.2018.05.004
5. Zhang LS, Davies SS. Microbial metabolism of dietary components to bioactive metabolites: Opportunities for new therapeutic interventions. *Genome Med.* 2016;8(1):1-18. doi:10.1186/s13073-016-0296-x
6. Lamas B, Natividad JM, Sokol H. Aryl hydrocarbon receptor and intestinal immunity. *Mucosal Immunol.* 2018;11(4):1024-1038. doi:10.1038/s41385-018-0019-2
7. Han H, Davidson LA, Fan Y, et al. Loss of aryl hydrocarbon receptor potentiates FoxM1 signaling to enhance self-renewal of colonic stem and progenitor cells. *EMBO J.* 2020;39(19). doi:10.15252/embj.2019104319
8. Metidji A, Omenetti S, Crotta S, et al. The Environmental Sensor AHR Protects from Inflammatory Damage by Maintaining Intestinal Stem Cell Homeostasis and Barrier Integrity. *Immunity.* 2018;49(2):353-362.e5. doi:10.1016/j.immuni.2018.07.010
9. Roager HM, Licht TR. Microbial tryptophan catabolites in health and disease. *Nat Commun.* 2018;9(1):1-10. doi:10.1038/s41467-018-05470-4
10. Agus A, Planchais J, Sokol H. Gut microbiota regulation of tryptophan metabolism in health and disease. *Cell Host Microbe.* 2018;23(6):716-724. doi:10.1016/j.chom.2018.05.003
11. Scott SA, Fu J, Chang P V. Microbial tryptophan metabolites regulate gut barrier function via the aryl hydrocarbon receptor. *Proc Natl Acad Sci.* 2020;117(32):19376-19387. doi:10.1073/pnas.2000047117

12. Natividad JM, Agus A, Planchais J, et al. Impaired Aryl Hydrocarbon Receptor Ligand Production by the Gut Microbiota Is a Key Factor in Metabolic Syndrome. *Cell Metab.* 2018;28(5):737-749.e4. doi:10.1016/j.cmet.2018.07.001
13. Lamas B, Hernandez-Galan L, Galipeau HJ, et al. Aryl hydrocarbon receptor ligand production by the gut microbiota is decreased in celiac disease leading to intestinal inflammation. *Sci Transl Med.* 2020;12(566):eaba0624. doi:10.1126/scitranslmed.aba0624
14. Wlodarska M, Luo C, Kolde R, et al. Indoleacrylic Acid Produced by Commensal *Peptostreptococcus* Species Suppresses Inflammation. *Cell Host Microbe.* 2017;22(1):25-37.e6. doi:10.1016/j.chom.2017.06.007
15. Islam J, Sato S, Watanabe K, et al. Dietary tryptophan alleviates dextran sodium sulfate-induced colitis through aryl hydrocarbon receptor in mice. *J Nutr Biochem.* 2017;42:43-50. doi:10.1016/j.jnutbio.2016.12.019
16. Capuano E, Pellegrini N. An integrated look at the effect of structure on nutrient bioavailability in plant foods. *J Sci Food Agric.* 2019;99(2):493-498. doi:10.1002/jsfa.9298
17. Dallas DC, Sanctuary MR, Qu Y, et al. Personalizing protein nourishment. *Crit Rev Food Sci Nutr.* 2017;57(15):3313-3331. doi:10.1080/10408398.2015.1117412
18. Zahir M, Fogliano V, Capuano E. Food matrix and processing modulate: In vitro protein digestibility in soybeans. *Food Funct.* 2018;9(12):6326-6336. doi:10.1039/c8fo01385c
19. Yao CK, Muir JG, Gibson PR. Review article: Insights into colonic protein fermentation, its modulation and potential health implications. *Aliment Pharmacol Ther.* 2016;43(2):181-196. doi:10.1111/apt.13456
20. Bhattarai RR, Dhital S, Wu P, Chen XD, Gidley MJ. Digestion of isolated legume cells in a stomach-duodenum model: Three mechanisms limit starch and protein hydrolysis. *Food Funct.* 2017;8(7):2573-2582. doi:10.1039/c7fo00086c
21. Aguilera JM. The food matrix: implications in processing, nutrition and health. *Crit Rev Food Sci Nutr.* 2019;59(22):3612-3629. doi:10.1080/10408398.2018.1502743
22. Park H, Jin U-H, Orr AA, et al. Isoflavones as Ah Receptor Agonists in Colon-Derived Cell Lines: Structure–Activity Relationships. *Chem Res Toxicol.* 2019;32(11):2353-2364. doi:10.1021/acs.chemrestox.9b00352
23. Jin UH, Cheng Y, Park H, et al. Short Chain Fatty Acids Enhance Aryl Hydrocarbon (Ah) Responsiveness in Mouse Colonocytes and Caco-2 Human Colon Cancer Cells. *Sci Rep.* 2017;7(1):1-12. doi:10.1038/s41598-017-10824-x

24. Marinelli L, Martin-Gallausiaux C, Bourhis JM, Béguet-Crespel F, Blottière HM, Lapaque N. Identification of the novel role of butyrate as AhR ligand in human intestinal epithelial cells. *Sci Rep*. 2019;9(1):1-14. doi:10.1038/s41598-018-37019-2
25. Comai S, Bertazzo A, Bailoni L, Zancato M, Costa CVL, Allegri G. Protein and non-protein (free and protein-bound) tryptophan in legume seeds. *Food Chem*. 2007;103(2):657-661. doi:10.1016/j.foodchem.2006.07.045
26. Koper JEB, Loonen LMP, Wells JM, Troise AD, Capuano E, Fogliano V. Polyphenols and tryptophan metabolites activate the aryl hydrocarbon receptor in an in vitro model of colonic fermentation. *Mol Nutr Food Res*. 2019;63(3):1-9. doi:10.1002/mnfr.201800722
27. Koper JEB, Kortekaas M, Loonen LMP, et al. Aryl hydrocarbon Receptor activation during in vitro and in vivo digestion of raw and cooked broccoli (brassica oleracea var. Italica). *Food Funct*. 2020;11(5):4026-4037. doi:10.1039/D0FO00472C
28. Donohoe DR, Collins LB, Wali A, Bigler R, Sun W, Bultman SJ. The Warburg Effect Dictates the Mechanism of Butyrate-Mediated Histone Acetylation and Cell Proliferation. *Mol Cell*. 2012;48(4):612-626. doi:10.1016/j.molcel.2012.08.033
29. Powell DN, Swimm A, Sonowal R, et al. Indoles from the commensal microbiota act via the AHR and IL-10 to tune the cellular composition of the colonic epithelium during aging. *Proc Natl Acad Sci*. Published online 2020:202003004. doi:10.1073/pnas.2003004117
30. Portune KJ, Beaumont M, Davila AM, Tomé D, Blachier F, Sanz Y. Gut microbiota role in dietary protein metabolism and health-related outcomes: The two sides of the coin. *Trends Food Sci Technol*. 2016;57:213-232. doi:10.1016/j.tifs.2016.08.011
31. Day L, Gomez J, Øiseth SK, Gidley MJ, Williams BA. Faster fermentation of cooked carrot cell clusters compared to cell wall fragments in vitro by porcine faeces. *J Agric Food Chem*. 2012;60(12):3282-3290. doi:10.1021/jf204974s
32. Jin U-H, Park H, Li X, et al. Structure-Dependent Modulation of Aryl Hydrocarbon Receptor-Mediated Activities by Flavonoids. *Toxicol Sci*. 2018;164(1):205-217. doi:10.1093/toxsci/kfy075
33. Windey K, De Preter V, Verbeke K. Relevance of protein fermentation to gut health. *Mol Nutr Food Res*. 2012;56(1):184-196. doi:10.1002/mnfr.201100542
34. Jin UH, Lee SO, Sridharan G, et al. Microbiome-derived tryptophan metabolites and their aryl hydrocarbon receptor-dependent agonist and antagonist activities. *Mol Pharmacol*. 2014;85(5):777-788. doi:10.1124/mol.113.091165

35. Cheng Y, Jin U-H, Allred CD, Jayaraman A, Chapkin RS, Safe S. Aryl Hydrocarbon Receptor Activity of Tryptophan Metabolites in Young Adult Mouse Colonocytes. *Drug Metab Dispos.* 2015;43(10):1536-1543. doi:10.1124/dmd.115.063677

Supporting information

**Table S3.1** Chemical composition<sup>1</sup> of experimental materials on a dry basis.

Samples	Protein <sup>2</sup> (%)	Carbohydrate <sup>3</sup> (%)	Fat <sup>4</sup> (%)
<i>Soy protein isolate*</i>	91	< 1	3.3
Single soybean cells	51.3	20.5	25.3
Clustered soybean cells	48.2	22.7	24.7

<sup>1</sup>Results are presented as the average of three replicates, except soy protein isolate\* that are from the label

<sup>2</sup>Protein content was determined by DUMAS (FlashSmart N/PROTEIN, Thermo Fisher Scientific)

<sup>3</sup>Carbohydrate content was determined by Total Dietary Fiber Assay Kit (K-TDFR-200A, Megazyme)

<sup>4</sup>Fat content was determined by Soxhlet extraction using hexane as a solvent.



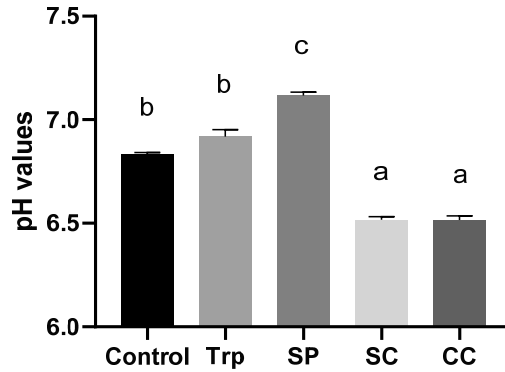


**Figure S3.1** The pH values of supernatants after 48 h fermentation. Control: fermentation without substrate; Trp: fermentation with tryptophan; SP: fermentation with isolated soybean protein; SC: fermentation with single soybean cells; CC: fermentation with clustered soybean cells. Results are presented as mean  $\pm$  SEM ( $n = 3$ ). Bars with different letters indicate treatments that are significantly different ( $p < 0.05$ , one-way ANOVA followed by a Tukey post-hoc test).

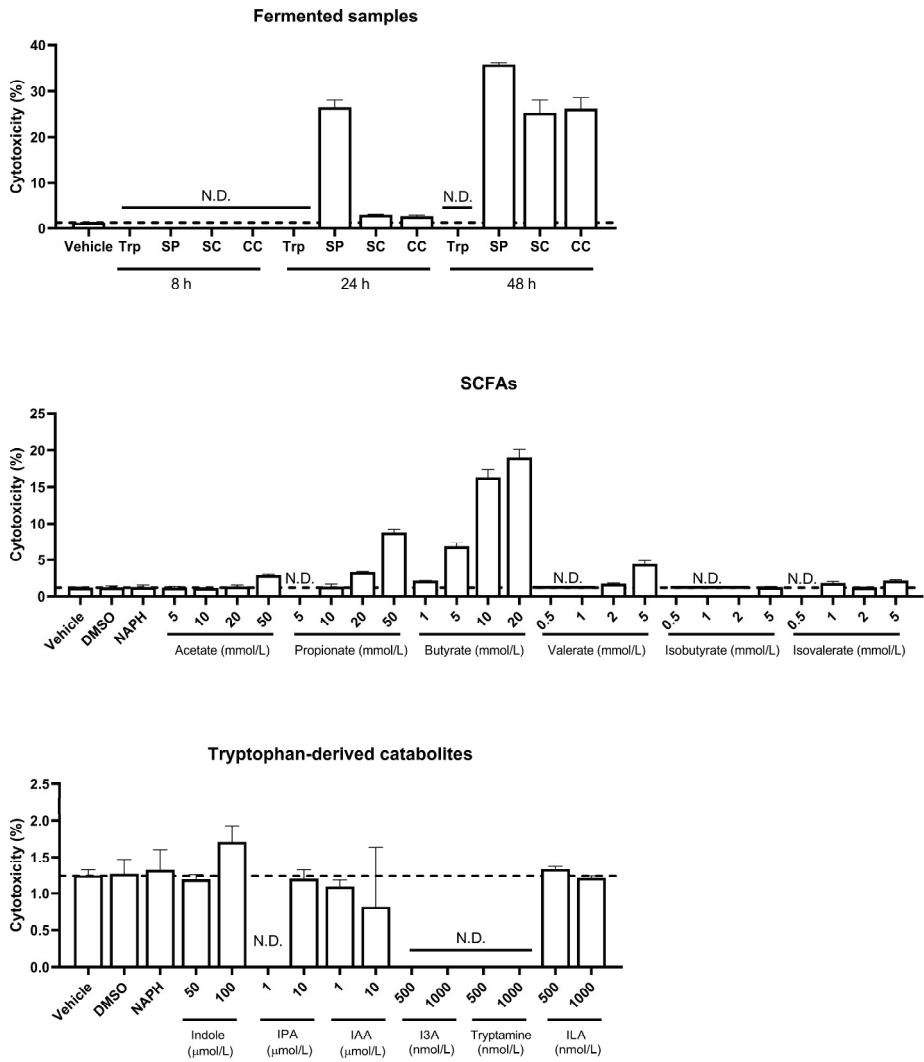


**Figure S3.2** Cytotoxicity of fermented samples, SCFAs, BCFAs, and tryptophan-derived catabolites. HepG2-Lucia™ AhR reporter cells were incubated for 48 h with vehicle (medium) or tested samples. Cytotoxicity was measured by the released lactate dehydrogenase (LDH) using CytoTox 96 Non-Radioactive Cytotoxicity Assay according to the manufacturer's instructions (Promega, USA). The maximum LDH release (positive control) was achieved by adding 10X Lysis Solution. Results are expressed as the percentage of the positive control (100%) with standard error of the mean (n = 3). N.D.: not detected.

## CHAPTER 4





# Distinct effects of fiber and colon segment on microbiota-derived indoles and short-chain fatty acids

**Zhan Huang<sup>1,2</sup>, Jos Boekhorst<sup>2</sup>, Vincenzo Fogliano<sup>1</sup>, Edoardo Capuano<sup>1</sup>, Jerry M. Wells<sup>2,\*</sup>**

<sup>1</sup>Food Quality and Design Group, Department of Agrotechnology and Food Sciences, Wageningen University, P.O. Box 17, 6700 AA, Wageningen, the Netherlands

<sup>2</sup>Host-Microbe Interactomics Group, Department of Animal Sciences, Wageningen University, P.O. Box 17, 6700 AA, Wageningen, the Netherlands



## Abstract

Effects of pectin, inulin, and their combination on the production of microbiota-derived indoles and short-chain fatty acids (SCFAs) in different colon segments were investigated in a batch system inoculated with microbiota from proximal colon (PC) and distal colon (DC) compartments of the Simulator of Human Intestinal Microbial Ecosystem. Bacteria from DC compartment had a higher abundance of Firmicutes and a stronger capacity to produce indoles and SCFAs than bacteria from PC compartment. Fiber supplementation significantly increased the production of SCFAs, indole-3-propionic acid, and indole-3-lactic acid, but decreased the production of oxindole, tryptamine, and serotonin. Pectin specifically promoted the production of indole-3-acetic acid and indole-3-aldehyde. Interestingly, supplementation of pectin or inulin increased the relative abundance of Bacteroidetes whereas supplementation of a mixture of two fibers decreased it. Overall, these results suggest that fiber supplementation and colon segment affect the composition of gut microbiota and microbial catabolism of tryptophan.

**Keywords:** pectin; inulin; colonic fermentation; short-chain fatty acids; indole derivatives; tryptophan

## 1. Introduction

Dietary fiber is a group of non-digestible carbohydrates plus lignin passing to the colon.<sup>1</sup> It is mainly present in nuts, legumes, cereals, fruits, and vegetables and is broadly categorized into soluble and insoluble fiber. Most insoluble fiber is not fermented or only poorly fermented in the colon and has a fecal bulking effect.<sup>2</sup> Conversely, soluble fiber is fermentable by gut microbiota,<sup>2</sup> producing short-chain-fatty acids (SCFAs) as metabolic by-products which play an important role in intestinal homeostasis and affect the tissues and organs beyond the gut.<sup>3</sup> Meta-analyses of prospective studies and randomized trials provide evidence for the important role of dietary fiber in the prevention of cardiovascular related mortality, type 2 diabetes, and colorectal cancer.<sup>4,5</sup> Dietary fiber is also able to promote the growth of beneficial bacteria in the gut.<sup>6</sup> Therefore, dietary fiber, mostly soluble fiber, is widely used to modulate the composition and metabolic profile of the gut microbial community.

SCFAs are the primary end products of fiber fermentation. It is well established that dietary fiber can promote the production of SCFAs in the gut. Recently, there is increasing interest in several indole derivatives originating from bacterial catabolism of tryptophan (Trp), such as indole-3-aldehyde (I3A), indole-3-propionic acid (IPA), and indole-3-acetic acid (IAA), due to their activation of the Aryl hydrocarbon Receptor (AhR), a cytosolic ligand-activated transcription factor that regulates intestinal immune homeostasis.<sup>7</sup> Moreover, IPA can regulate the intestinal barrier function by acting as a ligand of the Pregnane X Receptor (PXR), an effect highly potentiated in the presence of indole.<sup>8</sup> A recent human cohort study indicated that dietary fiber intake was positively associated with the circulating level of microbial produced IPA,<sup>9</sup> but there are no studies on the impact of fiber or combinations of fibers on the bacterial Trp catabolism for the production of indole derivatives in the gut.

The functional capacity of gut microbiota varies along the colon with proximal colon (PC) being the major location for saccharolytic fermentation, as most microbiota preferentially ferment carbohydrates.<sup>10</sup> When carbohydrates reaching the colon are depleted, bacteria tend to utilize other energy sources, such as peptides or amino acids, and this typically occurs in the distal colon (DC).<sup>11</sup> Interestingly, both PC and DC microbiota are dominated by *Bacteroidetes* and *Firmicutes* phyla,<sup>12</sup> but *Bacteroidetes* is more active in a close to neutral pH environment in the DC compared to mildly acidic conditions in the PC.<sup>13</sup> The nature of the substrates available to the microbial community and environmental conditions in the PC and DC would lead to a difference in the composition and metabolic activity of the microbiota. However, whether this



leads to a different utilization pattern of dietary fiber or a different Trp catabolism remains unknown.

In this study, we investigated the effect of pectin, inulin, and their combination on the microbiota composition and the production of SCFAs and indole derivatives by *ex vivo* human gut microbiota from proximal and distal colon compartments of the Simulator of Human Intestinal Microbial Ecosystem (SHIME®) model. We hypothesized that different fibers would have different effects on the composition and metabolic activity of gut microbiota and that this would also be influenced by the colon segment (proximal or distal) and the resident microbiota adapted to this niche.

## 2 Experimental Section

### 2.1 Materials and chemicals

Pectin from apple (product No. 93854) and inulin from chicory (product No. I2255) were purchased from Sigma Aldrich (St. Louis MO, USA), as well as other chemicals used in this study, unless stated otherwise.

### 2.2 Preparation of faecal inocula

Inocula for batch fermentation were collected from SHIME® (ProDigest, Belgium), a dynamic *in vitro* human gastrointestinal model to simulate the *in vivo* conditions.<sup>14</sup> In this study, SHIME® was used to mimic the proximal and distal colon and it was set up according to a previous study.<sup>15</sup> In brief, fresh fecal samples from two healthy donors who had no history of antibiotic usages in the last 6 months prior to donation were inoculated into the PC and DC compartments of SHIME®. As host genetics, sex, age, and diet affect the gut microbiota,<sup>16,17</sup> the two selected donors are Dutch female with similar ages, body mass index, and self-reported dietary habits, so as to reduce inter-individual differences in microbial functionality. The *ex vivo* human gut microbiota were stabilized for two weeks in SHIME® to produce a stable human microbial community by continuously feeding with adult SHIME® growth medium (PD-NM001B, ProDigest). The pH of PC compartment was kept between 5.6 and 5.9 and DC compartment was kept between pH 6.6 and 6.9. Bacteria adapted to PC compartment was referred to as PC bacteria and bacteria adapted to DC compartment as DC bacteria. Stabilized bacteria from each donor and each colon segment were subsequently used in the batch fermentation.

### 2.3 *In vitro* batch fermentation

The batch fermentation was performed in sterilized penicillin bottles containing 43 mL of autoclaved basal medium and 20 mL of autoclaved water (Control) or water containing 2 g/L pectin (P) or 2 g/L inulin (I) or a combination of 1 g/L pectin and 1 g/L inulin (P+I). The basal medium consisted of 2.0 g/L NaHCO<sub>3</sub>, 2.0 g/L yeast extract, 2.0 g/L special peptone, 1.0 g/L mucin, 0.5 g/L L-cysteine HCl, and 2.0 mL/L Tween 80. In addition, 2.11 g/L K<sub>2</sub>HPO<sub>4</sub> and 18.77 g/L KH<sub>2</sub>PO<sub>4</sub> were used in the fermentation with PC bacteria (PC fermentation) to create a pH between 5.6 and 5.9 and 12.34 g/L K<sub>2</sub>HPO<sub>4</sub> and 10.88 g/L KH<sub>2</sub>PO<sub>4</sub> were used in the fermentation with DC bacteria (DC fermentation) for a pH between 6.6 and 6.9. An additional

0.14 g/L of Trp was added to the basal medium for investigating the bacterial catabolism of Trp. Bottles were flushed with N<sub>2</sub>/CO<sub>2</sub> (80/20, v/v) gas mixture to create an anaerobic environment before adding 7 mL of the SHIME<sup>®</sup> inoculum from each donor and each colon segment, then incubated at 37 °C with gentle shaking. The batch fermentation was carried out in duplicate. After 24 h fermentation, 5 mL of fermented samples were immediately centrifuged at 12500 rpm for 5 min. The supernatants were filtered through a 0.20 µm regenerated cellulose filter and then frozen at -20 °C before quantification of metabolites. The pellets were frozen at -20 °C prior to the isolation of microbiota DNA.

#### 2.4 Quantification of SCFAs and branched-chain fatty acids (BCFAs)

SCFAs and BCFAs were measured as previously described.<sup>18</sup> In brief, the frozen supernatants were defrosted at 4 °C and then mixed with the internal standard (0.45 mg/mL 2-ethylbutyric acid in 0.3 mol/L HCl and 0.9 mol/L oxalic acid) at 2:1 (v/v) ratio for quantification via a Shimadzu GC-2014 (Kyoto, Japan) equipped with a flame-ionization detector and a capillary fatty acid-free Stabil wax-DA column (1 µm × 0.32 mm × 30 m) (Restek, Bellefonte, PA, USA). The injection volume was 0.5 µL and the carrier gas was nitrogen. The initial oven temperature was 100 °C for 0.35 min, and increased to 172 °C by 10.8 °C/min, then to 200 °C by 50 °C/min, and held for 1 min. The temperature of the injector and detector was 100 °C and 250 °C, respectively. Standard solutions of acetate, propionate, butyrate, valerate, isobutyrate, and isovalerate were prepared and used for identification and quantification. The results were processed using Chromeleon 7.2.10 (Thermo Fisher Scientific Inc., San Jose, CA).

#### 2.5 Quantification of Trp and indole derivatives

Trp and indole derivatives were measured via a Shimadzu Nexera XR LC-20ADxr UPLC system coupled with a Shimadzu LCMS-8050 mass spectrometer (Kyoto, Japan). Chromatographic separation was accomplished on a Phenomenex Kinetex 1.7 µm EVO C18 100 Å LC column (100 × 2.1 mm). The mobile phase and elution program were described elsewhere.<sup>18</sup> Indoles were identified by comparing the transitions (m/z) and retention time (RT) with reference standards including Trp (m/z 204.9 → 188.1; RT 3.08 min) and indole derivatives: serotonin (5HT; m/z 177.0 → 160.1; RT 1.66 min), kynurenine (Kyn; m/z 209.0 → 192.1; RT 1.92 min), tryptamine (TA; m/z 161.1 → 144.0; RT 2.11 min), oxindole (Oxi; m/z 134.0 → 77.1; RT 8.55 min), indole-3-lactic acid (ILA; m/z 205.9 → 118.1; RT 9.02 min), I3A (m/z 146.0 → 118.1; RT 9.26 min), IAA (m/z 176.0 → 130.1; RT 9.30 min), indole (Ind; m/z

118.2 → 91.1; RT 9.59 min), and IPA (m/z 190.1 → 130.0; RT 9.78 min). Data analysis was performed on LabSolutions LCMS 5.6 (Shimadzu Corporation, Japan).

## 2.6 Microbiota profiling

Bacterial DNA was extracted from the pellets according to the manufacturer instruction of DNeasy® PowerSoil® Kit (12888-50, Qiagen). The purified DNA was quantified by Qubit™ dsDNA BR Assay Kit (Q32853, Invitrogen) using Qubit 4 Fluorometer (Thermo Fisher Scientific Inc., USA) and then kept at -80 °C. The sequencing procedures were carried out by Novogene Europe (Cambridge, United Kingdom). In brief, PCR amplification of 16S rRNA gene (V3-V4 regions) was performed by using 341F (5'-CCTAYGGGRBGCASCAG-3') and 806R (5'-GGACTACNNGGTATCTAAT-3') primers connected with barcodes. PCR products of 450-550 bp were selected by 2% agarose gel electrophoresis. Same amounts of PCR products from each sample were pooled, end-repaired, A-tailed and further ligated with Illumina adapters. Libraries were sequenced on a paired-end Illumina platform (NovaSeq 6000) to generate 250bp paired-end raw reads. After receiving raw sequencing data, the FastQ files were trimmed with cutadapt 2.3.<sup>19</sup> We created amplicon sequence variants (ASVs) with DADA2,<sup>20</sup> and used the SILVA database v138 for taxonomic assignment.<sup>21</sup> We excluded ASVs with taxonomic assignment as eukaryote, mitochondria, and chloroplast.

## 2.7 Statistical analysis

Data were expressed as mean ± standard deviation (SD). Statistical analysis was performed by IBM SPSS Statistics 25 (SPSS Inc, Chicago, USA). Principal coordinate analysis (PCoA) was performed by Canoco 5.12 based on Bray-Curtis distance of microbial relative abundance at the genus level and default settings for the analysis type "Specialized analysis: Principal-coordinates". Shannon diversity was calculated in Python from the microbial relative abundance at the genus level. Differences in the concentrations of microbial metabolites were tested by one-way ANOVA followed by a Tukey post-hoc test, with a  $p < 0.05$  considered as statistical significance.

### 3 Results

#### 3.1 Microbial community

Shannon index describes the species richness in the ecosystem. After 24 h fermentation, PC bacteria had a lower alpha diversity than DC bacteria (Figure 4.1A). The inclusion of pectin and inulin slightly increased the Shannon index of bacteria compared to the control (Figure 4.1A). In the PCoA plot (Figure 4.1B), the first principal coordinate (PC1, 39.7%) explains the intragroup variation due to the colon segment and the second principal coordinate (PC2, 28.4%) explains the intergroup variation due to the fiber supplementation, in which the total amount of fibers was kept the same in the P, I, and P+I groups. The four groups were well-separated in the PC1 and PC2 (Figure 4.1B), suggesting a different composition of gut microbiota between PC and DC, and an effect of fibers on the microbiota of each donor.

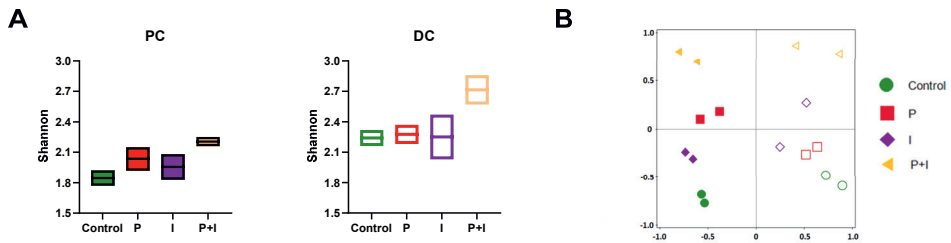


**Figure 4.1** Floating bars (min to max, line at mean) of Shannon index (A) and PCoA plot with Bray-Curtis dissimilarity metrics (B) of microbial relative abundance at the genus level after 24 h fermentation with inoculations from proximal colon (PC) and distal colon (DC) compartments of SHIME® using two donors. Control: fermentation without dietary fibers; P: fermentation with 2 g/L pectin; I: fermentation with 2 g/L inulin; P+I: fermentation with 1 g/L pectin and 1 g/L inulin. Closed symbols are PC samples and open symbols are DC samples.

At phylum level, the microbial community was dominated by *Bacteroidetes*, *Proteobacteria*, and *Firmicutes* in both colon segments (Figure 4.2). PC and DC bacteria had slight differences in microbial composition with a higher level of *Proteobacteria* and a lower level of *Firmicutes* in PC bacteria than in DC bacteria. The P and I groups had a higher percentage of *Bacteroidetes* and a lower percentage of *Proteobacteria* compared to the control group, although this effect was small for DC bacteria of donor 2. Interestingly, an opposite outcome was observed in the P+I group.

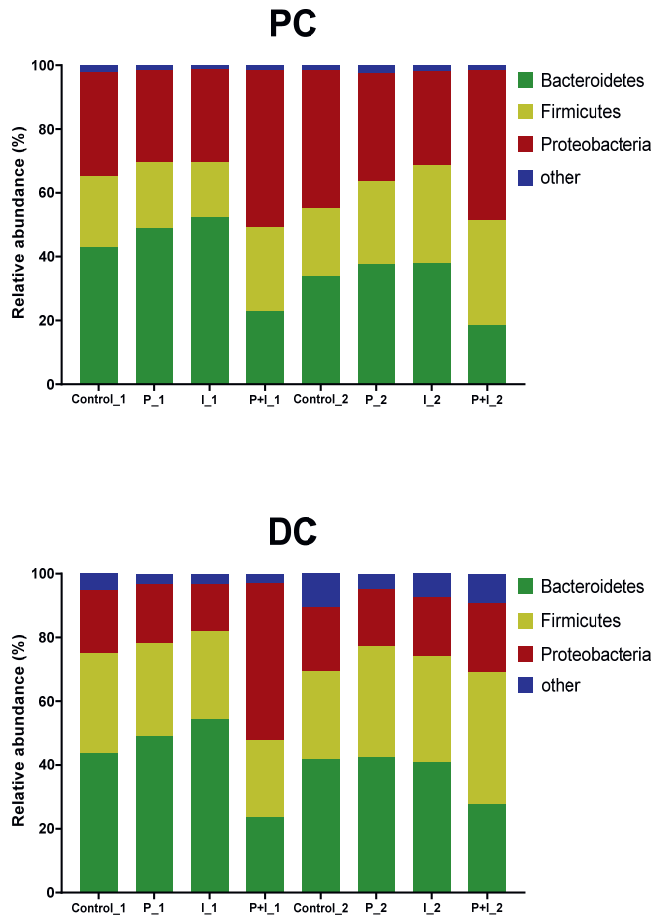


**Figure 4.2** Relative abundance (%) of microbiota at the phylum level after 24 h fermentation with inoculations from proximal colon (PC) and distal colon (DC) compartments of SHIME® using two donors. Control: fermentation without dietary fibers; P: fermentation with 2 g/L pectin; I: fermentation with 2 g/L inulin; P+I: fermentation with 1 g/L pectin and 1 g/L inulin; \_1: donor 1; \_2: donor 2.

At genus level, *Bacteroides* was overall the most abundant, followed by *Lachnoclostridium* and *Suttonella* (Figure 4.3). The relative abundance of *Citrobacter* and *Enterococcus* showed large variations between two donors, especially in PC bacteria. The relative abundance of *Lachnospiraceae* UCG-010 and *Pyramidobacter* was lower in PC bacteria than in DC bacteria. Addition of pectin or inulin resulted in a small increase in the relative abundance of *Bacteroides*, while addition of a mixture of the two fibers appeared to substantially lower the relative

abundance of *Bacteroides* compared to the control group. The effect of fiber on *Citrobacter*, *Suttonella*, and *Enterococcus* was different for each donor, hence repeat studies are needed to determine whether this variability is due to the donor variation in gut microbiome.

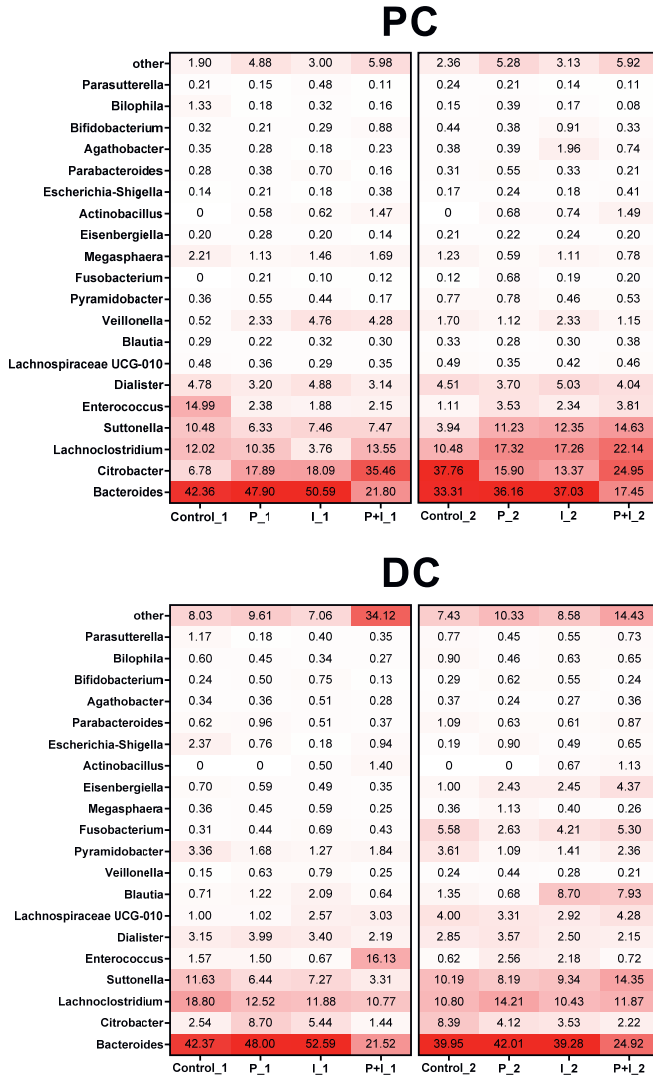
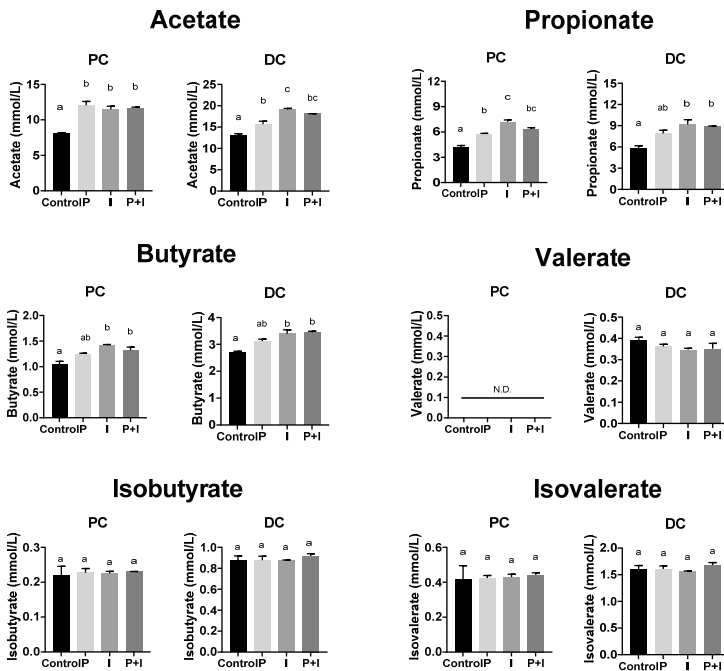


Figure 4.3 Heatmap of relative abundances (%) of microbiota at the genus level after 24 h fermentation with inoculations from proximal colon (PC) and distal colon (DC) compartments of SHIME® using two donors. Control: fermentation without dietary fibers; P: fermentation with 2 g/L pectin; I: fermentation with 2 g/L inulin; P+I: fermentation with 1 g/L pectin and 1 g/L inulin. \_1: donor 1; \_2: donor 2.

### 3.2 SCFAs and BCFAs

Figure 4.4 shows changes in SCFA and BCFA concentrations after 24 h fermentation. Acetate, propionate, and butyrate were the three major produced SCFAs with acetate being the most abundant as previously reported.<sup>22</sup> For all measured SCFA except valerate, which was only found in fermentations with DC bacteria, higher concentrations were observed in samples fermented with DC bacteria than with PC bacteria. Fiber supplementation significantly increased the production of acetate, propionate, and butyrate compared to the control group, but no significant differences were observed for valerate and BCFAs (isobutyrate and isovalerate). Addition of a mixture of the two fibers had a similar effect on SCFA and BCFA production as the addition of either pectin or inulin alone. Compared to pectin, inulin was more effective in increasing SCFA production, leading to significantly higher concentrations of propionate in the PC fermentation and acetate in DC fermentation.



**Figure 4.4** Concentrations of SCFAs and BCFAs after 24 h fermentation with inoculations from proximal colon (PC) and distal colon (DC) compartments of SHIME® using two donors. Control: fermentation without dietary fibers; P: fermentation with 2 g/L pectin; I: fermentation with 2 g/L inulin; P+I: fermentation with 1 g/L pectin and 1 g/L inulin. Bars not sharing any letters indicate treatments that are significantly different ( $p < 0.05$ , one-way ANOVA followed by a Tukey post-hoc test). N.D.: not detected.



### 3.3 Trp and indole derivatives

Trp was catabolized by gut microbiota to produce indole derivatives. After 24 h fermentation, the concentration of residual Trp in samples fermented with PC bacteria was about 40-fold higher than in samples fermented with DC bacteria (Figure 4.5), suggesting a stronger capacity of DC bacteria to utilize Trp. Fiber supplementation suppressed the bacterial catabolism of Trp by PC bacteria as P, I, and P+I groups had significant higher concentrations of residual Trp and thus lower concentrations of indole derivatives than the control group after 24 h fermentation. However, there were no significant differences in the concentration of indole derivatives produced by DC fermentation.

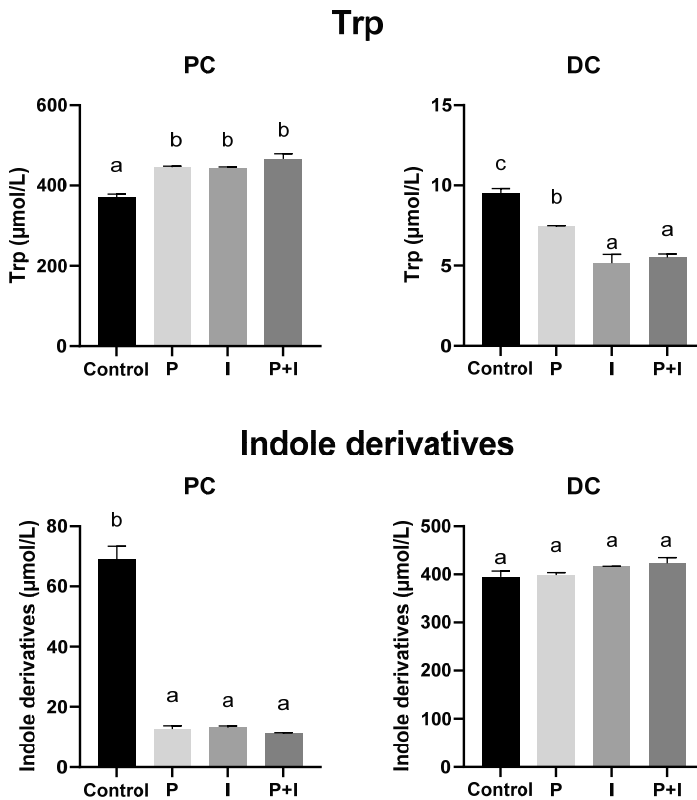


**Figure 4.5** Concentrations of Trp and indole derivatives after 24 h fermentation with inoculations from proximal colon (PC) and distal colon (DC) compartments of SHIME® using two donors. Control: fermentation without dietary fibers; P: fermentation with 2 g/L pectin; I: fermentation with 2 g/L inulin; P+I: fermentation with 1 g/L pectin and 1 g/L inulin. Bars not sharing any letters indicate treatments that are significantly different ( $p < 0.05$ , one-way ANOVA followed by a Tukey post-hoc test).

When looking at specific indole derivatives (Figure 4.6), Ind was produced in the greatest amount likely due to the fact that many *Citrobacter* spp. and *Bacteroides* spp. present in PC and DC bacteria express tryptophanase enzyme that converts Trp into Ind.<sup>23</sup> PC and DC bacteria showed different capacities to produce indole derivatives, showing high concentrations of ILA, TA, and 5HT in PC fermentation and high concentrations of Ind, Oxi, and IPA in DC fermentation. Fiber supplementation significantly decreased the production of Oxi, TA, and 5HT, but increased the production of IPA, IAA, and ILA by PC and DC bacteria, especially in the fermentation containing a mixture of the two fibers. Interestingly, fiber supplementation suppressed the production of Ind in the PC fermentation, but not in the DC fermentation. Fermentation with pectin yielded significant higher concentrations of IAA and I3A than fermentation with inulin, while fermentation with inulin promoted the production of Kyn and 5HT compared to fermentation with pectin.

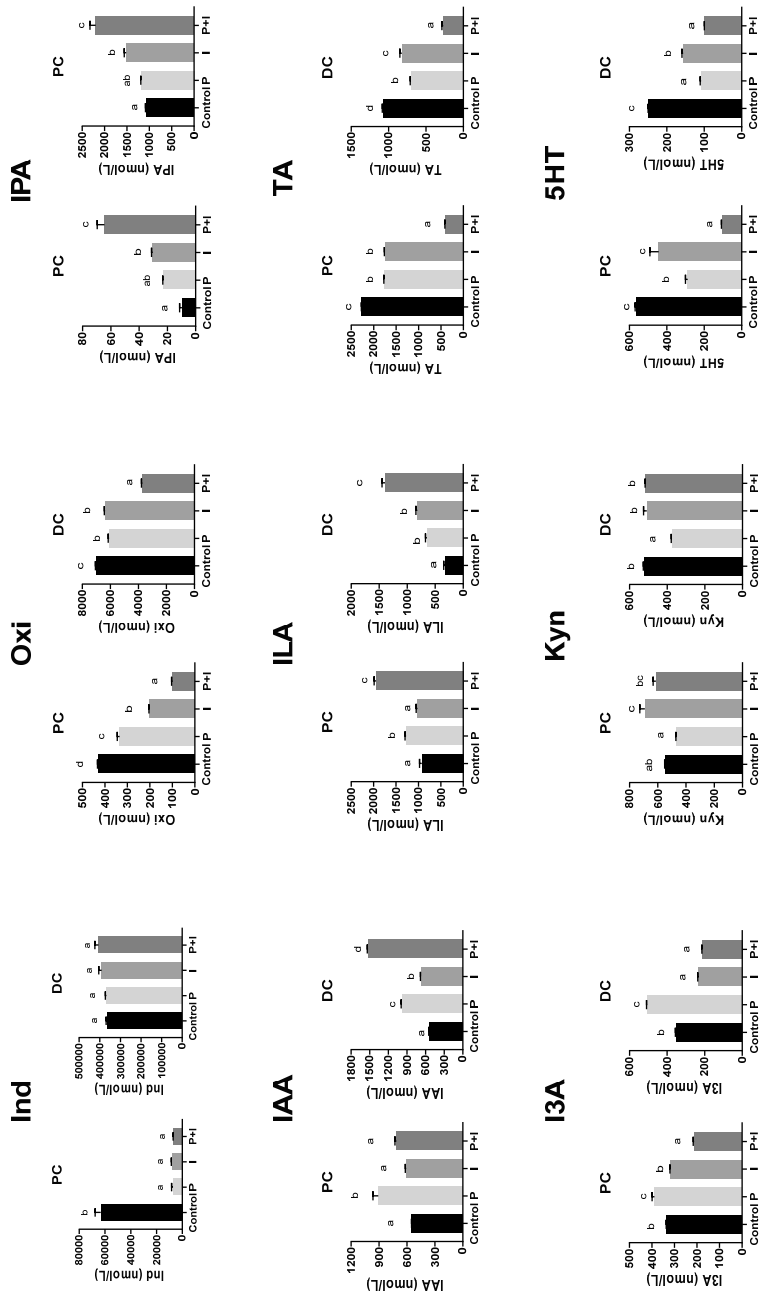


**Figure 4.6** Concentration of specific indole derivative after 24 h fermentation with inoculations from proximal colon (PC) and distal colon (DC) compartments of SHIME® using two donors. Control: fermentation without dietary fibers; P: fermentation with 2 g/L pectin; I: fermentation with 1 g/L inulin; P+I: fermentation with 1 g/L pectin and 1 g/L inulin. Bars not sharing any letters indicate treatments that are significantly different ( $p < 0.05$ , one-way ANOVA followed by a Tukey post-hoc test).



## 4 Discussion

Dietary fiber is recognized as an important component in a health-promoting diet, which can modulate the gut microbial community and promote the production of SCFAs in the colon so as to reduce the risks of several diseases, like inflammatory bowel disease, obesity, diabetes, and intestinal cancers.<sup>2,5</sup> Emerging data shows that indole derivatives produced from bacterial catabolism of Trp are also positively involved in the host-microbiota crosstalk in health and disease,<sup>24,25</sup> but how the production of indole derivatives is modulated by dietary fiber remains largely unknown. Hereby, in the current study, we used an *in vitro* experimental framework to investigate the effect of pectin and inulin on the production of SCFAs and indole derivatives by gut microbiota from PC and DC compartments of the SHIME<sup>®</sup> model.

We found that pectin and inulin induced a striking impact on gut microbiota after 24 h fermentation compared to the control. *Bacteroides* was enriched in the fermentation with pectin in line with the ability of species in this genus to utilize pectin as a carbon source.<sup>26</sup> In the PC fermentation, inulin also favored the growth of *Bacteroides* which can digest and metabolize inulin-type fructans.<sup>27</sup> An increased relative abundance of a specific taxon, genus or species depends on primary utilization of a specific carbohydrate or cross-feeding of products from primary degraders. As hypothesized, fiber supplementation increased the production of SCFAs in the *in vitro* fermentation system, thereby significantly decreasing the pH values (Figure S4.1). Acetate was the major produced SCFA in agreement with the abundance of *Bacteroidetes*, which contains many bacterial groups capable of producing acetate in the intestine.<sup>28</sup> Propionate is produced by a few dominant genera, including *Akkermansia muciniphila*, *Coprococcus catus*, and certain species of *Bacteroidetes*.<sup>29</sup> The increased relative abundance of *Bacteroidetes* is consistent with the increased production of acetate and propionate in the fermentation with pectin and inulin, especially with inulin. Isobutyrate and isovalerate are branched-chain fatty acids (BCFAs), which are exclusive products of fermentation of branched-chain amino acids. In our study, fermentation with fibers had no noticeable effects on the production of BCFAs. When the bacterial degradation of Trp is considered, supplementation of pectin and inulin markedly decreased the production of indole derivatives by PC bacteria. This could be explained by the microbial preference of carbohydrates over proteins as energy source.<sup>10</sup> However, this was not evident in DC fermentation, possibly due to the functional capacities of bacteria in the PC and DC. The PC bacteria hosts mainly saccharolytic specialists, while DC bacteria hosts more proteolytic specialists. Fermentation with pectin and inulin differently

altered the bacterial catabolism of Trp, resulting in different profiles of indole derivatives. An increased level of some specific catabolites, like IPA, IAA, and ILA, were observed in the fermentation with fibers. Although the conversion of indoles by gut microbiota is not well understood, several *Bacteroides* and *Bifidobacterium* species have been reported to be able to convert Trp into IAA and ILA.<sup>25</sup> Intake of fiber-rich foods was found to be positively associated with the serum level of microbial produced IPA.<sup>9</sup> Our study provided direct evidence that fermentation with pectin and inulin increased the production of IPA by gut microbiota. Together, these results confirmed the general observation that the type of fiber influences the microbiota composition and the microbial metabolites produced.

We observed that gut microbiota were differently modulated depending on whether fiber was added alone or in combination. To rule out an effect of the total amount of fibers, this was kept the same for all conditions. Compared to fermentation with pectin or inulin alone, the relative abundance of *Bacteroidetes* which contains the largest repertoire of carbohydrate-active enzymes,<sup>30</sup> was markedly reduced in the fermentation with a mixture of the two fibers. Additionally, the combination of pectin and inulin greatly promoted the production of IPA and ILA, and decreased the production of Oxi and TA, which suggests a synergistic or antagonistic effect on indoles production induced by fiber combination. These results highlight the importance to study the combination of different fibers rather than one specific fiber in the understanding of the health effects of fiber-rich foods where a complex mixture of fibers is always present.

We further clarified the differences in the composition and metabolic activity of gut microbiota from different colon segments (PC and DC). It is reported that the *in vivo* concentration of SCFAs decreases along the length of the colon,<sup>31</sup> possibly due to the decline in the supply of carbohydrates and the continuous absorption by colon epithelium. However, our results show that DC bacteria produced more SCFAs than PC bacteria when they were supplied with the same amount of fibers. This could be due to the higher relative abundance of *Firmicutes* found in DC bacteria compared to PC bacteria, which is active in the degradation of fibers to produce SCFAs, especially butyrate.<sup>32</sup> *Blautia* species are well-recognized butyrate-producing bacteria in the gut,<sup>33</sup> and they were relatively more abundant in DC bacteria compared to PC bacteria. The production of SCFAs is affected by the pH of fermentation environment, as some *Bacteroides* species grow well at pH 6.7 but poorly at pH 5.<sup>34</sup> A pH of 6.5 is able to increase the production of acetate and propionate compared to pH 5.5.<sup>35</sup> These results suggest that DC with a pH environment between 6.6 and 6.9 could be a more suitable target segment than PC

for promoting SCFA production. Proteolytic fermentation mainly occurs in the DC and this is evident in our study as significant more BCFAs and indole derivatives were produced in the DC fermentation than in the PC fermentation. The functional capacity of PC bacteria to catabolize Trp was relatively low as judged by large amounts of Trp remaining after 24 h fermentation and this capacity was further diminished by fiber supplementation. However, it is interesting to notice that some indole derivatives, like ILA, TA, and 5HT, were found at higher concentrations in the PC fermentation than in the DC fermentation, although less Trp was catabolized by PC bacteria. ILA secreted by *Bifidobacterium* spp. is an agonist of AhR.<sup>36</sup> TA and 5HT are neurotransmitters with documented effects on gastrointestinal motility.<sup>25,37</sup> These catabolites are considered beneficial to the host health, and therefore, strategies aiming to promote the production of these catabolites should target the PC.

## 5 Conclusions

In conclusion, our study showed that pectin and inulin had different effects on the composition and metabolic activity of gut microbiota, leading to different profiles of SCFAs and indole derivatives. Our study provides evidence for a novel potential mechanism by which dietary fiber can benefit the host, i.e. via modulating the bacterial catabolism of Trp, in particular promoting the production of IAA, ILA, and IPA which are the ligands of AhR and PXR.<sup>7,8</sup> Importantly, our study also showed that the proteolytic specialists in DC bacteria possessed a strong capacity to produce SCFAs when they were supplied with a sufficient amount of fiber. The bacterial catabolism of Trp was not limited in the DC as several catabolites, like ILA, TA, and 5HT, were produced in large amounts in the PC fermentation. These findings highlight the impact of microbiota metabolic functions in proximal and distal colon on fermentation of different fibers and production of beneficial metabolites which has implications for the design of health-promoting foods.



## **CRedit authorship contribution statement**

Zhan Huang: Conceptualization, Methodology, Investigation, Formal analysis, Writing – original draft, Writing – review & editing.

Jos Boekhorst: Formal analysis, Writing – review & editing.

Edoardo Capuano: Writing – review & editing, Supervision.

Vincenzo Fogliano: Writing – review & editing, Supervision.

Jerry M. Wells: Writing – review & editing, Supervision.

## **Declaration of Competing Interest**

The authors declare that they have no known competing financial interests or personal relationships that could have appeared to influence the work reported in this paper.

## **Acknowledgement**

The authors would like to thank Simen Fredriksen for the help in microbial analysis and the China Scholarship Council for the financial support to the first author.

## Reference

1. EFSA. Scientific Opinion on Dietary Reference Values for carbohydrates and dietary fibre. *EFSA J.* 2010;8(3):1462. doi:10.2903/j.efsa.2010.1462
2. Makki K, Deehan EC, Walter J, Bäckhed F. The impact of dietary fiber on gut microbiota in host health and disease. *Cell Host Microbe.* 2018;23(6):705-715. doi:10.1016/j.chom.2018.05.012
3. van der Hee B, Wells JM. Microbial regulation of host physiology by short-chain fatty acids. *Trends Microbiol.* 2021;29(8):700-712. doi:10.1016/j.tim.2021.02.001
4. Reynolds A, Mann J, Cummings J, Winter N, Mete E, Te Morenga L. Carbohydrate quality and human health: a series of systematic reviews and meta-analyses. *Lancet.* 2019;393(10170):434-445. doi:10.1016/S0140-6736(18)31809-9
5. Cui J, Lian Y, Zhao C, et al. Dietary fibers from fruits and vegetables and their health benefits via modulation of gut microbiota. *Compr Rev Food Sci Food Saf.* 2019;18(5):1514-1532. doi:10.1111/1541-4337.12489
6. Kuo S-M. The interplay between fiber and the intestinal microbiome in the inflammatory response. *Adv Nutr.* 2013;4(1):16-28. doi:10.3945/an.112.003046
7. Lamas B, Natividad JM, Sokol H. Aryl hydrocarbon receptor and intestinal immunity. *Mucosal Immunol.* 2018;11(4):1024-1038. doi:10.1038/s41385-018-0019-2
8. Venkatesh M, Mukherjee S, Wang H, et al. Symbiotic bacterial metabolites regulate gastrointestinal barrier function via the xenobiotic sensor PXR and toll-like receptor 4. *Immunity.* 2014;41(2):296-310. doi:10.1016/j.immuni.2014.06.014
9. Qi Q, Li J, Yu B, et al. Host and gut microbial tryptophan metabolism and type 2 diabetes: an integrative analysis of host genetics, diet, gut microbiome and circulating metabolites in cohort studies. *Gut.* 2022;71(6):1095-1105. doi:10.1136/gutjnl-2021-324053
10. Oliphant K, Allen-Verge E. Macronutrient metabolism by the human gut microbiome: major fermentation by-products and their impact on host health. *Microbiome.* 2019;7(1):91. doi:10.1186/s40168-019-0704-8

11. Windey K, De Preter V, Verbeke K. Relevance of protein fermentation to gut health. *Mol Nutr Food Res.* 2012;56(1):184-196. doi:10.1002/mnfr.201100542
12. Marzorati M, Vilchez-Vargas R, Bussche J Vanden, et al. High-fiber and high-protein diets shape different gut microbial communities, which ecologically behave similarly under stress conditions, as shown in a gastrointestinal simulator. *Mol Nutr Food Res.* 2017;61(1):1600150. doi:10.1002/mnfr.201600150
13. Duncan SH, Iyer A, Russell WR. Impact of protein on the composition and metabolism of the human gut microbiota and health. *Proc Nutr Soc.* 2021;80(2):173-185. doi:10.1017/S0029665120008022
14. Van de Wiele T, Van den Abbeele P, Ossieur W, Possemiers S, Marzorati M. The Simulator of the Human Intestinal Microbial Ecosystem (SHIME®). In: *The Impact of Food Bioactives on Health*. Springer International Publishing; 2015:305-317. doi:10.1007/978-3-319-16104-4\_27
15. Koper JEB, Loonen LMP, Wells JM, Troise AD, Capuano E, Fogliano V. Polyphenols and tryptophan metabolites activate the aryl hydrocarbon receptor in an in vitro model of colonic fermentation. *Mol Nutr Food Res.* 2019;63(3):1-9. doi:10.1002/mnfr.201800722
16. Lozupone CA, Stombaugh JI, Gordon JI, Jansson JK, Knight R. Diversity, stability and resilience of the human gut microbiota. *Nature.* 2012;489(7415):220-230. doi:10.1038/nature11550
17. Org E, Mehrabian M, Parks BW, et al. Sex differences and hormonal effects on gut microbiota composition in mice. *Gut Microbes.* 2016;7(4):313-322. doi:10.1080/19490976.2016.1203502
18. Huang Z, Schoones T, Wells JM, Fogliano V, Capuano E. Substrate-Driven Differences in Tryptophan Catabolism by Gut Microbiota and Aryl Hydrocarbon Receptor Activation. *Mol Nutr Food Res.* 2021;65(13):2100092. doi:10.1002/mnfr.202100092
19. Martin M. Cutadapt removes adapter sequences from high-throughput sequencing reads. *EMBnet.journal.* 2011;17(1):10. doi:10.14806/ej.17.1.200

20. Callahan BJ, McMurdie PJ, Rosen MJ, Han AW, Johnson AJA, Holmes SP. DADA2: High-resolution sample inference from Illumina amplicon data. *Nat Methods*. 2016;13(7):581-583. doi:10.1038/nmeth.3869
21. Quast C, Pruesse E, Yilmaz P, et al. The SILVA ribosomal RNA gene database project: improved data processing and web-based tools. *Nucleic Acids Res*. 2012;41(D1):D590-D596. doi:10.1093/nar/gks1219
22. Sánchez-Patán F, Barroso E, van de Wiele T, et al. Comparative in vitro fermentations of cranberry and grape seed polyphenols with colonic microbiota. *Food Chem*. 2015;183:273-282. doi:10.1016/j.foodchem.2015.03.061
23. Lee J-H, Lee J. Indole as an intercellular signal in microbial communities. *FEMS Microbiol Rev*. 2010;34(4):426-444. doi:10.1111/j.1574-6976.2009.00204.x
24. Agus A, Planchais J, Sokol H. Gut Microbiota Regulation of Tryptophan Metabolism in Health and Disease. *Cell Host Microbe*. 2018;23(6):716-724. doi:10.1016/j.chom.2018.05.003
25. Roager HM, Licht TR. Microbial tryptophan catabolites in health and disease. *Nat Commun*. 2018;9(1):1-10. doi:10.1038/s41467-018-05470-4
26. Luis AS, Briggs J, Zhang X, et al. Dietary pectic glycans are degraded by coordinated enzyme pathways in human colonic Bacteroides. *Nat Microbiol*. 2018;3(2):210-219. doi:10.1038/s41564-017-0079-1
27. Bai J, Li Y, Li T, et al. Comparison of different soluble dietary fibers during the in vitro fermentation process. *J Agric Food Chem*. 2021;69(26):7446-7457. doi:10.1021/acs.jafc.1c00237
28. Cummings JH, Pomare EW, Branch HWJ, Naylor CPE, MacFarlane GT. Short chain fatty acids in human large intestine, portal, hepatic and venous blood. *Gut*. 1987;28(10):1221-1227. doi:10.1136/gut.28.10.1221
29. Louis P, Flint HJ. Formation of propionate and butyrate by the human colonic microbiota. *Environ Microbiol*. 2017;19(1):29-41. doi:10.1111/1462-2920.13589
30. Korpela K. Diet, microbiota, and metabolic health: trade-off between saccharolytic and

- proteolytic fermentation. *Annu Rev Food Sci Technol*. 2018;9(1):65-84. doi:10.1146/annurev-food-030117-012830
31. Koh A, De Vadder F, Kovatcheva-Datchary P, Bäckhed F. From dietary fiber to host physiology: short-chain fatty acids as key bacterial metabolites. *Cell*. 2016;165(6):1332-1345. doi:10.1016/j.cell.2016.05.041
  32. Berry D. The emerging view of Firmicutes as key fibre degraders in the human gut. *Environ Microbiol*. 2016;18(7):2081-2083. doi:10.1111/1462-2920.13225
  33. Benítez-Páez A, Gómez del Pugar EM, López-Almela I, Moya-Pérez Á, Codoñer-Franch P, Sanz Y. Depletion of Blautia species in the microbiota of obese children relates to intestinal inflammation and metabolic phenotype worsening. Turnbaugh PJ, ed. *mSystems*. 2020;5(2). doi:10.1128/mSystems.00857-19
  34. Walker AW, Duncan SH, Carol McWilliam Leitch E, Child MW, Flint HJ. pH and peptide supply can radically alter bacterial populations and short-chain fatty acid ratios within microbial communities from the human colon. *Appl Environ Microbiol*. 2005;71(7):3692-3700. doi:10.1128/AEM.71.7.3692-3700.2005
  35. Walker AW., Duncan SH, Leitch ECM, Child MW., Flint HJ. pH and peptide supply can radically alter bacterial populations and short-chain fatty acid ratios within microbial communities from the human colon. *Appl Environ Microbiol*. 2005;71(7):3692-3700. doi:10.1128/AEM.71.7.3692-3700.2005
  36. Ehrlich AM, Pacheco AR, Henrick BM, et al. Indole-3-lactic acid associated with Bifidobacterium-dominated microbiota significantly decreases inflammation in intestinal epithelial cells. *BMC Microbiol*. 2020;20(1):357. doi:10.1186/s12866-020-02023-y
  37. Krautkramer KA, Fan J, Bäckhed F. Gut microbial metabolites as multi-kingdom intermediates. *Nat Rev Microbiol*. 2021;19(2):77-94. doi:10.1038/s41579-020-0438-4

## Supporting information

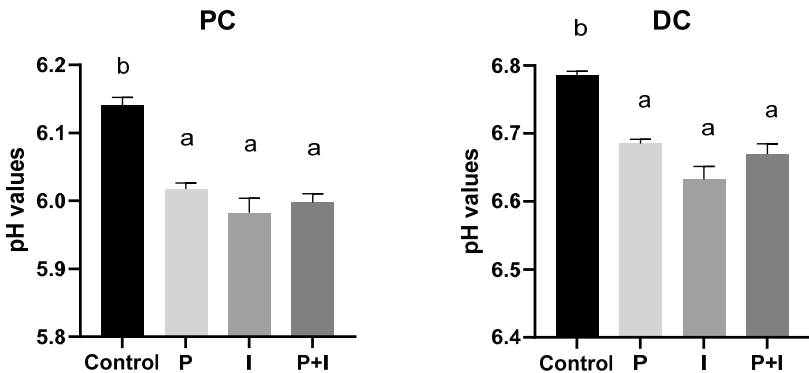


**Figure S4.1** pH values after 24 h fermentation with inoculations from proximal colon (PC) and distal colon (DC) compartments of SHIME® using two donors. Control: fermentation without dietary fibers; P: fermentation with 2 g/L pectin; I: fermentation with 2 g/L inulin; P+I: fermentation with 1 g/L pectin and 1 g/L inulin. Bars with different letters indicate treatments that are significantly different ( $p < 0.05$ , one-way ANOVA followed by a Tukey post-hoc test).

## CHAPTER 5

# 5





# Impact of high-fiber or high-protein diet on the capacity of human gut microbiota to produce tryptophan catabolites

**Zhan Huang<sup>1,2</sup>, Jos Boekhorst<sup>2</sup>, Vincenzo Fogliano<sup>1</sup>, Edoardo Capuano<sup>1,\*</sup>, Jerry M. Wells<sup>2,\*</sup>**

<sup>1</sup>Food Quality and Design Group, Department of Agrotechnology and Food Sciences, Wageningen University, P.O. Box 17, 6700 AA, Wageningen, the Netherlands

<sup>2</sup>Host-Microbe Interactomics Group, Department of Animal Sciences, Wageningen University, P.O. Box 17, 6700 AA, Wageningen, the Netherlands



## Abstract

Diet plays an important role in the modulation of gut microbiome, but there is little knowledge of how diets rich in fiber or proteins alter the functional capacity of the colon microbiota to produce beneficial tryptophan catabolites. In this study, the Simulator of the Human Intestinal Microbial Ecosystem (SHIME®) was used to mimic the *in vivo* human gut microbial communities of proximal colon (PC) and distal colon (DC). We investigated the effects of high-fiber-low-protein (HF) and high-protein-low-fiber (HP) diets on microbiota composition and microbial Trp catabolism in the PC and DC. We found that PC microbiota had a higher abundance of *Firmicutes* and a stronger capacity to produce kynurenine, serotonin (5-HT), indoleacrylic acid (IA), tryptamine, indole-3-lactic acid (ILA), and indole-3-aldehyde (I3A), whereas DC microbiota had a higher abundance of *Bacteroidetes* and a stronger capacity to produce indole-3-acetic acid (IAA), indole, indole-3-propionic acid (IPA), and oxindole. To investigate the effects of dietary interventions, HF and HP diets were inoculated in SHIME® over 2 weeks. A distinct effect of diet on microbiota composition was observed in the PC where the HF diet enriched the abundance of *Firmicutes*, and the HP diet enriched the abundance of *Proteobacteria*. The HF diet favored the microbial production of 5-HT, IA, I3A, ILA, IAA, and IPA, which is independent of tryptophan content, but largely dependent on abundance of specific microbes. Together, these findings provide a better understanding of the contribution of HF and HP diet to the microbial catabolism of Trp in the human colon.

**Keywords:** diet; SHIME; gut microbiota; tryptophan; indole derivatives

## 1 Introduction

There is a growing interest in manipulating the gut microbiota and microbiota-derived metabolites through diet to beneficially modulate host physiology.<sup>1–4</sup> The most studied microbial metabolites are short-chain fatty acids (SCFAs) mainly produced by colonic fermentation of undigested complex polysaccharides.<sup>5</sup> SCFAs have profound effects on gut homeostasis, exert anti-inflammatory and epigenetic effects, and affect physiology in other organs through G-protein-coupled receptors signaling.<sup>6–8</sup> Recently, indole derivatives originating from microbial catabolism of tryptophan (Trp) have received much attention, due to their AhR-dependent anti-inflammatory effects and modulation of innate lymphoid cells type 3 which produce IL-22,<sup>9,10</sup> a cytokine important for intestinal repair and barrier function.<sup>11</sup> Several studies have reported the beneficial effects of indole derivatives on host physiology.<sup>12–15</sup> Individuals with metabolic syndrome,<sup>15</sup> inflammatory bowel disease,<sup>16</sup> and celiac disease<sup>17</sup> have reduced concentration of indole derivatives in the faeces, presumably due to an altered gut microbial community. A large human cohort study on the correlation between circulating concentrations of Trp metabolites and incidence type 2 diabetes (T2D) showed that indole-3-propionic acid (IPA) was inversely associated with T2D risk.<sup>18</sup> Recently IPA was shown to promote regeneration and functional recovery of nerves after injury.<sup>19</sup> Together, these studies highlight the important role of microbiota-derived Trp catabolites in health and disease, and the need to find reliable strategies to promote the microbial production of these catabolites.

Several *Bacteroides* spp., *Clostridium* spp., *Bifidobacterium* spp., *Lactobacillus* spp., and *Peptostreptococcus* spp. have been reported to be able to convert Trp into indole derivatives,<sup>10,13,20,21</sup> but the complete set of taxa and the related microbial pathways are incomplete. Emerging evidence from animal and human studies suggests a potential role of diet in the manipulation of Trp catabolism by gut microbiota.<sup>22–24</sup> The fecal concentration of microbiota-derived Trp catabolites was increased in mice and pigs fed with a high-Trp diet.<sup>17,25</sup> A recent study showed that human intake of fiber-rich foods was positively associated with the serum concentrations of IPA,<sup>18</sup> a finding confirmed in older adults on a polyphenol-rich diet.<sup>26</sup> Previously, using an *in vitro* batch model of colonic fermentation, we demonstrated that dietary fibers (i.e. pectin and inulin) are able to promote the microbial production of IPA, indole-3-acetic acid (IAA), and indole-3-lactic acid (ILA).<sup>27</sup> However, the effects of long-term dietary habits on the microbial production of Trp catabolites in the intestine has not yet been systematically explored.

Here, we tested the effects of two different diets, a high-fiber-low-protein (HF) diet and a high-protein-low-fiber (HP) diet, on the microbial production of Trp catabolites in the proximal and distal colon using the simulator of human intestinal microbiota ecosystem (SHIME®), a dynamic gastrointestinal model for long-term microbiome intervention studies.<sup>28</sup> SHIME® was inoculated with *ex vivo* human gut microbiota to mimic the microbiological properties of the proximal and distal parts of the colon under representative *in vivo* environmental conditions. To determine effects of diet on the functional capacity of the microbiota as well as microbiota composition and diversity, we used 16S rRNA amplicon sequencing and shotgun metagenomic sequencing. In addition, we also quantified a panel of microbiota-derived Trp catabolites in the proximal colon (PC) and distal colon (DC) compartments of SHIME®, and correlated their concentration with the abundance of different taxa at each location to provide insights into the main producers of Trp catabolites in the human colon.

## 2 Materials and methods

### 2.1 Experimental design

SHIME® (ProDigest, Belgium) was set up as previously described.<sup>29</sup> Briefly, as shown in Figure 5.1a, SHIME® consisted of two units (SHIME\_1 and SHIME\_2). Each unit had one combined stomach and small intestine vessel (S1/S2) and was subdivided in two parallel PC and DC compartments, which were inoculated with fresh fecal samples from two healthy Dutch female donors aged 22 to 25 with a normal BMI value, similar dietary habits, and no history of antibiotic and probiotic use in the last 6 months prior to donation. The SHIME® system was kept at 37 °C by means of a warm water circulator (AC200, Thermo Fisher Scientific). The pH was maintained at 5.6-5.9 for PC compartments and at 6.6-6.9 for DC compartments by adding 0.5 M HCL (acid) or NaOH (base). In the rest of the manuscript microbiota adapted to the PC or DC compartment of SHIME® are referred to as PC or DC microbiota respectively. The feeding was programmed three times per day with an interval of eight hours. In each cycle, 224 mL fresh feed (pH 1.8-2.2) was pumped to S1/S2 and later was mixed with 96 mL pancreatic juice (12.5 g/L NaHCO<sub>3</sub>, 6 g/L Oxgall, and 0.9 g/L pancreatin) to simulate the digestion happening in the small intestine. After 90 min, the digesta was parallelly transferred to the series of PC and DC compartments within 60 min. The volume of PC and DC compartments was kept constant at 400 mL and 640 mL respectively all the time.

The experiment was conducted in five stages as illustrated in Figure 5.1b. To adapt to the new environment and produce a representative microbial community, the *ex vivo* human gut microbiota was stabilized for two weeks by continuously feeding with adult SHIME® growth medium (basal diet) (PD-NM001B, ProDigest). A control period supplied with basal diet for one week was placed to measure the baseline (day 1-7). Next was the dietary intervention for two weeks (day 8-23), in which SHIME\_1 unit was supplied with a HF diet and SHIME\_2 unit was supplied with a HP diet. This was followed by supplementation of the HF or HP diet with 0.2 g/L Trp for five days (day24-28). Lastly, the basal diet was used in a wash-out period of two weeks (day 29-42) to determine whether there were lasting effects of the different diets on the microbiota. The details of the diet composition are reported in Figure 5.1c. HF or HP diet was formulated by changing the composition and amounts of the ingredients in the basal diet, essentially as previously described.<sup>30</sup> The total consumption of base solution as an indicator of fermentation process is shown in Figure 5.1d, which was automatically added to neutralize the

SCFAs produced in the PC and DC compartments of SHIME<sup>®</sup> so as to maintain the pH range. Samples from the fermentor were collected once per day at the same time starting point from the control period, and they were immediately centrifuged after sampling (12500 rpm, 5 min, 4 °C). The supernatants were filtered using a 0.2 µm regenerated cellulose filter (Phenomenex, Torrance, CA) and stored at -20 °C until the Trp metabolites were measured. The pellets were kept at -80 °C for extraction of bacterial DNA and sequencing.





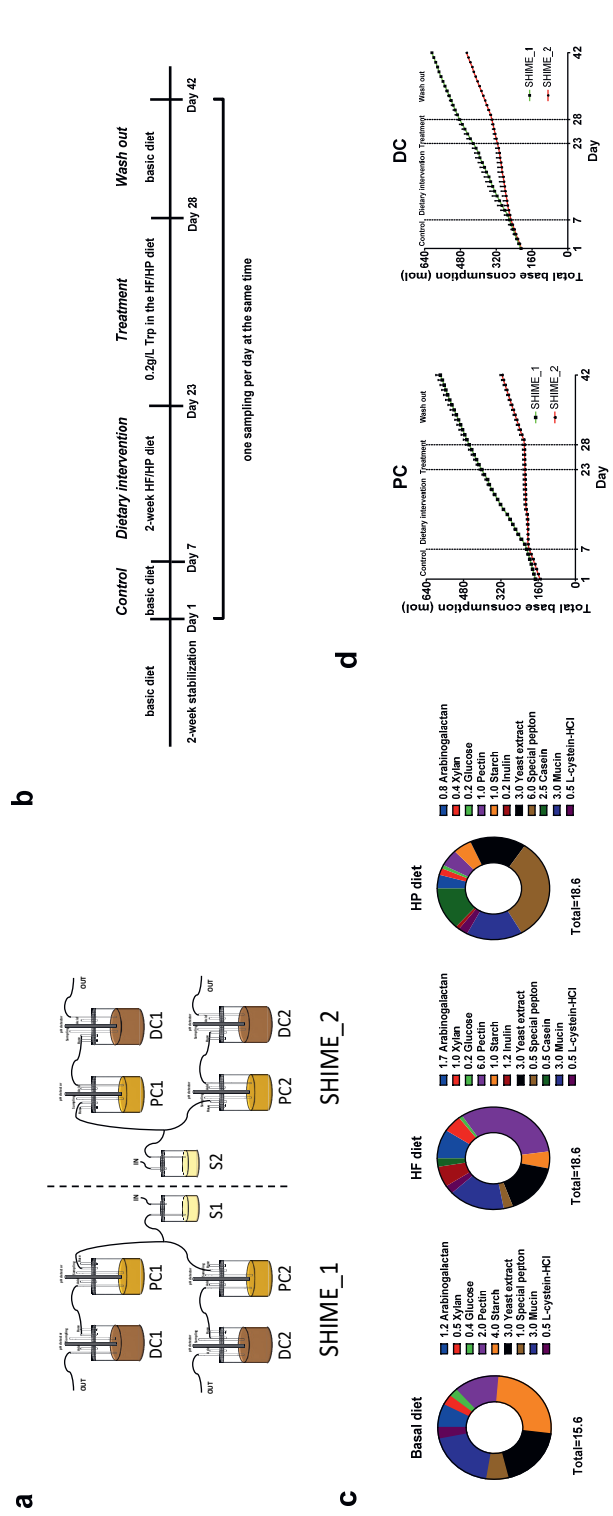


**Figure 5.1** The overview of the study design. **a** Design of the SHIME® model mimicking the proximal colon (PC) and distal colon (DC). **b** Schematic of the experimental procedure including 2-week microbiome stabilization, 1-week control period, 2-week dietary interventions, 1-week tryptophan (Trp) treatment, and 2-week wash-out. **c** Composition of the basal, high-fiber-low-protein (HF) and high-protein-low-fiber (HP) diets for SHIME® microbiota. **d** Total consumption of the base solution of the SHIME® model during the study. Control: SHIME® fed with basal diet to measure the baseline. Dietary intervention: SHIME\_1 fed with high-fiber-low-protein (HF) diet and SHIME\_2 fed with high-protein-low-fiber (HP) diet. Treatment: supplied 0.2 g/L tryptophan in the HF/HP diet. Wash out: SHIME® fed with basal diet. Data are presented as mean + SD (n = two biological donors).



## 2.2 LC-MS analysis of Trp catabolites

Trp catabolites in the supernatants were quantified as previously described.<sup>27,31</sup> Briefly, IPA, IAA, ILA, indole (Ind), oxindole (Oxi), indoleacrylic acid (IA), indole-3-aldehyde (I3A), tryptamine (TA), kynurenine (Kyn), and serotonin (5-HT) were measured via a Shimadzu Nexera XR LC-20ADxr UPLC system coupled with a Shimadzu LCMS-8050 mass spectrometer (Kyoto, Japan). Chromatographic separation was accomplished on a Phenomenex Kinetex 1.7  $\mu\text{m}$  EVO C18 100 Å LC column (100  $\times$  2.1 mm) using 0.1% formic acid in water (v : v) as mobile phase A and 0.1% formic acid in methanol (v : v) as mobile phase B. The identification was done by comparing the transitions and retention time with reference standards. Data analysis was performed on LabSolutions LCMS 5.6 (Shimadzu Corporation, Japan).

## 2.3 DNA extraction

Fermented samples from three time points (day 6, after stabilization and before dietary interventions; day 23, after two-week dietary interventions; and day 42, after two-week wash-out) were selected to extract bacterial genomic DNA from the pellet according to the manufacturer instruction of DNeasy® PowerSoil® Kit (12888-50, Qiagen). DNA quality and quantity were measured by Qubit™ dsDNA BR Assay Kit (Q32853, Invitrogen) using Qubit 4 Fluorometer (Thermo Fisher Scientific, USA) and then stored at -80 °C for further analysis.

## 2.4 16S rRNA amplicon sequencing

Bacterial genomic DNA samples were sent to Novogene Europe (Cambridge, UK) for library preparation and sequencing. Briefly, the V3-V4 region of the 16S rRNA gene was PCR amplified using 341F (5'-CCTAYGGGRBGCASCAG-3') and 806R (5'-GGA CTACNNGGGTATCTAAT-3') primers connected with barcodes. The PCR products were purified and then sequenced on a paired-end Illumina platform (NovaSeq 6000, Illumina) to generate 250 bp paired-end raw reads. The FastQ files were trimmed with cutadapt 2.3.<sup>32</sup> Amplicon sequence variants (ASVs) were created using DADA2<sup>33</sup> and taxonomic assignment was performed using SILVA database v138.<sup>34</sup> ASVs with taxonomic assignment as eukaryote, mitochondria, and chloroplast were excluded.

## 2.5 Shotgun metagenomics

Bacterial genomic DNA samples extracted from the pellet of day 23 (after dietary intervention) were selected in shotgun metagenomic sequencing performed by Novogene Europe (Cambridge, UK). Briefly, the genomic DNA was randomly sheared into short fragments and the obtained fragments were end repaired, A-tailed and further ligated with Illumina adapter. The fragments with adapters were PCR amplified, size selected, and purified. The library was checked with Qubit and real-time PCR for quantification and bioanalyzer for size distribution detection. Quantified libraries were pooled and sequenced on NovaSeq 6000 for 4 Gb raw data per sample. The original metagenomic sequencing data were analyzed with ATLAS on defaults settings to harvest the functional annotation information.<sup>35</sup> The genes involved in Kyoto Encyclopedia of Genes and Genomes (KEGG) annotation of Trp metabolism (map00380) together with other potential KEGG Orthology involved in the known pathway of microbial catabolism of Trp were chosen for further analysis.<sup>36–38</sup>

## 2.6 Statistical analysis

GraphPad Prism 9.1.0 (GraphPad Software, La Jolla, CA) was used for statistical analysis unless otherwise indicated. For microbial analysis, the Shannon index for  $\alpha$ -diversity (richness and diversity) was calculated in Python3 (<https://www.python.org>) and  $\beta$ -diversity (microbial similarity or dissimilarity) was assessed by calculating a matrix of dissimilarities using the Bray-Curtis method on the relative abundance of microbiota at genus level and then visualized using principal coordinate analysis (PCoA) by Canoco 5.14. Correlations between gut microbiota and quantified Trp catabolites were assessed with Spearman's correlations in Scientific Python (<https://scientific-python.org>), in which gut microbiota is filtered by the average abundance ( $> 1\%$ ) and prevalence ( $> 70\%$ ). The  $p$ -value was adjusted for multiple tests using the false discovery rate (FDR) correction by Benjamini and Hochberg (<https://tools.carbocation.com/FDR>). An FDR corrected  $p$ -value (FDR- $p$ )  $< 0.05$  is considered as significant correlation and  $< 0.15$  is considered as a speculative correlation, warranting further investigation. Significant differences in microbial community indicators and Trp catabolites between the two colon segments and diets were determined using the Student's  $t$ -test. Statistical significance is represented as  $*p < 0.05$ ,  $**p < 0.01$ ,  $***p < 0.001$ , and  $****p < 0.0001$ . Sample size and statistical tests are also indicated in the figure caption.

### 3 Results

#### 3.1 Microbiota composition and diversity varies between PC and DC and between HF and HP diets

After stabilization time in the SHIME<sup>®</sup>, we compared the diversity and composition of the PC and DC microbiota. We normally compare samples on day 7 of stabilization but the initial quality control of the sequencing results suggested a contamination and thus the day 6 samples were used. These results showed the PC microbiota to have a significantly lower Shannon index of  $\alpha$ -diversity than the DC microbiota as (Figure 5.2a). The PCoA plot of  $\beta$ -diversity, a measure of compositional similarity, revealed differences between PC and DC microbiota as well as between donor 1 and donor 2 (Figure 5.2b). To further understand these microbial dissimilarities, we evaluated their taxonomic compositions. At the phylum level, the microbial community was dominated by *Bacteroidetes*, *Firmicutes*, and *Proteobacteria*. PC microbiota had a higher abundance of *Firmicutes* and *Proteobacteria*, but a lower abundance of *Bacteroidetes*, *Desulfobacterota*, and *Synergistota* than DC microbiota (Figure 5.2c). At the genus level, *Lachnospirillum*, *Dialister* and *Megasphaera* were more abundant in PC microbiota than in DC microbiota, whereas DC microbiota had a higher abundance of *Parabacteroides* and *Pyramidobacter* than PC microbiota (Figure 5.2c).

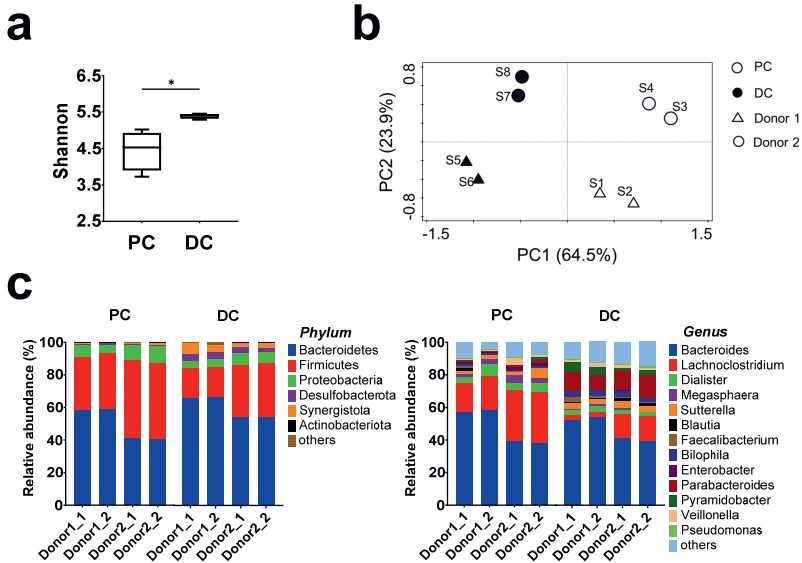


**Figure 5.2** The SHIME® microbiota in the proximal and distal colon compartments at Day 6. **a** alpha diversity (Shannon at genus level). **b** beta diversity (PCoA with Bray-Curtis dissimilarity at genus level). **c** taxonomy (phylum and genus) of proximal colon (PC) and distal colon (DC) microbiota. Data were from two biological donors after stabilization and before dietary interventions and analyzed by Student's t test. Significance is reported as  $*p < 0.05$ . In PCoA plots, each point represents one observation (S1-S8). Donor 1 is represented by a triangle and Donor 2 is represented by a circle. Open symbols are PC samples. Black closed symbols are DC samples.

To understand how changes in the diet influence PC and DC microbiota, we conducted a two-week dietary intervention by using HF and HP diets. The PC microbiota exposed to HF diet had a significantly lower  $\alpha$ -diversity than that exposed to HP diet (Figure 5.3a). Similarly, the microbiota  $\beta$ -diversity varied between HF and HP diets, especially for the PC microbiota (Figure 5.3b). A detailed investigation of diet effect on the composition of PC microbiota revealed that HF diet resulted in a prevalence of *Firmicutes* including several genera, such as *Lachnospirillum*, *Megasphaera*, *Tyzzelerella*, and *Veillonella*, whereas HP diet resulted in a prevalence of *Proteobacteria* represented by the genus *Enterobacter* (Figure 5.3c). The relative abundance of *Bacteroidetes* dominated by the genus *Bacteroides* was less in PC microbiota exposed to HF diet rather than the HP diet, but this was reversed for DC microbiota (Figure 5.3c).

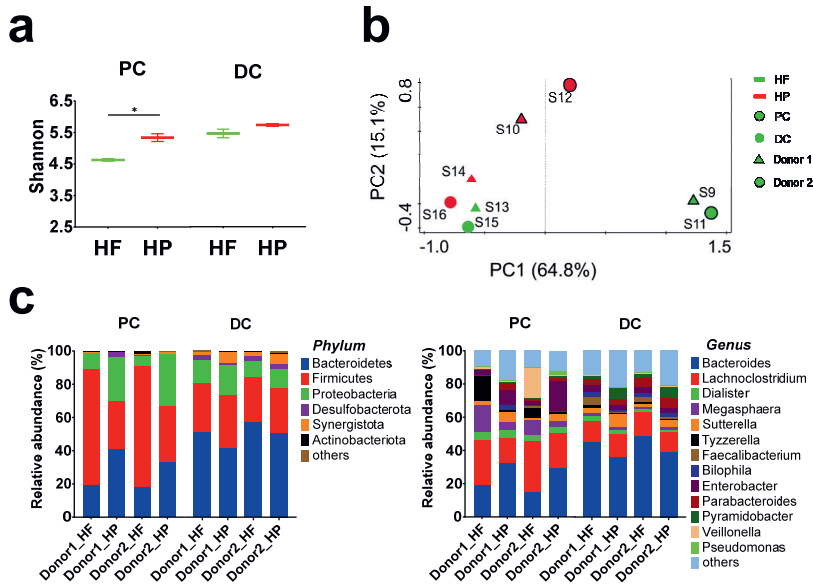


**Figure 5.3** The SHIME® microbiota in the proximal and distal colon compartments at Day 23. **a** alpha diversity (Shannon at genus level). **b** beta diversity (PCoA with Bray-Curtis dissimilarity at genus level). **c** taxonomy (phylum and genus) of proximal colon (PC) and distal colon (DC) microbiota. Data were from two biological donors after 2-week dietary interventions by high-fiber-low-protein diet (HF, green) and high-protein-low-fiber diet (HP, red) and analyzed by Student's t test. Significance is reported as \* $p < 0.05$ . In PCoA plots, each point represents one observation (S9-S16). Donor 1 is represented by a triangle and Donor 2 is represented by a circle. Symbols with black outline are PC samples. Symbols without black outline are DC samples.

After the 2-week dietary exposure and then a further period of 5 days with increased Trp supplementation, the SHIME® feed was switched to the basal diet to see if the microbiota might revert to the pre-intervention state or not. At the end of the experiment the PC microbiota from the different donors cluster together in a PCoA plot of Bray-Curtis dissimilarity at the genus level whereas there was more variability in the biological replicates of the DC microbiota from donor 1 and donor 2 (Figure 5.4). An increased abundance of the phylum *Proteobacteria* and the genus *Enterobacter* was observed in the PC microbiota compared to the pre-intervention state at day 6 (Figure 5.4c). Similar increases in the phylum *Proteobacteria* were also observed in DC microbiota (Figure 5.4c). These results suggest that the two-week wash-out after a dietary intervention cannot reverse the effects of the dietary modulation on the microbiota, which is further confirmed in the PCoA plot of microbiota Bray-Curtis dissimilarity of all samples (Figure 5.5).

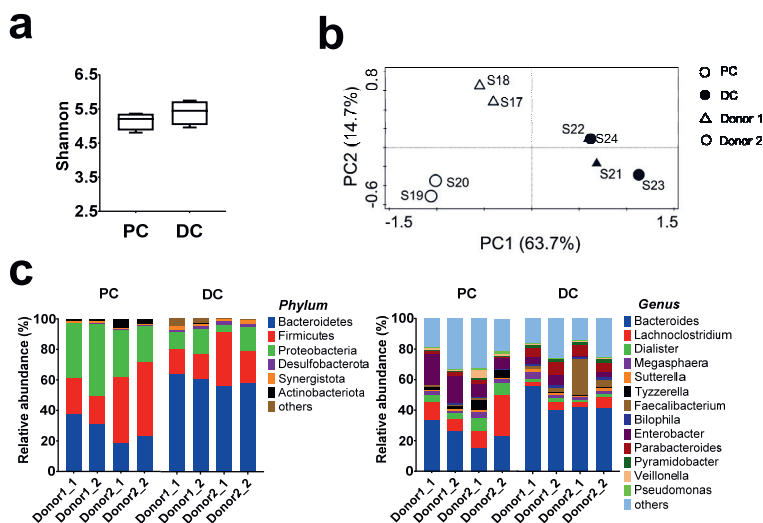


**Figure 5.4** The SHIME® microbiota in the proximal and distal colon compartments at Day 42. **a** alpha diversity (Shannon at genus level). **b** beta diversity (PCoA with Bray-Curtis dissimilarity at genus level). **c** taxonomy (phylum and genus) of proximal colon (PC) and distal colon (DC) microbiota. Data were from two biological donors after 2-week wash-out and analyzed by Student's t test. Significance is reported as  $*p < 0.05$ . In PCoA plots, each point represents one observation (S17-S24). Donor 1 is represented by a triangle and Donor 2 is represented by a circle. Open symbols are PC samples. Black closed symbols are DC samples.

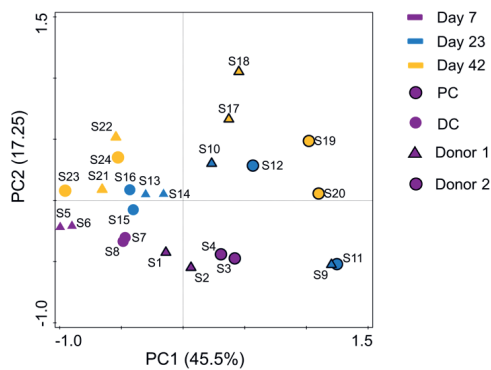


**Figure 5.5** PCoA plot with Bray-Curtis dissimilarity of all microbiota compositional profiles from selected time points at genus level. Each point represents one observation (S1-S24). Donor 1 is represented by a triangle and Donor 2 is represented by a circle. Symbols with black outline are PC samples. Symbols without black outline are DC samples.



### 3.2 Colon segment differs in the microbial catabolism of Trp

We next examined the microbial production of Trp catabolites in the PC and DC compartments of SHIME<sup>®</sup>. In line with microbiota composition, notable differences in the quantification of Trp catabolites were observed between PC and DC samples at day 6, with Kyn, 5-HT, IA, TA, ILA, and I3A in higher concentrations in PC samples than the DC samples, whereas IAA and especially Ind were more abundant in DC samples than in the PC samples (Figure 5.6a). IPA and Oxi were only measurable in the DC samples (Figure 5.6a).

As indicated by the overall concentration of Trp catabolites (Figure 5.6b), the DC is the main site for microbial catabolism of Trp and it is dominated by the production of Ind which accounts for over 90% of the measured catabolites (Figure 5.6c). The panel of Trp catabolites in the PC samples is completely different to DC samples, which was more balanced with IA (38.90%), ILA (21.32%), and Kyn (14.09%) being the main catabolites (Figure 5.6c).

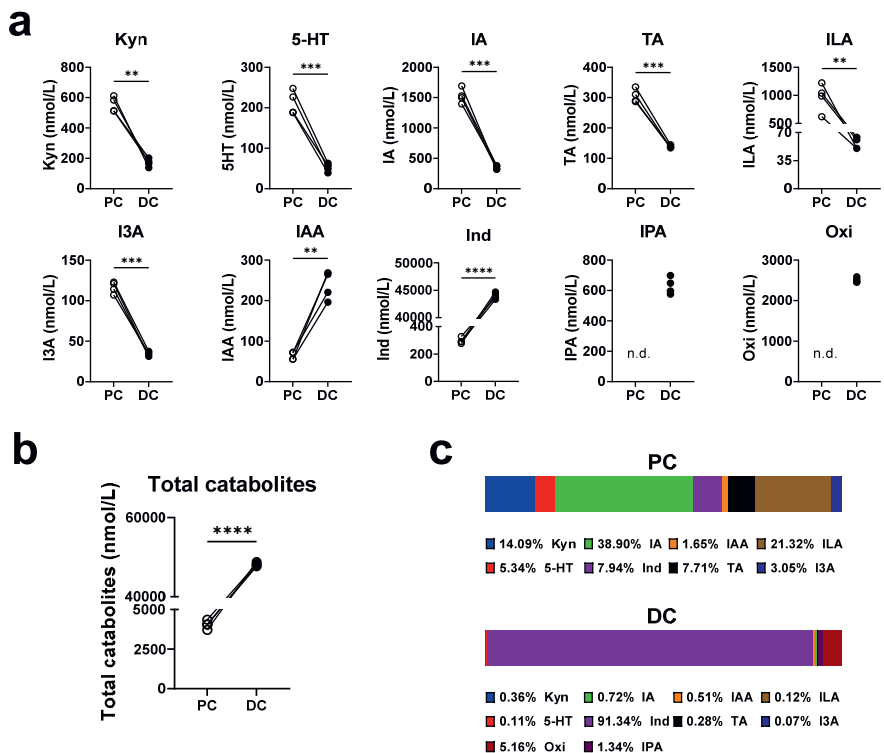


**Figure 5.6** Difference in microbial production of tryptophan catabolites between proximal and distal colon. **a** Concentration of individual tryptophan metabolites (kynurenine, Kyn; serotonin, 5-HT; indoleacrylic acid, IA; tryptamine, TA; indole-3-lactic acid, ILA; indole-3- aldehyde, I3A; indole, Ind; indole-3-acetic acid, IAA; indole-3-propionic acid, IPA; oxindole, Oxi) in the proximal colon (PC) and distal colon (DC) compartments of SHIME®. **b** Overall concentration of all identified catabolites in the PC and DC compartments of SHIME®. **c** Average percent abundance of each catabolite relative to total catabolites in the PC and DC compartments of SHIME®. Data were from two biological donors in duplicate at Day 6 and analyzed by paired Student’s t test. Significance is reported as \*\* $p < 0.01$ , \*\*\* $p < 0.001$ , and \*\*\*\* $p < 0.0001$ .

### 3.3 HF and HP diets differentially shift the microbial catabolism of Trp

Trp catabolism by the PC and DC microbiota rapidly changed in response to the different diets and during dietary intervention, with the HF diet resulting in higher concentrations of 5-HT, IA, IAA, ILA, I3A, and IPA than the HP diet in both PC and DC samples (Figure 5.7a). The HP diet resulted in higher concentrations of Ind, TA, Kyn, and Oxi than the HF diet (Figure 5.7b). However, compared to the control period, both dietary interventions rapidly reduced the

microbial production of 5-HT, IA, and TA and slowly reduced the microbial production of I3A in both PC and DC SHIME® compartments (Figure 5.7). Similar decreases were also observed for ILA and Kyn production in the PC compartment (Figure 5.7). When the microbiota was exposed to HP and HF diets, the concentration of Ind in PC samples rapidly increased and then decreased (Figure 5.7b). In DC samples, the HF dietary intervention stimulated increased production of IPA compared to the control period (Figure 5.7a), whereas the HP dietary intervention stimulated increased production of Ind and Oxi (Figure 5.7b).

At the end of dietary intervention, we supplied 0.2 g/L free Trp in the HF or HP diet to verify the Trp catabolizing ability of the microbiota adapted to HF and HP diets. As expected, Trp supplementation increased the microbial production of Trp catabolites in both PC and DC compartments of SHIME® (Figure 5.7). The microbiota adapted to the HF diet had a stronger capacity to produce 5-HT, IA, IAA, ILA, I3A, and IPA than the microbiota adapted to HP diet, whereas the microbiota adapted to HP diet possessed a stronger capacity to produce TA, Kyn, Ind, and Oxi than the microbiota adapted to HF diet (Figure 5.7). These results were in line with the effect of the dietary modulation of Trp catabolism by HF and HP diets.

We next examined whether dietary interventions have a lasting effect on the microbial catabolism of Trp beyond the intervention stage. After a two-week wash-out period, the concentration of Trp catabolites in PC and DC samples became more similar to the pre-intervention state (Figure 5.7). However, in the wash-out period, the microbiota adapted to HF diet retained a strong capacity to produce ILA and IPA, while a strong capacity to produce Kyn was retained in the microbiota after adaptation to HP diet (Figure 5.7). Furthermore, in the wash-out period the microbiota pre-adapted to the HF diet had a stronger capacity to produce TA than the microbiota adapted to the HP diet, which was different to what was observed in the dietary intervention period (Figure 5.7b).



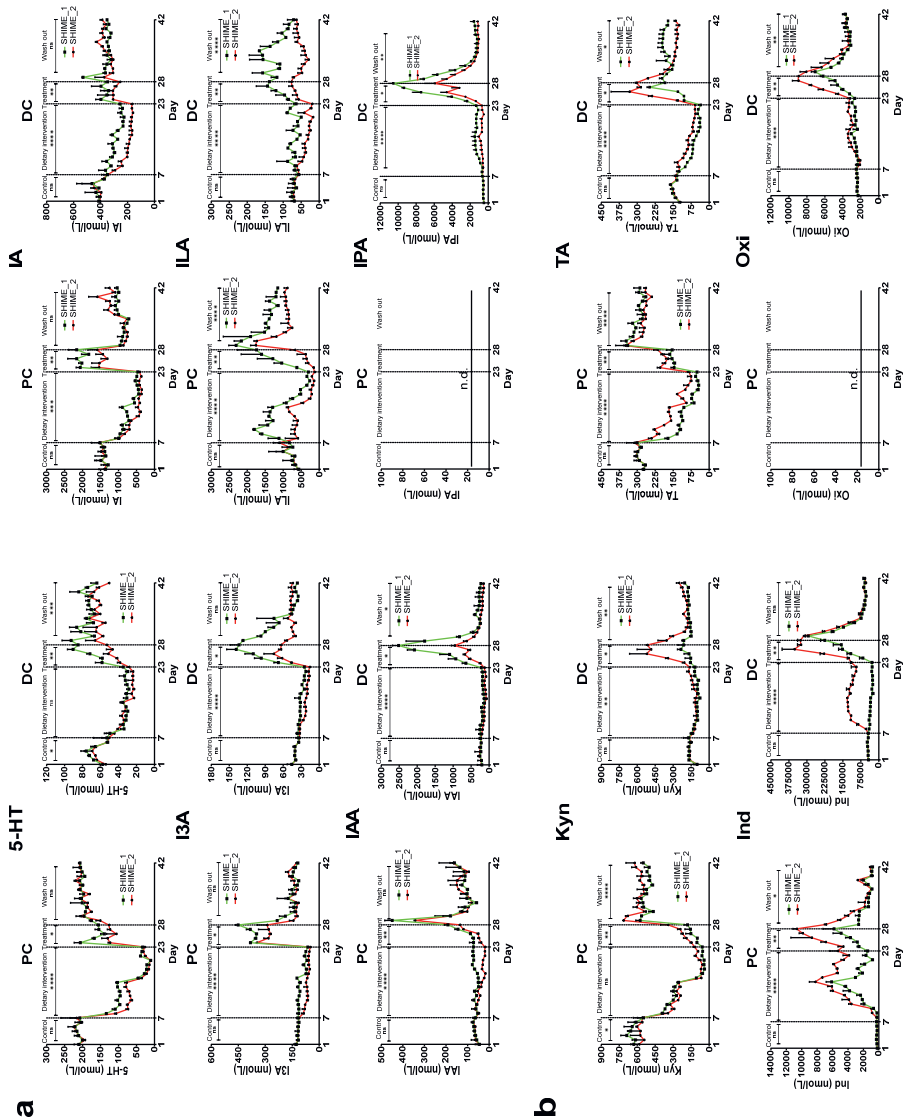


(Figure legend on next page)

**Figure 5.7** Microbial production of tryptophan catabolites during the experimental period. **a** Tryptophan catabolites with higher concentrations after high-fiber-low-protein (HF) diet compared to high-protein-low-fiber (HP) diet during dietary intervention. 5-HT, serotonin; IAA, indole-3-acetic acid; ILA, indole-3-lactic acid; I3A, indole-3-aldehyde; IPA, indole-3-propionic acid. **b** Tryptophan catabolites with higher concentrations after HP diet compared to HF diet during dietary intervention. Kyn, kynurenine; TA, tryptamine; Ind, indole; Oxi, oxindole. PC: proximal colon. DC: distal colon. Control: SHIME® fed with basal diet to measure the baseline. Dietary intervention: SHIME\_1 fed with HF diet and SHIME\_2 fed with HP diet. Treatment: supplied 0.2 g/L tryptophan in the HF/HP diet. Wash out: SHIME® fed with basal diet n.d.: not detected. Data are presented as mean + SD (n = two biological donors) and analyzed by paired Student's t test between SHIME\_1 and SHIME\_2 in each period. Significance is reported as ns  $p > 0.05$ , \* $p < 0.05$ , \*\* $p < 0.01$ , \*\*\* $p < 0.001$ , and \*\*\*\* $p < 0.0001$ .

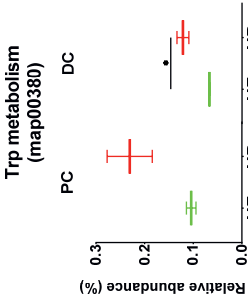
### 3.4 Diet modulates the genetic potential of the microbiota to produce Trp catabolites

We next analyzed metagenomic sequencing data at day 23 to investigate the diet effect on the functional profiling of the microbiome regarding Trp catabolism. The selected genetic potential of PC and DC microbiota to produce Trp metabolites was assessed by determining the normalized relative abundance of DNA sequence reads mapping to the superpathway of KEGG Trp metabolism (map00380). Genes involved in Trp metabolism were relatively more abundant in the PC microbiota than in DC microbiota (Figure 5.8a), and nearly all the abundant KEGG Orthology (KO) in the map00380 was enriched by the HP diet, with the exception of K10217 in PC microbiota and K01667 in DC microbiota (Figure 5.8b). A search was then performed for all known enzymes or KOs involved in the microbial catabolism of Trp.<sup>36–38</sup> A total of six relevant KOs were found, as well as two candidate genes (K00170 and K00172) responsible for the conversion of indole-3-pyruvic acid to IAA (Figure 5.8c).<sup>20</sup> The HP diet enriched the KOs involved in the biosynthesis of Kyn (K00453 and K07130), IAA (K04103 and K00128), and IPA (K00249) in both PC and DC microbiota, whereas the HF diet enriched the K00172 (Figure 5.8c and Figure S5.1). Interestingly, the effect of diet on the abundance of K01667 and K00170 varied between the PC and DC microbiota (Figure 5.8c and Figure S5.1).

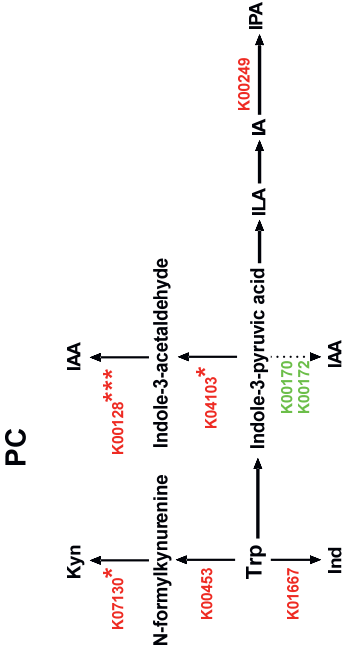




a



c



b

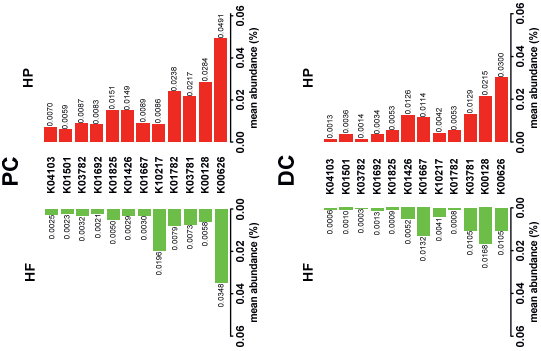


(Figure legend on next page)

**Figure 5.8** Differential functions of the microbiome regarding tryptophan catabolism between HF and HP diets. **a** Comparison of microbial Kyoto Encyclopedia of Genes and Genomes (KEGG) pathway of tryptophan (Trp) metabolism (map00380) between proximal colon (PC) and distal colon (DC) microbiota exposed to high-fiber-low-protein (HF, green) diet and high-protein-low-fiber (HP, red). **b** The mean abundance of the top 12 abundant KEGG Orthology (KO) in the map00380. **c** Cartoon displaying the Trp catabolism to kynurenine (Kyn), indole (Ind), indole-3-acetic acid (IAA), and indole-3-propionic acid (IPA) and the KO involved in each pathway and identified in the PC and DC microbiota exposed to HF and HP diets. The color represents the relatively high abundance of KO in which diet with significance marked by asterisks. Details are given in **Fig. S1**. Data were from two biological donors at Day 23 and analyzed by Student's *t* test. Significance is reported as \* $p < 0.05$ , \*\* $p < 0.01$ , and \*\*\* $p < 0.001$ . ILA: indole-3-lactic acid; IA: indoleacrylic acid. K00626: acetyl-CoA C-acetyltransferase (EC 2.3.1.9); K00128: aldehyde dehydrogenase (EC 1.2.1.3); K03781: catalase (EC 1.11.1.6); K01782: 3-hydroxyacyl-CoA dehydrogenase (EC 1.1.1.35); K10217: aminomuconate-semialdehyde dehydrogenase (EC 1.2.1.32); K01667: tryptophanase (EC 4.1.99.1); K01426: amidase (EC 3.5.1.4); K01825: 3-hydroxyacyl-CoA dehydrogenase (EC 1.1.1.35); K01692: enoyl-CoA hydratase (EC:4.2.1.17); K03782: catalase-peroxidase (EC 1.11.1.21); K01501: nitrilase (EC 3.5.5.1); K04103: indolepyruvate decarboxylase (EC 4.1.1.74); K00453: tryptophan 2,3-dioxygenase (EC 1.13.11.11); K07130: arylformamidase (EC 3.5.1.9); K00249: acyl-CoA dehydrogenase (EC 1.3.8.7); K00170: pyruvate ferredoxin oxidoreductase B (EC:1.2.7.1); K00172: pyruvate ferredoxin oxidoreductase C (EC 1.2.7.1); ILA: indole-3-lactic acid; IA: indoleacrylic acid.

### 3.5 Correlation between gut microbiota and Trp catabolites

We further identified the correlation between gut microbiota and Trp catabolites. The microbial genera that made up less than 1% of the total counts and occurring in less than 70% of samples were removed from the analysis. Overall, although the correlations were relatively weak after FDR correction, significant differences in the correlation patterns of PC and DC microbiota for Trp catabolites were observed, for example *Megasphaera* in PC microbiota was negatively correlated with most of Trp catabolites produced in the PC compartment of SHIME®, but positive correlations between *Megasphaera* and most of Trp catabolites were observed in DC samples (Figure 5.9). In PC samples, a significantly positive correlation was observed between *Bifidobacterium* and IAA (FDR- $p < 0.05$ ) and potentially negative correlations were observed between *Megasphaera* and Kyn and between *Sutterella* and IAA (FDR- $p < 0.15$ ) (Figure 5.9). In DC samples, *Megasphaera* was positively correlated with Oxi (FDR- $p < 0.05$ ), as well as *Enterobacter* (FDR  $< 0.15$ ); *Faecalibacterium* was positively correlated with IPA (FDR- $p < 0.15$ ); *Veillonella* was positively correlated with IAA (FDR- $p < 0.15$ ); uncultured\_f\_Lachnospiraceae was negatively correlated with I3A (FDR- $p < 0.15$ ) and TA (FDR- $p < 0.05$ ); *Sutterella* was negatively correlated with IPA (FDR- $p < 0.15$ ); and *Bilophila* was negatively correlated with Ind and Oxi (FDR- $p < 0.15$ ) (Figure 5.9).



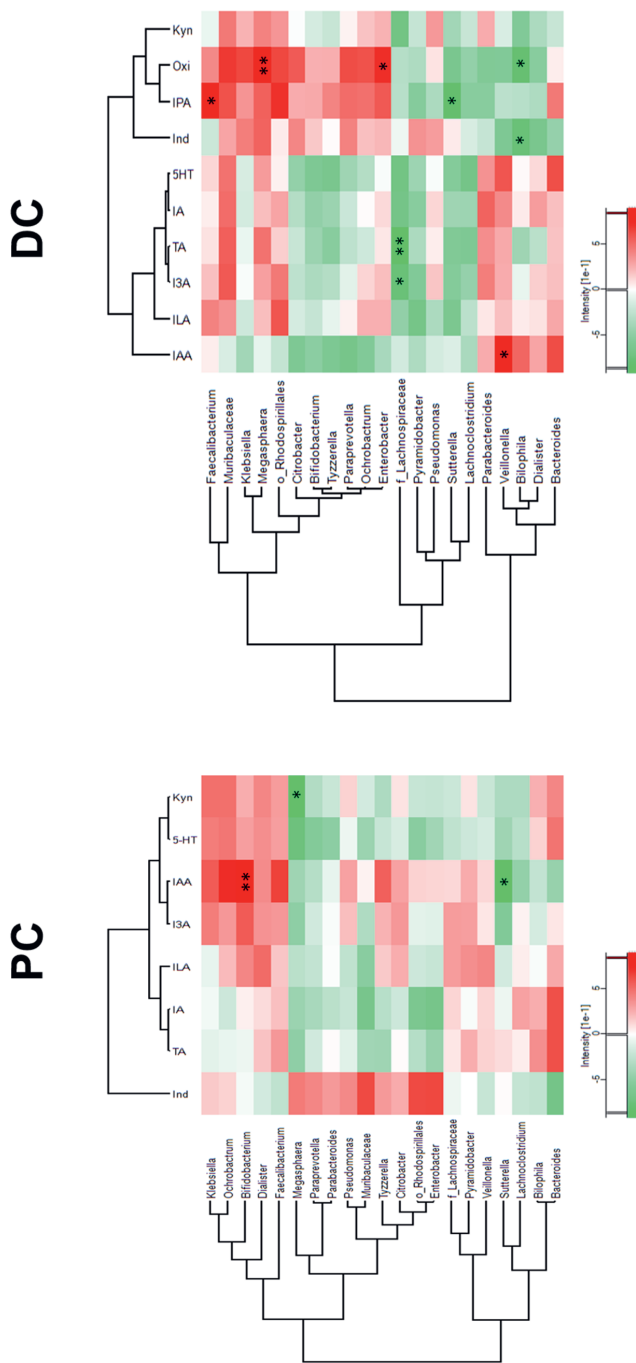


**Figure 5.9** Correlations between gut microbiota and tryptophan catabolites. The microbial genera with a mean relative abundance >1% and represented in >70% of proximal colon (PC) or distal colon (DC) microbial samples obtained from Day 6, Day 23, and Day 42 were correlated to their corresponding quantified tryptophan catabolites through non-parametric Spearman rank analysis. The heatmap was plotted based on  $r$  values. The red color means positive correlation and the green color means negative correlation. \*\*Significant correlation with FDR-corrected  $p$  value <0.05. \*Potential correlation with FDR-corrected  $p$  value <0.15. Kyn: kynurenine; 5-HT: serotonin; IA: indoleacrylic acid; Ind: indole; IAA: indole-3-acetic acid; TA: tryptamine; ILA: indole-3-lactic acid; I3A: indole-3-aldehyde; Oxi: oxindole; IPA: indole-3-propionic acid.



## 4 Discussion

Given the beneficial role of microbiota-derived Trp catabolites in intestinal homeostasis and immune regulation,<sup>10,39,40</sup> we investigated how HF or HP diet influences the capacity of human gut microbiota to produce Trp catabolites in SHIME®. We found that the composition and function of human gut microbiota differed in the different colon segments, i.e. proximal and distal colon. After the *ex vivo* human gut microbiota was stabilized in SHIME®, DC microbiota showed a higher diversity than PC microbiota, consistent with a previous study in humans.<sup>41</sup> The major intestinal phyla *Bacteroidetes* and *Firmicutes* were present in both PC and DC microbiota but *Bacteroidetes* was more abundant in the DC microbiota (~ 60% versus 50%) and *Firmicutes* was more abundant in PC microbiota (~ 40% versus 25%). The acidic pH of 5.6-5.9 in the PC compartment of SHIME® provides a competitive advantage for acid-tolerant bacterial species, mostly from *Firmicutes*,<sup>42</sup> to grow in this niche, whereas members of *Bacteroidetes* grow poorly in acidic conditions and grow optimally in the DC compartment where the pH was maintained at 6.6-6.9.<sup>43</sup> The substrates available for metabolism can also influence the microbiota composition. In the colon, the microbiota preferentially utilizes fermentable carbohydrates over proteins for growth.<sup>44</sup> Consequently, proximal colon is the main site for saccharolytic fermentation and when fermentable carbohydrates are depleted, the microbiota switch to other energy sources, such as peptides or amino acids, and this typically occurs in the distal colon.<sup>45</sup> *Firmicutes* consists of many degraders of complex carbohydrates, but *Bacteroidetes*, mostly *Bacteroides* spp., has the largest repertoire of carbohydrate-active enzymes of all intestinal microbiota.<sup>46</sup> However, *Bacteroides* spp. are usually considered as generalists because of their capacity to utilize a large range of substrates for growth also including proteins.<sup>43</sup>

The microbial production of Trp catabolites is not limited to specialized protein degraders or to the distal colon. Several Trp catabolites, such as Kyn, 5-HT, IA, TA, ILA, and I3A, were quantified at high concentrations in PC samples. This may be due to the high abundance of acid-tolerant bacteria in PC microbiota,<sup>43</sup> e.g. *Bifidobacterium* spp. (Figure S5.2), which is capable of converting Trp into ILA.<sup>47</sup> Kyn and 5-HT are two well-known endogenous Trp metabolites, but a growing body of literature suggests that they can also be produced by gut microbiota.<sup>4,15,23,38,48</sup> Our data further support this notion. We also identified the enzymes responsible for Kyn biosynthesis, Trp 2,3-dioxygenase (K00453) and arylformamidase

(K07130),<sup>37</sup> which were more abundant in PC microbiota than in DC microbiota (Figure S5.1). However, the enzymes for microbial biosynthesis of 5-HT were not found.<sup>38</sup>

In line with the distal colon being the most active location of proteolytic fermentation of proteins,<sup>43</sup> large amounts of Trp catabolites were identified in the DC samples, especially Ind via the activity of tryptophanase (K01667).<sup>49</sup> Within the human gut microbiota, tryptophanase is widely expressed in the commensal *Bacteroides* species,<sup>22</sup> which are suggested to be active in the distal colon and inactive in the proximal colon because of the environmental pH.<sup>50</sup> Several *Bacteroides* species have also been reported to produce IAA.<sup>51</sup>

One stark difference in Trp catabolism between PC and DC microbiota was the production of IPA and Oxi, which was only identified in DC samples. IPA has recently received increased attention for its association with gut barrier integrity and cognitive performance,<sup>12,19</sup> as well as its protective role in disease.<sup>52,53</sup> To date, only a small number of bacteria, mostly *Clostridium* spp.,<sup>20,54</sup> have been identified for IPA production. Very little information is available on the microbial production of Oxi. A recent study indicated that Oxi is present at a considerable concentration in human stool and it can activate human AhR at physiologically relevant concentrations.<sup>23</sup> However, the physiological significance of Oxi as well as the identity of the bacteria producing it in the human gut are currently unknown. Our correlation analyses suggest that *Megasphaera* and *Enterobacter* might be the main contributors to Oxi production in the distal colon.

In addition to intestinal location-specific differences, we also demonstrated the diet-induced modifications to microbiota composition and microbiota-derived Trp catabolites. Changes in microbial community reflect trade-offs between primary utilization of fermentable carbohydrates versus proteins in the diet. A study on professional athletes revealed that athletes have a high diversity of gut microbiota and this is positively correlated with the high level of protein consumption.<sup>55</sup> We also found that HP diet increased the diversity of PC and DC microbiota compared to HF diet. A distinct diet effect on microbiota composition was observed in PC microbiota: the HF diet favored fiber-degrading bacteria, especially those from *Firmicutes*, whereas the HP diet allowed the increase of acid-sensitive *Proteobacteria*.<sup>56</sup> Surprisingly, a similar effect was not observed in DC microbiota. One possible explanation is the high abundance of *Bacteroides* in DC microbiota, which is able to cope with the different diets using its large repertoire of degrading enzymes.<sup>43</sup>



The modification of microbiota composition induced by the different diets has been previously associated with changes in Trp catabolism. For example, the 4-day Mediterranean diet has been reported to increase the concentration of IAA, IPA, and ILA in the plasma of individuals.<sup>24</sup> Our data demonstrated that, compared to a HP diet, the HF diet favored the microbial production of 5-HT, IA, IAA, ILA, I3A, and IPA. This suggests that some of the fiber-degrading bacteria enriched by HF diet may have the capacity to specifically catabolize Trp. It is important to notice that the HF diet has a lower content of protein compared to the HP diet, and therefore a lower content of precursor Trp. Therefore, we speculate that the effect of fiber on microbial catabolism of Trp is independent of protein or Trp content, but largely dependent on the effect of the diet on the abundance of microbes able to catabolize Trp.

Compared to HF diet, HP diet favored the microbial production of TA, Kyn, Ind, and Oxi, but this may be due to the higher content of Trp in the HP diet. Thus, we analyzed the functional capacity of the colon microbiota to produce beneficial tryptophan catabolites by shotgun metagenomic sequencing. The HP diet increased the genetic potential of PC and DC microbiota for Kyn biosynthesis compared to the HF diet, as well as the PC microbiota for Ind biosynthesis. Interestingly, the HP diet reduced the genetic potential of DC microbiota for Ind biosynthesis, which was not in agreement with the higher concentration of Ind in DC samples after the HP dietary intervention. Similar inconsistencies were also observed for IAA and IPA production and measured gene abundances. This may be due to the fact that the identified Trp catabolic genes are not all expressed in PC and DC microbiota.<sup>57</sup>

The diet effect on gut microbiome is rapid and reproducible.<sup>58</sup> Previous trials in humans showed gut microbiota can recover from dietary interventions to its pre-intervention baseline state after a wash-out period of 3-4 weeks.<sup>59,60</sup> However, an intensive wash-out of 2 weeks in SHIME<sup>®</sup> was unable to reverse the diet effect on PC and DC microbiota, and even resulted in a different microbial community compared to the pre-intervention state. A recent study demonstrated that the rapid evolution of the gut microbiota occurs in the response to dietary change influencing the microbiota-dependent phenotypes in humans.<sup>61</sup>

SHIME<sup>®</sup> allows a good representation of the *in vivo* gut microbial communities and offers unique advantages in studying site-specific difference in human gut microbiome and long-term dietary intervention, but it can only be performed with a limited number of donors. This limits statistical power and studies with different donors would be needed to translate the findings to a broader group of individuals. To increase the confidence in our findings, we longitudinally

measured the catabolite data and run the SHIME® for a long period of time (~ 8 weeks), but to completely understand the complexity of the Trp catabolism by gut microbiota, more in-depth metagenomic and metatranscriptomic analysis need to be performed on a large number of human fecal donors.

Despite the limitations, this study presents the first detailed observation of the site-specific differences in microbiota composition and microbiota-associated Trp catabolism of the human PC and DC microbiota, and provides the first detailed characterization of the shifts in microbial catabolism of Trp under contrasting diets differing in the relative abundance of fiber and proteins. This study highlights the bacterial genera that are likely to be the main contributors to the microbial catabolism of Trp in the human colon. The results of this study pave the way for the design of site-specific therapeutic treatments and dietary interventions targeting the Trp catabolism by gut microbiota.

## **Acknowledgement**

The authors would like to thank Simen Fredriksen for the help in data management and the China Scholarship Council for the financial support to the first author.

## **Competing Interests**

The authors declare no competing interests.

## Reference

1. Wastyk HC, Fragiadakis GK, Perelman D, et al. Gut-microbiota-targeted diets modulate human immune status. *Cell*. 2021;184(16):4137-4153. doi:10.1016/j.cell.2021.06.019
2. Louis P, Hold GL, Flint HJ. The gut microbiota, bacterial metabolites and colorectal cancer. *Nat Rev Microbiol*. 2014;12(10):661-672. doi:10.1038/nrmicro3344
3. Armet AM, Deehan EC, O'Sullivan AF, et al. Rethinking healthy eating in light of the gut microbiome. *Cell Host Microbe*. 2022;30(6):764-785. doi:10.1016/j.chom.2022.04.016
4. Krautkramer KA, Fan J, Bäckhed F. Gut microbial metabolites as multi-kingdom intermediates. *Nat Rev Microbiol*. 2021;19(2):77-94. doi:10.1038/s41579-020-0438-4
5. Flint HJ, Scott KP, Duncan SH, Louis P, Forano E. Microbial degradation of complex carbohydrates in the gut. *Gut Microbes*. 2012;3(4). doi:10.4161/gmic.19897
6. Koh A, De Vadder F, Kovatcheva-Datchary P, Bäckhed F. From dietary fiber to host physiology: short-chain fatty acids as key bacterial metabolites. *Cell*. 2016;165(6):1332-1345. doi:10.1016/j.cell.2016.05.041
7. van der Hee B, Wells JM. Microbial regulation of host physiology by short-chain fatty acids. *Trends Microbiol*. 2021;29(8):700-712. doi:10.1016/j.tim.2021.02.001
8. Makki K, Deehan EC, Walter J, Bäckhed F. The impact of dietary fiber on gut microbiota in host health and disease. *Cell Host Microbe*. 2018;23(6):705-715. doi:10.1016/j.chom.2018.05.012
9. Qiu J, Heller JJ, Guo X, et al. The Aryl Hydrocarbon Receptor Regulates Gut Immunity through Modulation of Innate Lymphoid Cells. *Immunity*. 2012;36(1):92-104. doi:10.1016/j.immuni.2011.11.011
10. Roager HM, Licht TR. Microbial tryptophan catabolites in health and disease. *Nat Commun*. 2018;9(1):1-10. doi:10.1038/s41467-018-05470-4
11. Ouyang W, O'Garra A. IL-10 Family Cytokines IL-10 and IL-22: from Basic Science

- to Clinical Translation. *Immunity*. 2019;50(4):871-891. doi:10.1016/j.immuni.2019.03.020
12. Venkatesh M, Mukherjee S, Wang H, et al. Symbiotic bacterial metabolites regulate gastrointestinal barrier function via the xenobiotic sensor PXR and toll-like receptor 4. *Immunity*. 2014;41(2):296-310. doi:10.1016/j.immuni.2014.06.014
  13. Wlodarska M, Luo C, Kolde R, et al. Indoleacrylic Acid Produced by Commensal *Peptostreptococcus* Species Suppresses Inflammation. *Cell Host Microbe*. 2017;22(1):25-37.e6. doi:10.1016/j.chom.2017.06.007
  14. Bhattarai Y, Williams BB, Battaglioli EJ, et al. Gut Microbiota-Produced Tryptamine Activates an Epithelial G-Protein-Coupled Receptor to Increase Colonic Secretion. *Cell Host Microbe*. 2018;23(6):775-785.e5. doi:10.1016/j.chom.2018.05.004
  15. Natividad JM, Agus A, Planchais J, et al. Impaired Aryl Hydrocarbon Receptor Ligand Production by the Gut Microbiota Is a Key Factor in Metabolic Syndrome. *Cell Metab*. 2018;28(5):737-749.e4. doi:10.1016/j.cmet.2018.07.001
  16. Lamas B, Richard ML, Leducq V, et al. CARD9 impacts colitis by altering gut microbiota metabolism of tryptophan into aryl hydrocarbon receptor ligands. *Nat Med*. 2016;22(6):598-605. doi:10.1038/nm.4102
  17. Lamas B, Hernandez-Galan L, Galipeau HJ, et al. Aryl hydrocarbon receptor ligand production by the gut microbiota is decreased in celiac disease leading to intestinal inflammation. *Sci Transl Med*. 2020;12(566):eaba0624. doi:10.1126/scitranslmed.aba0624
  18. Qi Q, Li J, Yu B, et al. Host and gut microbial tryptophan metabolism and type 2 diabetes: an integrative analysis of host genetics, diet, gut microbiome and circulating metabolites in cohort studies. *Gut*. 2022;71(6):1095-1105. doi:10.1136/gutjnl-2021-324053
  19. Serger E, Luengo-Gutierrez L, Chadwick JS, et al. The gut metabolite indole-3 propionate promotes nerve regeneration and repair. *Nature*. Published online June 22, 2022. doi:10.1038/s41586-022-04884-x

20. Dodd D, Spitzer MH, Van Treuren W, et al. A gut bacterial pathway metabolizes aromatic amino acids into nine circulating metabolites. *Nature*. 2017;551(7682):648-652. doi:10.1038/nature24661
21. Cervantes-Barragan L, Chai JN, Tianero MD, et al. *Lactobacillus reuteri* induces gut intraepithelial CD4 + CD8 $\alpha\alpha$  + T cells. *Science (80- )*. 2017;357(6353):806-810. doi:10.1126/science.aah5825
22. Devlin AS, Marcobal A, Dodd D, et al. Modulation of a Circulating Uremic Solute via Rational Genetic Manipulation of the Gut Microbiota. *Cell Host Microbe*. 2016;20(6):709-715. doi:10.1016/j.chom.2016.10.021
23. Dong F, Hao F, Murray IA, et al. Intestinal microbiota-derived tryptophan metabolites are predictive of Ah receptor activity. *Gut Microbes*. 2020;12(1):1788899. doi:10.1080/19490976.2020.1788899
24. Zhu C, Sawrey-Kubicek L, Beals E, et al. Human gut microbiome composition and tryptophan metabolites were changed differently by fast food and Mediterranean diet in 4 days: a pilot study. *Nutr Res*. 2020;77:62-72. doi:10.1016/j.nutres.2020.03.005
25. Liang H, Dai Z, Liu N, et al. Dietary L-tryptophan modulates the structural and functional composition of the intestinal microbiome in weaned piglets. *Front Microbiol*. 2018;9(AUG). doi:10.3389/fmicb.2018.01736
26. Peron G, Meroño T, Gargari G, et al. A Polyphenol-Rich Diet Increases the Gut Microbiota Metabolite Indole 3-Propionic Acid in Older Adults with Preserved Kidney Function. *Mol Nutr Food Res*. Published online April 6, 2022:2100349. doi:10.1002/mnfr.202100349
27. Huang Z, Boekhorst J, Fogliano V, Capuano E, Wells JM. Distinct effects of fiber and colon segment on microbiota-derived indoles and short-chain fatty acids. *Food Chem*. 2023;398:133801. doi:10.1016/j.foodchem.2022.133801
28. Van de Wiele T, Van den Abbeele P, Ossieur W, Possemiers S, Marzorati M. The Simulator of the Human Intestinal Microbial Ecosystem (SHIME®). In: *The Impact of Food Bioactives on Health*. Springer International Publishing; 2015:305-317. doi:10.1007/978-3-319-16104-4\_27

29. Koper JEB, Loonen LMP, Wells JM, Troise AD, Capuano E, Fogliano V. Polyphenols and tryptophan metabolites activate the aryl hydrocarbon receptor in an in vitro model of colonic fermentation. *Mol Nutr Food Res.* 2019;63(3):1-9. doi:10.1002/mnfr.201800722
30. Marzorati M, Vilchez-Vargas R, Bussche J Vanden, et al. High-fiber and high-protein diets shape different gut microbial communities, which ecologically behave similarly under stress conditions, as shown in a gastrointestinal simulator. *Mol Nutr Food Res.* 2017;61(1):1600150. doi:10.1002/mnfr.201600150
31. Huang Z, Schoones T, Wells JM, Fogliano V, Capuano E. Substrate-Driven Differences in Tryptophan Catabolism by Gut Microbiota and Aryl Hydrocarbon Receptor Activation. *Mol Nutr Food Res.* 2021;65(13):2100092. doi:10.1002/mnfr.202100092
32. Martin M. Cutadapt removes adapter sequences from high-throughput sequencing reads. *EMBnet.journal.* 2011;17(1):10. doi:10.14806/ej.17.1.200
33. Callahan BJ, McMurdie PJ, Rosen MJ, Han AW, Johnson AJA, Holmes SP. DADA2: High-resolution sample inference from Illumina amplicon data. *Nat Methods.* 2016;13(7):581-583. doi:10.1038/nmeth.3869
34. Quast C, Pruesse E, Yilmaz P, et al. The SILVA ribosomal RNA gene database project: improved data processing and web-based tools. *Nucleic Acids Res.* 2012;41(D1):D590-D596. doi:10.1093/nar/gks1219
35. Kieser S, Brown J, Zdobnov EM, Trajkovski M, McCue LA. ATLAS: a Snakemake workflow for assembly, annotation, and genomic binning of metagenome sequence data. *BMC Bioinformatics.* 2020;21(1):257. doi:10.1186/s12859-020-03585-4
36. Li X, Zhang B, Hu Y, Zhao Y. New Insights Into Gut-Bacteria-Derived Indole and Its Derivatives in Intestinal and Liver Diseases. *Front Pharmacol.* 2021;12. doi:10.3389/fphar.2021.769501
37. Kaur H, Bose C, Mande SS. Tryptophan Metabolism by Gut Microbiome and Gut-Brain-Axis: An in silico Analysis. *Front Neurosci.* 2019;13(1365):1-17. doi:10.3389/fnins.2019.01365

38. Valles-Colomer M, Falony G, Darzi Y, et al. The neuroactive potential of the human gut microbiota in quality of life and depression. *Nat Microbiol.* 2019;4(4):623-632. doi:10.1038/s41564-018-0337-x
39. Gao J, Xu K, Liu H, et al. Impact of the gut microbiota on intestinal immunity mediated by tryptophan metabolism. *Front Cell Infect Microbiol.* 2018;8(13):1-22. doi:10.3389/fcimb.2018.00013
40. Agus A, Planchais J, Sokol H. Gut Microbiota Regulation of Tryptophan Metabolism in Health and Disease. *Cell Host Microbe.* 2018;23(6):716-724. doi:10.1016/j.chom.2018.05.003
41. James KR, Gomes T, Elmentaite R, et al. Distinct microbial and immune niches of the human colon. *Nat Immunol.* 2020;21(3):343-353. doi:10.1038/s41590-020-0602-z
42. Duncan SH, Iyer A, Russell WR. Impact of protein on the composition and metabolism of the human gut microbiota and health. *Proc Nutr Soc.* 2021;80(2):173-185. doi:10.1017/S0029665120008022
43. Korpela K. Diet, microbiota, and metabolic health: trade-off between saccharolytic and proteolytic fermentation. *Annu Rev Food Sci Technol.* 2018;9(1):65-84. doi:10.1146/annurev-food-030117-012830
44. Oliphant K, Allen-Vercoe E. Macronutrient metabolism by the human gut microbiome: major fermentation by-products and their impact on host health. *Microbiome.* 2019;7(1):91. doi:10.1186/s40168-019-0704-8
45. Hamer HM, De Preter V, Windey K, Verbeke K. Functional analysis of colonic bacterial metabolism: relevant to health? *Am J Physiol Liver Physiol.* 2012;302(1):G1-G9. doi:10.1152/ajpgi.00048.2011
46. Kaoutari A El, Armougom F, Gordon JI, Raoult D, Henrissat B. The abundance and variety of carbohydrate-active enzymes in the human gut microbiota. *Nat Rev Microbiol.* 2013;11(7):497-504. doi:10.1038/nrmicro3050
47. Aragozzini F, Ferrari A, Pacini N, Gualandris R. Indole-3-lactic acid as a tryptophan metabolite produced by *Bifidobacterium* spp. *Appl Environ Microbiol.* 1979;38(3):544-



546. doi:10.1128/aem.38.3.544-546.1979
48. Koper JE, Troise AD, Loonen LM, et al. Tryptophan Supplementation Increases the Production of Microbial-Derived AhR Agonists in an In Vitro Simulator of Intestinal Microbial Ecosystem. *J Agric Food Chem.* 2022;70(13):3958-3968. doi:10.1021/acs.jafc.1c04145
  49. Lee J-H, Lee J. Indole as an intercellular signal in microbial communities. *FEMS Microbiol Rev.* 2010;34(4):426-444. doi:10.1111/j.1574-6976.2009.00204.x
  50. Walker AW, Duncan SH, Carol McWilliam Leitch E, Child MW, Flint HJ. pH and peptide supply can radically alter bacterial populations and short-chain fatty acid ratios within microbial communities from the human colon. *Appl Environ Microbiol.* 2005;71(7):3692-3700. doi:10.1128/AEM.71.7.3692-3700.2005
  51. Russell WR, Duncan SH, Scobbie L, et al. Major phenylpropanoid-derived metabolites in the human gut can arise from microbial fermentation of protein. *Mol Nutr Food Res.* 2013;57(3):523-535. doi:10.1002/mnfr.201200594
  52. Xiao HW, Cui M, Li Y, et al. Gut microbiota-derived indole 3-propionic acid protects against radiation toxicity via retaining acyl-CoA-binding protein. *Microbiome.* 2020;8(1):69. doi:10.1186/s40168-020-00845-6
  53. Xue H, Chen X, Yu C, et al. Gut Microbially Produced Indole-3-Propionic Acid Inhibits Atherosclerosis by Promoting Reverse Cholesterol Transport and Its Deficiency Is Causally Related to Atherosclerotic Cardiovascular Disease. *Circ Res.* 2022;131(5):404-420. doi:10.1161/CIRCRESAHA.122.321253
  54. Wikoff WR, Anfora AT, Liu J, et al. Metabolomics analysis reveals large effects of gut microflora on mammalian blood metabolites. *Proc Natl Acad Sci U S A.* 2009;106(10):3698-3703. doi:10.1073/pnas.0812874106
  55. Clarke SF, Murphy EF, O'Sullivan O, et al. Exercise and associated dietary extremes impact on gut microbial diversity. *Gut.* 2014;63(12):1913-1920. doi:10.1136/gutjnl-2013-306541
  56. Duncan SH, Louis P, Thomson JM, Flint HJ. The role of pH in determining the species

- composition of the human colonic microbiota. *Environ Microbiol.* 2009;11(8):2112-2122. doi:10.1111/j.1462-2920.2009.01931.x
57. Li F, Hitch TCA, Chen Y, Creevey CJ, Guan LL. Comparative metagenomic and metatranscriptomic analyses reveal the breed effect on the rumen microbiome and its associations with feed efficiency in beef cattle. *Microbiome.* 2019;7(1):6. doi:10.1186/s40168-019-0618-5
58. David LA, Maurice CF, Carmody RN, et al. Diet rapidly and reproducibly alters the human gut microbiome. *Nature.* 2014;505(7484):559-563. doi:10.1038/nature12820
59. Liu F, Li P, Chen M, et al. Fructooligosaccharide (FOS) and Galactooligosaccharide (GOS) Increase Bifidobacterium but Reduce Butyrate Producing Bacteria with Adverse Glycemic Metabolism in healthy young population. *Sci Rep.* 2017;7(1):11789. doi:10.1038/s41598-017-10722-2
60. Burton KJ, Rosikiewicz M, Pimentel G, et al. Probiotic yogurt and acidified milk similarly reduce postprandial inflammation and both alter the gut microbiota of healthy, young men. *Br J Nutr.* 2017;117(9):1312-1322. doi:10.1017/S0007114517000885
61. Dapa T, Ramiro RS, Pedro MF, Gordo I, Xavier KB. Diet leaves a genetic signature in a keystone member of the gut microbiota. *Cell Host Microbe.* 2022;30(2):183-199. doi:10.1016/j.chom.2022.01.002

## Supporting information

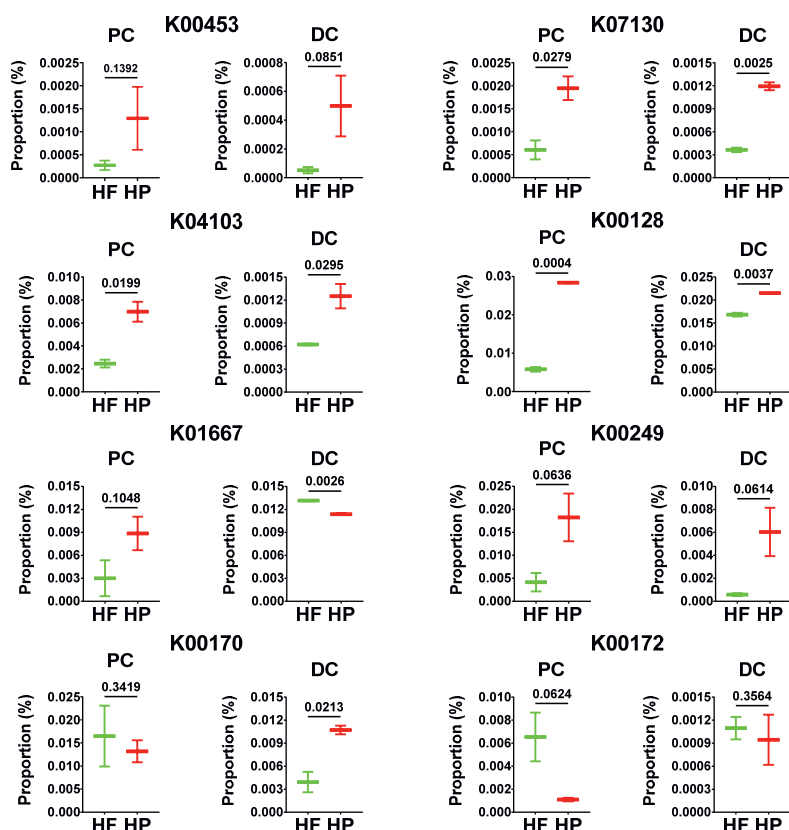


**Figure S5.1** Comparison of the specific KEGG Orthology in the identified tryptophan catabolism pathway. PC: proximal colon. DC: distal colon. HF: high-fiber-low-protein diet. HP: high-protein-low-fiber diet. Data were from two biological donors at Day 23 and were analyzed by Student's t test. The *p* value is shown in each plot and lower than 0.05 is considered as significant difference. K00128: aldehyde dehydrogenase (EC 1.2.1.3); K01667: tryptophanase (EC 4.1.99.1); K04103: indolepyruvate decarboxylase (EC 4.1.1.74); K00453: tryptophan 2,3-dioxygenase (EC 1.13.11.11); K00249: acyl-CoA dehydrogenase (EC 1.3.8.7); K00170: pyruvate ferredoxin oxidoreductase B (EC:1.2.7.1); K00172: pyruvate ferredoxin oxidoreductase C (EC 1.2.7.1); K07130: arylformamidase (EC 3.5.1.9)

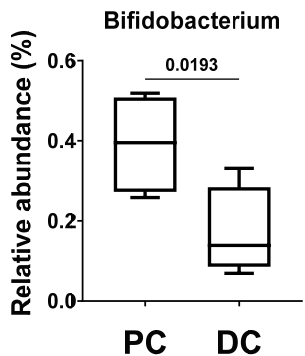


**Figure S5.2** The relative abundance of *Bifidobacterium* in proximal colon (PC) and distal colon (DC) bacteria. Data were from two biological donors in duplicate at Day 6 and analyzed by Student’s t test. The *p* value is shown in the plot and lower than 0.05 is considered as significant difference.

## CHAPTER 6





## General discussion





## 1 The gut bridge connecting food science to human nutrition

“Hunger breeds discontentment” is an old proverb in China. It highlights the most basic and important role of foods for human beings. It also drives food scientists to devote themselves to improving the knowledge on what we should eat. The nutritional and health quality of foods usually refer to the amount of nutrients and bioactive compounds available to be absorbed by the host, but since the discovery and exploration of gut microbiota in recent decades,<sup>1–3</sup> the concept of healthy foods has extended. Microbiome research has revealed the enormous functional potential of the gut microbiota for the host,<sup>4</sup> and this is rapidly changing the approach to food design, where we consider not only the needs of our body but also the needs of our intestinal microorganisms.<sup>5,6</sup> Accordingly, this thesis aims to provide insights into the design of healthy foods that target the gut microbiota to improve health.

The gut microbiota derives energy from ingested food components and produces metabolites that play significant roles in host physiology, of which tryptophan (Trp) catabolites are of particular interest.<sup>7</sup> Microbial catabolism of Trp generates several bioactive catabolites, such as indole (Ind), indole-3-propionic acid (IPA), indole-3-acetic acid (IAA), indole-3-aldehyde (I3A), indole-3-lactic acid (ILA), and tryptamine (TA), which positively modulate the intestinal barrier integrity and immune homeostasis by binding to the pregnane X receptor (PXR) and the aryl hydrocarbon receptor (AhR).<sup>8</sup> Reduced concentration of these catabolites have also been reported in the fecal samples of individuals with several diseases,<sup>9–13</sup> indicating that they could be therapeutic targets. However, factors influencing Trp catabolism by gut microbiota are not well understood, especially the dietary factors, and no studies have examined the site-specific differences in the microbial production of Trp catabolites along the intestine. Therefore, in this thesis, we investigated the effect of the food matrix (**Chapter 2 and 3**), food components (**Chapter 4**), and habitual diets (**Chapter 5**) on the Trp catabolism by gut microbiota. We also investigated the differences in the microbial production of Trp catabolites in the small and large intestine (**Chapter 2**) and in the proximal and distal parts of the colon (**Chapter 4 and 5**). The main findings of these chapters are presented in Table 6.1 and are generally discussed to give a broader perspective regarding the topic of this thesis.

**Table 6.1** Summary of the main findings of this thesis.

Objective	Main findings
<b>Chapter 2:</b>	
<ul style="list-style-type: none"> <li>To investigate the food-derived tryptophan catabolites present in the ileum and colon of pigs</li> </ul>	<ul style="list-style-type: none"> <li>➤ Tryptophan catabolites in ileal digesta of pigs are dominated by indole, indole-3-lactic acid, indole-3-propionic acid, and indole-3-acetic acid.</li> <li>➤ Tryptophan catabolites in faeces of pigs are dominated by skatole, oxindole, and indole.</li> <li>➤ The concentration and composition of tryptophan catabolites in ileal digesta and faeces of pigs is food-specific.</li> </ul>
<b>Chapter 3:</b>	
<ul style="list-style-type: none"> <li>To explore the role of food matrix in tryptophan catabolism by gut microbiota and the resulting AhR activation</li> </ul>	<ul style="list-style-type: none"> <li>➤ Food structure modulates the accessibility of tryptophan to microbiota.</li> <li>➤ The compositional differences in the food matrix differently modulate the microbial production of tryptophan catabolites.</li> <li>➤ Butyrate, as well as acetate and propionate, potentially synergizes with tryptophan catabolites to activate AhR.</li> </ul>
<b>Chapter 4:</b>	
<ul style="list-style-type: none"> <li>To examine effects of fiber and colon segment on the microbial production of short-chain fatty acids and tryptophan catabolites</li> </ul>	<ul style="list-style-type: none"> <li>➤ Fiber supplementation promotes the microbial production of acetate, propionate, and butyrate, indole-3-propionic acid, indole-3-lactic acid, and indole-3-acetic acid, but reduces the microbial production of oxindole, tryptamine, and serotonin.</li> <li>➤ DC microbiota<sup>a</sup> has a stronger capacity to produce short-chain fatty acids than PC microbiota<sup>b</sup></li> </ul>
<b>Chapter 5:</b>	
<ul style="list-style-type: none"> <li>To demonstrate the site-specific differences and diet-induced modifications in microbiota composition and microbiota-associated tryptophan catabolism</li> </ul>	<ul style="list-style-type: none"> <li>➤ PC microbiota has a higher abundance of <i>Firmicutes</i> and a stronger capacity to produce kynurenine, serotonin, indoleacrylic acid, tryptamine, indole-3-lactic acid, and indole-3-aldehyde.</li> <li>➤ DC microbiota has a higher abundance of <i>Bacteroidetes</i> and a stronger capacity to produce indole-3-acetic acid, indole, indole-3-propionic acid, and oxindole.</li> <li>➤ Compared to high-protein-low-fiber diet, high-fiber-low-protein diet favors the microbial production of serotonin, indoleacrylic acid, indole-3-aldehyde, indole-3-lactic acid, indole-3-acetic acid, and indole-3-propionic acid.</li> </ul>

<sup>a</sup> Human fecal microbiota adapted to the distal colon compartment of SHIME®<sup>b</sup> Human fecal microbiota adapted to the proximal colon compartment of SHIME®

## 2 Site-specific difference in microbial production of Trp catabolites

Most studies examining relationships between gut microbiota and host metabolism have primarily relied on fecal or colonic luminal samples,<sup>14–17</sup> and relatively little attention has been given to the microbiome in the small intestine. In **Chapter 2**, we employed an animal model of growing pigs to investigate the ileal and colonic production of microbiota-derived Trp catabolites. We found that some catabolites, like I3A, ILA, and IAA, were identified in ileal digesta of pigs (Figure 6.1), especially the ILA which was quantified at a higher concentration in ileal digesta than in faeces of pigs. Previously, these catabolites were also identified in ileal fluid samples of ileostomy patients.<sup>18</sup> ILA formation occurs via the action of the enzyme indolelactate dehydrogenase, which is expressed in *Lactobacillus* spp.<sup>19,20</sup> In the porcine intestine, the genus *Lactobacillus* is estimated to constitute 5% of the bacteria in the small intestine and approximately 0.1% of the bacteria in the colon.<sup>21</sup> These levels are similar to the abundance of *Lactobacillus* found in humans, ranging from 6% in the small intestine to 0.3% in the colon.<sup>21</sup> These findings suggest that small bowel microbiota plays a role in the catabolism of Trp, especially in the ILA biosynthesis.

In **Chapter 2**, we found that Trp catabolites, except for ILA, were more abundant in faeces than in ileal digesta of pigs, and the overall concentration of Trp catabolites in faeces was over five-fold higher than that in ileal digesta, which could be due to the large abundance and extensive metabolic capacity of the microbiota in the colon.<sup>22</sup> This finding suggested that the colon is the main site for microbial catabolism of Trp. Given that the microbiota composition and function varies along the colon (i.e., proximal and distal colon),<sup>23</sup> we hypothesized that it may also influence the microbial catabolism of Trp. To address this and mimic the *in vivo* human gut microbial communities of proximal and distal parts of the colon, we used the Simulator of Human Intestinal Microbial Ecosystem (SHIME®) in **Chapter 5**. The colonic microbiota prefers to utilize fermentable carbohydrates over proteins as the energy source, with the proximal part of the colon being the main site for saccharolytic fermentation and distal part of the colon being the main site for proteolytic fermentation.<sup>24,25</sup> Some studies reported that saccharolytic specialists in the proximal part of the colon can produce a variety of Trp catabolites, for example, *Bifidobacterium* spp. convert Trp to ILA,<sup>26</sup> *Lactobacillus* spp. convert Trp to ILA and I3A,<sup>27</sup> and *Ruminococcus gnavus* convert Trp to tryptamine (TA).<sup>28</sup> In agreement with these studies,

we identified these catabolites in PC samples<sup>c</sup>, together with Ind, IAA, kynurenine (Kyn), serotonin (5-HT), and indoleacrylic acid (IA) (Figure 6.1). Proteolytic fermentation by the microbiota occurs predominantly in the distal part of the colon where we indeed measured highest concentrations of Trp catabolites in DC samples<sup>d</sup>, with Ind accounting for over 90% of all Trp catabolites (Figure 6.1). For individual Trp catabolites, PC samples had higher concentrations of Kyn, 5-HT, IA, TA, ILA, and I3A than DC samples, whereas DC samples were more abundant in IAA and especially Ind. Interestingly, oxindole (Oxi) and IPA were identified in DC samples but not in PC samples. Together, these results provide insights into the site-specific difference in microbial production of Trp catabolites along the intestine.

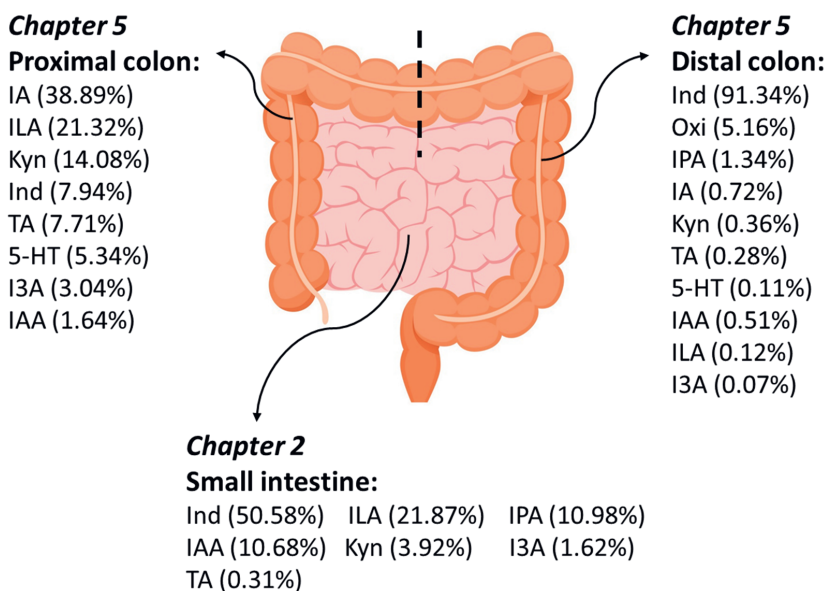


**Figure 6.1** The production of microbiota-derived tryptophan catabolites along the intestine.

Data are from **Chapter 2** and **Chapter 5** and presented in the mean abundance. Ind: indole; Ska: skatole; ILA: indole-3-lactic acid; Oxi: oxindole; 5-HT: serotonin; I3A: indole-3-aldehyde; TA: tryptamine; Kyn: kynurenine; IAA: indole-3-acetic acid; IA: indoleacrylic acid; IPA: indole-3-propionic acid

<sup>c</sup> Fermented samples from proximal colon compartment of SHIME®

<sup>d</sup> Fermented samples from distal colon compartment of SHIME®

### 3 Role of food matrix in Trp catabolism by gut microbiota

The food matrix is typically used to indicate the diversity in the chemical composition of food and its structural organization at macro-, meso-, and microscopic levels.<sup>29</sup> The matrix can influence the release, accessibility, digestibility, and fermentability of food compounds.<sup>30</sup> Human uptake of Trp is highly dependent on the foods included in the diet as Trp is an essential amino acid. Thus, it is reasonable to hypothesize that food matrix influences the Trp catabolism by gut microbiota, a research question not currently addressed in the published literature.

In *Chapter 2*, we fed pigs with eighteen different diets and each diet had a tested food as the protein source, including algae (seaweed, spirulina), fungi (mushrooms, yeast, quorn), seeds (kidney beans, linseed, buckwheat, amaranth), cereals (wheat flour, oatmeal, millet, rice crackers, cornflakes), animal products (chicken, fish, eggs), and potato protein. Trp is released from the proteolytic digestion of proteins in the small intestine,<sup>31</sup> where small bowel microbiota can compete with epithelial cells for the released Trp.<sup>32</sup> Animal protein generally has a higher level of Trp and a higher digestibility than plant protein,<sup>33</sup> as an intact plant cell wall and anti-nutritional compounds in plant foods protect the intracellular plant protein against digestive enzymes.<sup>34,35</sup> However, food processing can increase the digestibility of plant protein by breaking the cell wall and inactivating the anti-nutritional factors.<sup>36</sup> Therefore in the small intestine, animal foods would release more Trp than unprocessed plant foods and consequently, we found the highest overall concentration of Trp catabolites in ileal digesta of pigs fed with eggs, followed by chicken. Additionally, potato protein induced a similar overall concentration of Trp catabolites in ileal digesta as chicken, although it has a lower Trp content. A relatively low overall concentration of Trp catabolites was observed in ileal digesta of pigs fed with unprocessed plant foods. However, we also observed that fish has a similar protein digestibility,<sup>37</sup> and Trp content as chicken, but induced in a lower level of Trp catabolites than chicken in the ileal digesta, which suggests the presence of other factors affecting the microbial production of Trp catabolites in the small intestine.

The more protein is digested in the small intestine, the less protein will reach the colon; hence, it is reasonable to hypothesize that unprocessed plant foods can produce higher concentrations of Trp catabolites in the faeces than other highly digestible foods. Nevertheless, our data do not support this hypothesis. One possible explanation is that plant foods also contain sufficient amounts of dietary fibers which are fermented in preference to proteins by the microbiota.<sup>24</sup> Another limiting factor could be the content of Trp available to colonic microbiota. After

passing to the colon, although colonic microbiota can secrete carbohydrate-active enzymes that are able to break down the plant cell wall,<sup>38</sup> still some proteins remained undigested.

To simplify the effect of food matrix in microbial catabolism of Trp, we conducted a batch fermentation using human fecal microbiota supplied with free Trp, soybean protein, single and clustered soybean cells (**Chapter 3**). These four substrates contain an equimolar amount of Trp, but with different accessibility to the microbiota. The more complex the structure, the less tryptophan was catabolized. However, more TA was found in the fermentation with soybean cells, although less Trp was catabolized, potentially due to the effect of polysaccharides in the plant cell wall on the microbiota. Collectively, as shown in Figure 6.2, these results demonstrate that food matrix plays a role in the microbial production of Trp catabolites in the intestine, possibly via a direct effect on the amount of Trp available in the lumen and/or an indirect effect on the microbiota composition and metabolic activity regarding Trp catabolism. Depending on food processing and formulation, food products with high bioavailability will have small intestine absorption and with low bioavailability will have colon biotransformation and absorption (Figure 6.2). To better understand the role of the food matrix further *in vitro* studies isolating the effect of each dietary factor on the microbial catabolism of Trp are needed.

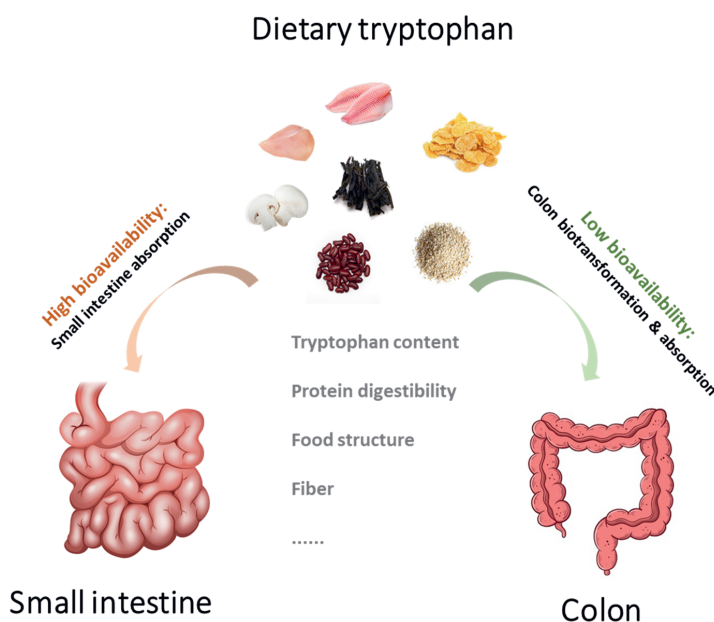


**Figure 6.2** Food matrix plays a role in the tryptophan bioavailability and microbial production of tryptophan catabolites in the intestine.

## 4 Fiber as a modulator of Trp catabolism by gut microbiota

A diverse body of literature supports the beneficial effect of fiber on host physiology through fermentation by the gut microbiota with production of beneficial short-chain fatty acids (SCFAs) as end products.<sup>39</sup> Results in **Chapter 3** suggested that fiber may also modulate the microbial catabolism of Trp. Therefore, in **Chapter 4**, we examined the effect of pectin, inulin, and their combination on the catabolism of Trp by PC microbiota<sup>e</sup> and DC microbiota<sup>f</sup>. Increasing the availability of fermentable carbohydrates to intestinal microbiome was previously reported to reduce the protein fermentation in the colon.<sup>38</sup> Our results in **Chapter 4** demonstrated that this was possible with PC microbiota, but not with DC microbiota with respect to microbial Trp catabolism. One possible explanation for the differential effect of fibers is the different functional metabolic capacity of PC and DC microbiota. Fermentable fiber is a preferred energy source for microbial growth,<sup>24</sup> but it can be used in different metabolic activities dependent on the functional profiles of microbiota. Fiber supplementation promoted the microbial production of IPA and ILA, but reduced the microbial production of Oxi, TA, and 5-HT, especially in the fermentation with the combined fibers. Fermentation with pectin specifically promoted the microbial production of IAA and I3A. These results indicate that the type and usage of fiber influence the Trp catabolism by gut microbiota.

In **Chapter 5**, we explored the effect of fiber on microbial catabolism of Trp under the habitual diets and resembling *in vivo* conditions of the colon. We formulated two extreme diets: high-fiber-low-protein (HF) diet and high-protein-low-fiber (HP) diet, and conducted a two-week microbiome intervention study using SHIME<sup>®</sup>. Compared to control period before dietary intervention, the composition of SHIME<sup>®</sup> microbiota<sup>g</sup> was greatly altered by HF and HP diets, especially the PC microbiota, and this was associated with changes in the microbial metabolic activity regarding Trp catabolism. The HF diet had less proteins and therefore less Trp than HP diet, but it favored the production of 5-HT, IA, IAA, ILA, I3A, and IPA by both PC and DC microbiota compared to HP diet, suggesting that the effect of HF diet on the microbial production of these catabolites was independent of protein or Trp content. The HF diet increased the abundance of fiber-degrading bacteria,<sup>40</sup> some of which may have the capability to specifically catabolize Trp, such as *Bifidobacterium* spp., which can convert Trp into IAA

<sup>e</sup> Human fecal microbiota adapted to the PC compartment of SHIME<sup>®</sup>

<sup>f</sup> Human fecal microbiota adapted to the DC compartment of SHIME<sup>®</sup>

<sup>g</sup> Human fecal microbiota adapted to the conditions of SHIME<sup>®</sup>

and ILA.<sup>8,26</sup> A recent study also showed that the circulating concentration of IPA was positively associated with intake of fiber-rich foods and inversely associated with type 2 diabetes risk.<sup>41</sup> Together, these results demonstrate a potential role of fiber in health as a modulator of Trp catabolism by gut microbiota.



## 5 Relevance of *in vitro* models in microbiology

Gut microbiota is closely related to human nutrition and health.<sup>1</sup> It is modulated by many factors, such as genetics, age, sex, stress, and drugs,<sup>42,43</sup> but diet, specifically food components, is recognized as the main driver of microbiota composition and function.<sup>44</sup> A wide range of strategies have been developed to advance the knowledge on gut microbiome, including *in vitro* models, animal models, and human studies.<sup>45,46</sup> *In vivo* approaches provide information with physiological relevance, but *in vitro* models are still essential, especially for isolating the effect of foods or food components on gut microbiome for more mechanistic insights.

Typically, *in vitro* models can be divided in two types: static batch systems used in **Chapter 3** and continuous culture systems, like SHIME<sup>®</sup> used in **Chapter 5**. Batch fermentation is relatively simple and convenient, and can be performed in test tubes or vessels. It has a high flexibility and scalability, which enables many hypotheses to be tested at once and within a time period of 24–48 h.<sup>47</sup> It is useful for assessing the fermentation rate/extent of different food components.<sup>48</sup> In **Chapter 3**, batch fermentation was used to characterize the catabolism kinetics of Trp by gut microbiota, in which we found that the more time Trp is exposed to microbiota, the more Trp catabolites were produced until all the available Trp was depleted. Therefore, increasing the passage time of Trp in the colon could be an effective way to promote the microbial production of Trp catabolites.

However, the outcome of batch fermentation is considered less physiologically relevant and therefore, SHIME<sup>®</sup> was developed.<sup>49</sup> It is a complex and fully automated system allowing a better representation of the gut microbial communities than batch fermentation.<sup>50</sup> SHIME<sup>®</sup> employs distinct serially connected bioreactors to mimic the gastrointestinal digestion and colonic fermentation in different colon segments under resembling *in vivo* environmental conditions.<sup>50</sup> A SHIME<sup>®</sup> experiment is time-consuming, but the microbiota can be kept stable over a long period of time, even several weeks, by continuously feeding with SHIME<sup>®</sup> growth medium<sup>h</sup> three times per day with an interval of eight hours. It offers unique advantages to study the long-term microbiome interventions and site-specific differences in the composition and function of colonic microbiota. By using SHIME<sup>®</sup> in **Chapter 5**, we demonstrated that microbiota composition and microbiota-associated Trp catabolism varied between PC and DC microbiota and between HF and HP diets. These findings provided insights into the design of

<sup>h</sup> A commercial product (PD-NM001B) from ProDigest, Belgium.

site-specific therapeutic treatments and dietary modifications targeting microbial catabolism of Trp.

SHIME<sup>®</sup> is a continuous system which leads to the variation of substrates available to microbiota in the PC and DC compartments. To well understand the specific role of PC and DC microbiota in Trp catabolism, we used a combination of SHIME<sup>®</sup> and a static batch fermentation in **Chapter 4**. The stabilized microbiota from PC and DC compartments of SHIME<sup>®</sup> was inoculated into the batch vessels supplied with the same medium, but the initial environmental pH was adjusted to 5.6-5.9 for fermentation with PC microbiota and 6.6-6.9 for fermentation with DC microbiota. Results showed that the functional difference between PC and DC microbiota was well maintained in batch cultures in terms of Trp catabolism compared with findings from **Chapter 5**. As expected, DC microbiota possessed a stronger capacity to catabolize Trp than PC microbiota, which could be due to the successful control of the pH during the 24 h fermentation. These findings suggest an approach of studying separately microbiota populations adapted to different parts of the colon *in vitro*.

*In vitro* models have certain limitations. Lack of co-culture with host cells means that microbial metabolites accumulate in the batch culture,<sup>46</sup> which may have feedback regulation on gut microbiota metabolism, and also alter the dynamics of metabolite production by providing substrates and intermediates at concentrations that would not be found *in vivo* due to host absorption. *In vitro* culturing methods cause shifts in the abundance of microbial taxa compared to the inoculum,<sup>51,52</sup> and this may affect the microbial responses to external stimuli. Additionally, the inoculum itself may not represent the whole of the microbiota inhabiting in the intestine. Therefore, conclusions from *in vitro* studies may be over- or under-estimated and warrant verification by comparison to *in vivo* studies.

## 6 Implications for food design targeting gut microbiota

The knowledge accumulated on the effect of certain microbial metabolites on intestinal and systemic health have prompted scholars to propose the idea of designing microbiota-directed foods (MDFs).<sup>53</sup> Unlike the dietary fiber-based prebiotics, MDF represents a “food” composed of one or more substrates for microbial metabolism capable of manipulating the microbiome in a selective manner that is beneficial for the host. This can involve nutrients, converted by the microbiota into beneficial metabolites.<sup>53</sup> One such example provided in this thesis is the use of Trp and fiber in an MDF.

A small fraction of Trp from ingested foods can be catabolized by gut microbiota in the intestine, especially in the colon, resulting in a variety of Trp catabolites.<sup>8</sup> Numerous studies have demonstrated the contribution of microbiota-derived Trp catabolites to host physiology.<sup>9,54</sup> The most investigated mechanism of action is their ability to activate the AhR,<sup>55</sup> which was confirmed in **Chapter 3** using a reporter cell line from human HepG2 cells. Some studies indicated that microbiota-derived Trp catabolites, like IPA, IAA, Ind, and indole-3-acetamide, can also activate PXR to regulate the intestinal barrier function.<sup>56,57</sup> Therefore, we tested these Trp catabolites in the porcine intestinal organoids for the induction of PXR-regulated gene expression of Cyp3a29,<sup>58</sup> at their reported effective concentrations.<sup>56,57</sup> Rifampicin was used a control agonist of PXR.<sup>59</sup> As shown in Figure 6.3, stimulation with Ind (1 mM) and IPA (100  $\mu$ M) induced Cyp3a29 expression on porcine intestinal organoids. These data support the role of these microbiota-derived Trp catabolites as potential AhR and PXR activators in the intestine. Given Trp can be absorbed in the small intestine, a suitable carrier system for Trp has to be produced in MDFs or the natural plant cells with an intact cell wall which protects the intracellular protein and Trp against the digestive enzymes.

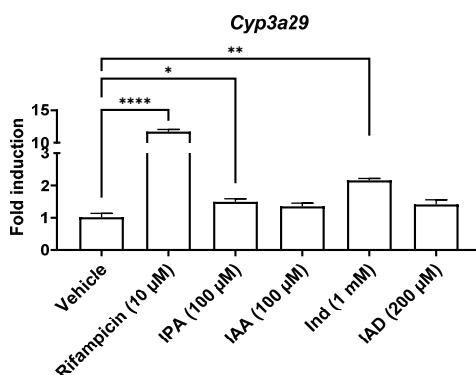


**Figure 6.3** RT-qPCR analysis of Cyp3a29 mRNA levels in porcine intestinal organoids treated with 0.1% DMSO (Vehicle), rifampicin, indole-3-propionic acid (IPA), indole-3-acetic acid (IAA), indole (Ind), and indole-3-acetamide (IAD) for 24 hours. Data are expressed as fold change compared to housekeeping gene Hprt1 (n=3) and analyzed by Student's t test. Significance is reported as \* $p < 0.05$ , \*\* $p < 0.01$ , and \*\*\*\* $p < 0.0001$ .

Fiber, mostly fermentable fiber, is widely studied for its modulation of the composition and metabolic profile of gut microbiota.<sup>60</sup> In **Chapter 4** and **Chapter 5**, we revealed that fermentable fiber can promote the microbial production of Trp-derived AhR and PXR activators, potentially due to the increased abundance of certain fiber-degrading bacteria. Fermentable fiber can also promote the microbial production of SCFAs.<sup>39</sup> Recent studies showed that butyrate can activate AhR,<sup>61</sup> as also demonstrated in **Chapter 3**, and enhance the AhR activation by microbiota-derived ligands.<sup>62</sup> As shown in Figure 6.4, the AhR activation on HepG2-Lucia™ reporter cells was synergistically increased when Trp catabolites were combined with butyrate, suggesting a synergistic effect of butyrate in the presence of an AhR activator. Therefore, fiber capable of supporting the microbial production of butyrate and Trp-derived AhR activators should be considered in the design of MDFs containing Trp.

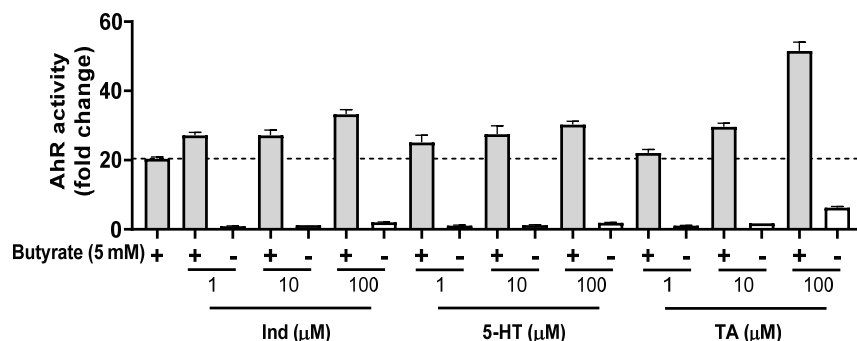


**Figure 6.4** AhR activity in HepG2-Lucia™ AhR reporter cells treated with butyrate (5 mM) in presence (+) or absence (-) with indole (Ind), serotonin (5-HT), and tryptamine (TA) for 48 hours. Data are expressed as luciferase fold change over 0.1% DMSO.

SCFAs are the metabolites mainly produced in the colon through the anaerobic fermentation of indigestible carbohydrates and are considered beneficial for the host.<sup>63</sup> The *in vivo* concentration of SCFAs declines along the colon.<sup>64</sup> This could be due to the reduced availability of fermentable carbohydrates and the continuous absorption by colon epithelium. Our data in **Chapter 4** demonstrated that fermentation with DC microbiota produced more SCFAs than fermentation with PC microbiota when they were supplied with the same amount of fiber, suggesting that DC microbiota may possess a stronger capacity to produce SCFAs than PC microbiota. Similar results were also reported by Rovalino-Córdova and colleagues.<sup>65</sup> These findings underscore the application of slowly fermentable fiber in the design of MDFs to promote the production of SCFAs, especially butyrate in the distal part of the colon, where more abundant Trp catabolites were presented at physiologically relevant concentrations to activate the AhR. Globally, the future for food design should be more specific and functional.

## 7 Future perspectives

Results presented in this thesis increased the understanding of microbial catabolism of Trp in the intestine and revealed the role of dietary factors in modulating the production of microbiota-derived Trp catabolites. Here, we proposed some ideas enlightened by this thesis for possible future research which are discussed in more detail below.

*Small bowel microbiota in host physiology.* Despite growing literature demonstrating the importance of gut microbiota in health and disease, most studies focus on fecal microbiota and much less is known about the role of small bowel microbiota in host physiology. Evidence from ileostomy patients,<sup>18</sup> and **Chapter 2** suggests that small bowel microbiota can produce Trp-derived AhR ligands, like Ind, IAA, and I3A. In the small intestine, lack of AhR ligands compromises the maintenance of intraepithelial lymphocytes, resulting in heightened immune activation and increased vulnerability to epithelial damage.<sup>66</sup> Dysbiosis in small intestine has been reported in many human diseases,<sup>67</sup> but whether this is associated with impaired AhR ligand production from Trp and contribute to disease pathogenesis has not yet been explored. Additionally, it would also be meaningful to investigate the effect of dietary perturbations on the composition and function of small bowel microbiota.

*Physiological significances of microbiota-derived Trp catabolites.* Using porcine intestinal organoids and a reporter cell line from human HepG2 cells, we demonstrated the AhR and PXR activation potential of microbiota-derived Trp catabolites. However, more studies should be conducted to understand the exact role of each Trp catabolite in host physiology and unravel their mechanisms in different segments and cells of the intestine by use of animal models and most importantly the human cells, as AhR and PXR responses are species-dependent. Specifically, human AhR has a higher affinity than mouse AhR for Trp-derived ligands,<sup>68</sup> and IPA is a mouse PXR ligand, but not an efficient human PXR ligand.<sup>69</sup> Besides AhR and PXR, other mechanisms of action of microbiota-derived Trp catabolites should also be explored, e.g. G-protein-coupled receptor.<sup>70</sup>

*Main producers of microbiota-derived Trp catabolites in the human intestine.* Although a number of bacterial species capable of producing Trp catabolites have been identified,<sup>8</sup> the main contributors to microbial catabolism of Trp in the human intestine are still unclear. In **Chapter 5**, we provided some evidence, but more in-depth research linking the abundances of bacterial species with concentrations of Trp catabolites in a large number of human fecal samples and if

possible, human ileal fluid samples, as well as *in vitro* and *in silico* verification is needed to determine the contributors. Additionally, Trp catabolites can also be produced by other microorganisms than bacteria, like fungi.<sup>71</sup> Therefore, the profiling of gut microbiota regarding Trp catabolism should not be limited to bacteria.

*Physiological effects of diet targeting Trp catabolism by gut microbiota.* Given the biological effects of microbiota-derived Trp catabolites and their perturbations in disease,<sup>8,54</sup> Trp catabolism by gut microbiota can be a potential target in disease prevention strategy. In **Chapter 4** and **Chapter 5**, we showed that fiber or HF diet can promote the *in vitro* microbial production of some Trp-derived AhR and PXR activators, which proves the cause-and-effect relationships. Therefore, dietary intervention studies targeting Trp catabolism by gut microbiota on special populations are of particular interest for future research.

## References

1. Sekirov I, Russell SL, Caetano M Antunes L, Finlay BB. Gut microbiota in health and disease. *Physiol Rev*. 2010;90(3):859-904. doi:10.1152/physrev.00045.2009
2. The Human Microbiome project Consortium. Structure, function and diversity of the healthy human microbiome. *Nature*. 2012;486(7402):207-214. doi:10.1038/nature11234
3. The Human Microbiome project Consortium. A framework for human microbiome research. *Nature*. 2012;486(7402):215-221. doi:10.1038/nature11209
4. Lozupone CA, Stombaugh JI, Gordon JI, Jansson JK, Knight R. Diversity, stability and resilience of the human gut microbiota. *Nature*. 2012;489(7415):220-230. doi:10.1038/nature11550
5. Armet AM, Deehan EC, O'Sullivan AF, et al. Rethinking healthy eating in light of the gut microbiome. *Cell Host Microbe*. 2022;30(6):764-785. doi:10.1016/j.chom.2022.04.016
6. Ercolini D, Fogliano V. Food Design to Feed the Human Gut Microbiota. *J Agric Food Chem*. 2018;66(15):3754-3758. doi:10.1021/acs.jafc.8b00456
7. Agus A, Planchais J, Sokol H. Gut Microbiota Regulation of Tryptophan Metabolism in Health and Disease. *Cell Host Microbe*. 2018;23(6):716-724. doi:10.1016/j.chom.2018.05.003
8. Roager HM, Licht TR. Microbial tryptophan catabolites in health and disease. *Nat Commun*. 2018;9(1):1-10. doi:10.1038/s41467-018-05470-4
9. Gao J, Xu K, Liu H, et al. Impact of the gut microbiota on intestinal immunity mediated by tryptophan metabolism. *Front Cell Infect Microbiol*. 2018;8(13):1-22. doi:10.3389/fcimb.2018.00013
10. Natividad JM, Agus A, Planchais J, et al. Impaired Aryl Hydrocarbon Receptor Ligand Production by the Gut Microbiota Is a Key Factor in Metabolic Syndrome. *Cell Metab*. 2018;28(5):737-749.e4. doi:10.1016/j.cmet.2018.07.001
11. Lamas B, Richard ML, Leducq V, et al. CARD9 impacts colitis by altering gut microbiota metabolism of tryptophan into aryl hydrocarbon receptor ligands. *Nat Med*. 2016;22(6):598-605. doi:10.1038/nm.4102
12. Choi S-C, Brown J, Gong M, et al. Gut microbiota dysbiosis and altered tryptophan catabolism contribute to autoimmunity in lupus-susceptible mice. *Sci Transl Med*. 2020;12(551):eaax2220. doi:10.1126/scitranslmed.aax2220



13. Lamas B, Hernandez-Galan L, Galipeau HJ, et al. Aryl hydrocarbon receptor ligand production by the gut microbiota is decreased in celiac disease leading to intestinal inflammation. *Sci Transl Med*. 2020;12(566):eaba0624. doi:10.1126/scitranslmed.aba0624
14. Rooks MG, Garrett WS. Gut microbiota, metabolites and host immunity. *Nat Rev Immunol*. 2016;16(6):341-352. doi:10.1038/nri.2016.42
15. De Filippis F, Pasolli E, Tett A, et al. Distinct Genetic and Functional Traits of Human Intestinal Prevotella copri Strains Are Associated with Different Habitual Diets. *Cell Host Microbe*. 2019;25(3):444-453.e3. doi:10.1016/j.chom.2019.01.004
16. Dapa T, Ramiro RS, Pedro MF, Gordo I, Xavier KB. Diet leaves a genetic signature in a keystone member of the gut microbiota. *Cell Host Microbe*. 2022;30(2):183-199. doi:10.1016/j.chom.2022.01.002
17. Wastyk HC, Fragiadakis GK, Perelman D, et al. Gut-microbiota-targeted diets modulate human immune status. *Cell*. 2021;184(16):4137-4153. doi:10.1016/j.cell.2021.06.019
18. Koper JEB, Kortekaas M, Loonen LMP, et al. Aryl hydrocarbon Receptor activation during in vitro and in vivo digestion of raw and cooked broccoli ( brassica oleracea var. Italica ). *Food Funct*. 2020;11(5):4026-4037. doi:10.1039/D0FO00472C
19. Wilck N, Matus MG, Kearney SM, et al. Salt-responsive gut commensal modulates TH17 axis and disease. *Nature*. 2017;551(7682):585-589. doi:10.1038/nature24628
20. Cervantes-Barragan L, Chai JN, Tianero MD, et al. Lactobacillus reuteri induces gut intraepithelial CD4 + CD8 $\alpha\alpha$  + T cells. *Science (80- )*. 2017;357(6353):806-810. doi:10.1126/science.aah5825
21. Heeney DD, Gareau MG, Marco ML. Intestinal Lactobacillus in health and disease, a driver or just along for the ride? *Curr Opin Biotechnol*. 2018;49:140-147. doi:10.1016/j.copbio.2017.08.004
22. Martinez-Guryn K, Leone V, Chang EB. Regional diversity of the gastrointestinal microbiome. *Cell Host Microbe*. 2019;26(3):314-324. doi:10.1016/j.chom.2019.08.011
23. James KR, Gomes T, Elmentaite R, et al. Distinct microbial and immune niches of the human colon. *Nat Immunol*. 2020;21(3):343-353. doi:10.1038/s41590-020-0602-z
24. Oliphant K, Allen-Vercoe E. Macronutrient metabolism by the human gut microbiome: major fermentation by-products and their impact on host health. *Microbiome*. 2019;7(1):91. doi:10.1186/s40168-019-0704-8
25. Hamer HM, De Preter V, Windey K, Verbeke K. Functional analysis of colonic

- bacterial metabolism: relevant to health? *Am J Physiol Liver Physiol*. 2012;302(1):G1-G9. doi:10.1152/ajpgi.00048.2011
26. Aragozzini F, Ferrari A, Pacini N, Gualandris R. Indole-3-lactic acid as a tryptophan metabolite produced by *Bifidobacterium* spp. *Appl Environ Microbiol*. 1979;38(3):544-546. doi:10.1128/aem.38.3.544-546.1979
  27. Zelante T, Iannitti RG, Cunha C, et al. Tryptophan Catabolites from Microbiota Engage Aryl Hydrocarbon Receptor and Balance Mucosal Reactivity via Interleukin-22. *Immunity*. 2013;39(2):372-385. doi:10.1016/j.immuni.2013.08.003
  28. Williams BB, Van Benschoten AH, Cimermancic P, et al. Discovery and characterization of gut microbiota decarboxylases that can produce the neurotransmitter tryptamine. *Cell Host Microbe*. 2014;16(4):495-503. doi:10.1016/j.chom.2014.09.001
  29. Capuano E, Oliviero T, van Boekel MAJS. Modeling food matrix effects on chemical reactivity: Challenges and perspectives. *Crit Rev Food Sci Nutr*. 2018;58(16):2814-2828. doi:10.1080/10408398.2017.1342595
  30. Aguilera JM. The food matrix: implications in processing, nutrition and health. *Crit Rev Food Sci Nutr*. 2019;59(22):3612-3629. doi:10.1080/10408398.2018.1502743
  31. Snook JT, Meyer JH. Response of digestive enzymes to dietary protein. *J Nutr*. 1964;82(4):409-414. doi:10.1093/jn/82.4.409
  32. Savage DC. Gastrointestinal Microflora in Mammalian Nutrition. *Annu Rev Nutr*. 1986;6(1):155-178. doi:10.1146/annurev.nu.06.070186.001103
  33. Day L, Cakebread JA, Loveday SM. Food proteins from animals and plants: Differences in the nutritional and functional properties. *Trends Food Sci Technol*. 2022;119:428-442. doi:10.1016/j.tifs.2021.12.020
  34. Day L, Cakebread JA, Loveday SM. Food proteins from animals and plants: Differences in the nutritional and functional properties. *Trends Food Sci Technol*. 2022;119:428-442. doi:10.1016/j.tifs.2021.12.020
  35. Capuano E, Pellegrini N. An integrated look at the effect of structure on nutrient bioavailability in plant foods. *J Sci Food Agric*. 2019;99(2):493-498. doi:10.1002/jsfa.9298
  36. Sá AGA, Moreno YMF, Carciofi BAM. Food processing for the improvement of plant proteins digestibility. *Crit Rev Food Sci Nutr*. 2020;60(20):3367-3386. doi:10.1080/10408398.2019.1688249
  37. Faber TA, Bechtel PJ, Hernot DC, et al. Protein digestibility evaluations of meat and fish substrates using laboratory, avian, and ileally cannulated dog assays. *J Anim Sci*.

- 2010;88(4):1421-1432. doi:10.2527/jas.2009-2140
38. Korpela K. Diet, microbiota, and metabolic health: trade-off between saccharolytic and proteolytic fermentation. *Annu Rev Food Sci Technol*. 2018;9(1):65-84. doi:10.1146/annurev-food-030117-012830
  39. Makki K, Deehan EC, Walter J, Bäckhed F. The impact of dietary fiber on gut microbiota in host health and disease. *Cell Host Microbe*. 2018;23(6):705-715. doi:10.1016/j.chom.2018.05.012
  40. Flint HJ, Scott KP, Duncan SH, Louis P, Forano E. Microbial degradation of complex carbohydrates in the gut. *Gut Microbes*. 2012;3(4). doi:10.4161/gmic.19897
  41. Qi Q, Li J, Yu B, et al. Host and gut microbial tryptophan metabolism and type 2 diabetes: an integrative analysis of host genetics, diet, gut microbiome and circulating metabolites in cohort studies. *Gut*. 2022;71(6):1095-1105. doi:10.1136/gutjnl-2021-324053
  42. Org E, Mehrabian M, Parks BW, et al. Sex differences and hormonal effects on gut microbiota composition in mice. *Gut Microbes*. 2016;7(4):313-322. doi:10.1080/19490976.2016.1203502
  43. Voreades N, Kozil A, Weir TL. Diet and the development of the human intestinal microbiome. *Front Microbiol*. 2014;5(495). doi:10.3389/fmicb.2014.00494
  44. Sheflin AM, Melby CL, Carbonero F, Weir TL. Linking dietary patterns with gut microbial composition and function. *Gut Microbes*. 2017;8(2):113-129. doi:10.1080/19490976.2016.1270809
  45. Venema K, Van Den Abbeele P. Experimental models of the gut microbiome. *Best Pract Res Clin Gastroenterol*. 2013;27(1):115-126. doi:10.1016/j.bpg.2013.03.002
  46. Fritz J V, Desai MS, Shah P, Schneider JG, Wilmes P. From meta-omics to causality: Experimental models for human microbiome research. *Microbiome*. 2013;1(1):14. doi:10.1186/2049-2618-1-14
  47. Pérez-Burillo S, Molino S, Navajas-Porras B, et al. An in vitro batch fermentation protocol for studying the contribution of food to gut microbiota composition and functionality. *Nat Protoc*. 2021;16(7):3186-3209. doi:10.1038/s41596-021-00537-x
  48. Wang M, Wichienchot S, He X, Fu X, Huang Q, Zhang B. In vitro colonic fermentation of dietary fibers: Fermentation rate, short-chain fatty acid production and changes in microbiota. *Trends Food Sci Technol*. 2019;88:1-9. doi:10.1016/j.tifs.2019.03.005
  49. Molly K, Vande Woestyne M, Verstraete W. Development of a 5-step multi-chamber

- reactor as a simulation of the human intestinal microbial ecosystem. *Appl Microbiol Biotechnol*. 1993;39(2):254-258. doi:10.1007/BF00228615
50. Van de Wiele T, Van den Abbeele P, Ossieur W, Possemiers S, Marzorati M. The Simulator of the Human Intestinal Microbial Ecosystem (SHIME®). In: *The Impact of Food Bioactives on Health*. Springer International Publishing; 2015:305-317. doi:10.1007/978-3-319-16104-4\_27
  51. Auchtung JM, Robinson CD, Britton RA. Cultivation of stable, reproducible microbial communities from different fecal donors using minibioreactor arrays (MBRAs). *Microbiome*. 2015;3(1):42. doi:10.1186/s40168-015-0106-5
  52. McDonald JAK, Schroeter K, Fuentes S, et al. Evaluation of microbial community reproducibility, stability and composition in a human distal gut chemostat model. *J Microbiol Methods*. 2013;95(2):167-174. doi:10.1016/j.mimet.2013.08.008
  53. Barratt MJ, Lebrilla C, Shapiro H-Y, Gordon JI. The Gut Microbiota, Food Science, and Human Nutrition: A Timely Marriage. *Cell Host Microbe*. 2017;22(2):134-141. doi:10.1016/j.chom.2017.07.006
  54. Agus A, Planchais J, Sokol H. Gut microbiota regulation of tryptophan metabolism in health and disease. *Cell Host Microbe*. 2018;23(6):716-724. doi:10.1016/j.chom.2018.05.003
  55. Lamas B, Natividad JM, Sokol H. Aryl hydrocarbon receptor and intestinal immunity. *Mucosal Immunol*. 2018;11(4):1024-1038. doi:10.1038/s41385-018-0019-2
  56. Venkatesh M, Mukherjee S, Wang H, et al. Symbiotic bacterial metabolites regulate gastrointestinal barrier function via the xenobiotic sensor PXR and toll-like receptor 4. *Immunity*. 2014;41(2):296-310. doi:10.1016/j.immuni.2014.06.014
  57. Illés P, Krasulová K, Vyhliďalová B, et al. Indole microbial intestinal metabolites expand the repertoire of ligands and agonists of the human pregnane X receptor. *Toxicol Lett*. 2020;334:87-93. doi:10.1016/j.toxlet.2020.09.015
  58. He Y, Zhou X, Li X, et al. Relationship between CYP3A29 and pregnane X receptor in landrace pigs: Pig CYP3A29 has a similar mechanism of regulation to human CYP3A4. *Comp Biochem Physiol Part - C Toxicol Pharmacol*. 2018;214:9-16. doi:10.1016/j.cbpc.2018.08.006
  59. Chrencik JE, Orans J, Moore LB, et al. Structural disorder in the complex of human pregnane X receptor and the macrolide antibiotic rifampicin. *Mol Endocrinol*. 2005;19(5):1125-1134. doi:10.1210/me.2004-0346
  60. Loo YT, Howell K, Chan M, Zhang P, Ng K. Modulation of the human gut microbiota

- by phenolics and phenolic fiber-rich foods. *Compr Rev Food Sci Food Saf*. 2020;19(4):1268-1298. doi:10.1111/1541-4337.12563
61. Marinelli L, Martin-Gallausiaux C, Bourhis JM, Béguet-Crespel F, Blottière HM, Lapaque N. Identification of the novel role of butyrate as AhR ligand in human intestinal epithelial cells. *Sci Rep*. 2019;9(1):1-14. doi:10.1038/s41598-018-37019-2
  62. Modoux M, Rolhion N, Lefevre JH, et al. Butyrate acts through HDAC inhibition to enhance aryl hydrocarbon receptor activation by gut microbiota-derived ligands. *Gut Microbes*. 2022;14(1). doi:10.1080/19490976.2022.2105637
  63. Silva YP, Bernardi A, Frozza RL. The Role of Short-Chain Fatty Acids From Gut Microbiota in Gut-Brain Communication. *Front Endocrinol (Lausanne)*. 2020;11:25. doi:10.3389/fendo.2020.00025
  64. Cummings JH, Pomare EW, Branch HWJ, Naylor CPE, MacFarlane GT. Short chain fatty acids in human large intestine, portal, hepatic and venous blood. *Gut*. 1987;28(10):1221-1227. doi:10.1136/gut.28.10.1221
  65. Rovalino-Córdova AM, Fogliano V, Capuano E. In vitro colonic fermentation of red kidney beans depends on cotyledon cells integrity and microbiota adaptation. *Food Funct*. 2021;12(11):4983-4994. doi:10.1039/d1fo00321f
  66. Li Y, Innocentin S, Withers DR, et al. Exogenous Stimuli Maintain Intraepithelial Lymphocytes via Aryl Hydrocarbon Receptor Activation. *Cell*. 2011;147(3):629-640. doi:10.1016/j.cell.2011.09.025
  67. Kastl AJ, Terry NA, Wu GD, Albenberg LG. The Structure and Function of the Human Small Intestinal Microbiota: Current Understanding and Future Directions. *Cell Mol Gastroenterol Hepatol*. 2020;9(1):33-45. doi:10.1016/j.jcmgh.2019.07.006
  68. Hubbard TD, Murray IA, Bisson WH, et al. Adaptation of the human aryl hydrocarbon receptor to sense microbiota-derived indoles. *Sci Rep*. 2015;5(1):12689. doi:10.1038/srep12689
  69. Dvořák Z, Sokol H, Mani S. Drug Mimicry: Promiscuous Receptors PXR and AhR, and Microbial Metabolite Interactions in the Intestine. *Trends Pharmacol Sci*. 2020;41(12):900-908. doi:10.1016/j.tips.2020.09.013
  70. Bhattarai Y, Williams BB, Battaglioli EJ, et al. Gut Microbiota-Produced Tryptamine Activates an Epithelial G-Protein-Coupled Receptor to Increase Colonic Secretion. *Cell Host Microbe*. 2018;23(6):775-785.e5. doi:10.1016/j.chom.2018.05.004
  71. Zelante T, Choera T, Beauvais A, et al. *Aspergillus fumigatus* tryptophan metabolic route differently affects host immunity. *Cell Rep*. 2021;34(4):108673.

doi:10.1016/j.celrep.2020.108673

A





# Appendix

Summary

Acknowledgements

About the author



## Summary

Gut microbiota has been widely acknowledged for its essential role in human and animal health, via the production of a variety of metabolites that impact locally and systemically with aspects of host physiology. In recent years, microbiota-derived tryptophan (Trp) catabolites have gained increasing interest. Specific microbial catabolites of tryptophan can bind and activate the aryl hydrocarbon receptor (AhR), indirectly enhancing intestinal epithelial barrier function, and contributing to intestinal homeostasis. These catabolites are also suggested to be therapeutic targets in treating several diseases. It was shown that fiber-rich foods, can potentially modulate the microbial catabolism of Trp and promote the production of beneficial Trp catabolites. Therefore, this thesis aimed to gain a better understanding of the effects of dietary components on the modulation of Trp catabolism by gut microbiota. The findings highlight the necessity to consider the microbial pathway of Trp catabolism in diet-microbiome interactions.

In **Chapter 1**, we provided a brief overview of the current knowledge regarding the Trp catabolism by gut microbiota and described the aims, the hypotheses, methodology and the content of the thesis.

In **Chapter 2**, we used growing pigs as a model to investigate the microbiota-derived Trp catabolites present in the ileum and colon. We fed pigs with eighteen different diets and each diet had a tested food as the protein source, including algae (seaweed, spirulina), fungi (mushrooms, yeast, quorn), seeds (kidney beans, linseed, buckwheat, amaranth), cereals (wheat flour, oatmeal, millet, rice crackers, cornflakes), animal products (chicken, fish, eggs), and potato protein. The protein content in each diet was kept the same at 100 g/kg dry matter, except for rice crackers and cornflakes. Microbiota-derived Trp catabolites were extracted from ileal digesta and faeces of pigs and quantified by LC-MS. Indole (Ind), indole-3-propionic acid (IPA), indole-3-acetic acid (IAA), indole-3-lactic acid (ILA), kynurenine (Kyn), tryptamine (TA), and indole-3-aldehyde (I3A) were identified in ileal digesta. These catabolites were also identified in faeces together with skatole (Ska), oxindole (Oxi), serotonin (5-HT), and 3-indoleacrylic acid (IA). The concentration of total catabolites in faeces was higher (~200-1200 nmol/g) than that in ileal digesta (~10-50 nmol/g). Trp catabolites in ileal digesta were dominated by Ind, whereas feeding pigs with millet, kidney beans, and yeast inhibited the production of Ind in the small intestine and shifted the Trp catabolism to IAA, IPA, and ILA production. Trp catabolites in faeces were dominated by Ska, but feeding pigs with mushrooms shifted the catabolism to TA and Ind biosynthesis and feeding pigs with buckwheat shifted the catabolism to TA, IPA, Ind,

and Oxi biosynthesis. Additionally, we also examined the AhR activation potential of ileal digesta and faeces of pigs. Extracts from ileal digesta failed to elicit a significant activation of AhR, while extracts from faeces significantly activated AhR.

In **Chapter 3**, we used static *in vitro* batch fermentation inoculated with human fecal microbiota to explore the role of food matrix in Trp catabolism by gut microbiota and the resulting AhR activation. We used four different soybean preparations to reproduce different level of structural complexity of a plant matrix: single cells, cell clusters, isolated soybean protein and free Trp. These preparations contained an equimolar amount of Trp. Human fecal microbiota was able to degrade the plant cell wall and break down the intracellular proteins. The more complex the structure, the less Trp was catabolized. Ind was the main catabolite produced from Trp, followed by IPA and IAA. Despite more catabolism of Trp in the fermentation with free Trp, IAA and I3A were more abundant in the fermentation with soybean protein, and TA was more abundant in the fermentation with soybean cells. Fermentation with soybean cells resulted in the highest AhR activity, but this was because of the high level of propionate and butyrate in the fermented samples. These fatty acids were produced from co-fermentation of polysaccharides in the plant cell wall, and were shown to be able to activate AhR at concentrations above 5 mmol/L. Similar levels of AhR activation were also observed in acetate, valerate, and isovalerate, whereas isobutyrate had no AhR activity and antagonized the AhR activation induced by  $\beta$ -naphthoflavone, a potent AhR agonist.

In **Chapter 4**, we used static *in vitro* batch fermentation inoculated with stabilized microbiota from proximal colon (PC) and distal colon (DC) compartments of the Simulator of Human Intestinal Microbial Ecosystem (SHIME<sup>®</sup>) to examine the effect of fiber (pectin, inulin, and their combination) and colon segment (PC and DC) on microbial composition and production of Trp catabolites and short-chain fatty acids (SCFAs). Microbiota from PC compartment (PC microbiota) had a higher relative abundance of Proteobacteria than microbiota from DC compartment (DC microbiota). Fermentation with pectin and inulin increased the relative abundance of Bacteroidetes in both PC and DC microbiota, but fermentation with combined fibers decreased it. Acetate, propionate, and butyrate were the main SCFAs produced and more abundant in the fermentation with DC microbiota (DC fermentation) than in the fermentation with PC microbiota (PC fermentation). DC fermentation also yielded higher levels of Ind, Oxi, and IPA than PC fermentation. Fiber supplementation promoted the microbial production of acetate, propionate, butyrate, IPA, and ILA, but reduced the microbial production of Oxi, TA, and 5-HT. Interestingly, fiber supplementation suppressed Ind production in PC fermentation,

but not in DC fermentation. Pectin specifically favored the microbial production of IAA and I3A.

In **Chapter 5**, we used SHIME® to demonstrate the site-specific differences and diet-induced modifications in microbiota composition and microbiota-associated Trp catabolism. SHIME® was set up to mimic the *in vivo* gut microbial communities of PC and DC by using human fecal microbiota from two healthy donors. After stabilization time in PC and DC compartments of SHIME®, PC microbiota had a higher relative abundance of Firmicutes and Proteobacteria, but a lower relative abundance of Bacteroidetes than DC microbiota. Kyn, 5-HT, IA, TA, ILA, and I3A were quantified at higher levels in samples from PC compartment (PC samples) than those from DC compartment (DC samples), whereas IAA and especially Ind were more abundant in DC samples than in PC samples. IPA and Oxi were identified in DC samples, but not in PC samples. Trp catabolism by PC microbiota was dominated by IA, ILA, and Kyn production, whereas Trp catabolism by DC microbiota was dominated Ind production, which accounts for over 90% of the examined catabolites. By changing the composition of the basal diet for microbiota in SHIME®, we formulated two extreme diets: high-fiber-low-protein (HF) diet and high-protein-low-fiber (HP) diet and conducted a two-week intervention study using these two diets. HF and HP diets markedly altered the composition of PC microbiota compared to baseline, in which HF diet increased the relative abundance of Firmicutes including several genera, such as *Lachnoclostridium*, *Megasphaera*, and *Tyzzereella*, and the HP diet increased the relative abundance of *Proteobacteria*, mostly through an increase in the genus *Enterobacter*. Compared to HP diet, HF diet favored the microbial production of 5-HT, IA, IAA, ILA, I3A, and IPA. Given the HF diet had less proteins and therefore less Trp than HP diet, the effect of HF diet on the microbial production of these catabolites was independent of protein or Trp content.

**Chapter 6** provides a general discussion of the results described in this thesis and some considerations about the use of *in vitro* models in microbiology. We also discussed the potential implications of the main findings in the design of novel healthy foods and some ideas for possible future research regarding the topic of this thesis.



## Acknowledgements

Time flies, I complete my PhD journey at Wageningen University & Research. It is my honor to be a student under the direction of Dr. Edoardo Capuano, Prof. Vincenzo Fogliano, and Prof. Jerry M. Wells. It is my honor to be a FQDer and a HMIer. It is my pleasure to meet so many colleagues and friends over here in Wageningen.

V and Jerry, thank you for being my promotor and standing by me. You gave me the opportunity to become part of the FQD and HMI groups and so much freedom to navigate my study and research. I have a great time working in both of your groups. V, thank you for your encouragement, guidance, and supervision. I have a lot of respect for you, although sometimes I do not follow your suggestions. Jerry, I learn a lot from uncountable discussions, meetings, and personal conversations with you. Thank you for your inspiration, idea, and creativity. I always lose myself under your pet phrase “Oh, good! Nice! Well-done, Zhan!”. Edo, my co-promotor, I cannot thank you more for supporting me during the four years. You are always available and ready to help when I encounter problems or burst into your office with any questions. Thank you very much for helping me during the most difficult time of my life. You always tell me be positive be happy. Thank you very much for taking care and making time for me. I will not let you down. V, Jerry, and Edo, we are a team.

Jiaxin, Danlei, Zhuang, Zulin, Lintianxiang, Yangwenshan, Xiaolin, and Tiantong, it is nice to meet you. I enjoy a lot being with you, having the dinner, playing mahjong, travelling, and chatting. Thank you very much for brightening my life and bringing me a lot of wonderful memories. I wish you the best of everything for all the years ahead.

Sonja, Nikkie, Roseanne, and Huyen in ANU, Pieter Gremmen in ETE, and Harry in FPH, thank you for your great help and coach in several parts of my research. Sonja and Nikkie, thank you very much for your valuable feedbacks on my manuscript of pig study. Geert and Christos, thank you very much for your help in my PhD project. Geert, I valued a lot the period we were together using the old LC-MS. You taught me a lot of things about the usage and theory of LC-MS. You helped me multiple times to fix the GC. With your training, I think I am a junior analyst and engineer now. The gentleman Christos, you make my work smoother and always help me fix the problems with LC-MS. You are so kind and polite. Jos and Simen, thank you for your help in microbiota analysis. Jos, thank you very much for your assistance in bioinformatics and valuable comments on my manuscripts. You further my research and make

my life much easier. Jonna, Erik, and Bart, thank you very much for your guidance in the experimental skills. Jonna, you are so nice and sweet, it is my great pleasure to meet you. I am very grateful for the things you taught me. Hoping one day I can meet you again. Erik, it is nice having you in the lab. We have so many conversations about research about life. You bring me a lot of laughs and jokes. You are one of the most important people in my PhD journey, just like you stand by me in my defense. Bart, you are my colleague, my teacher, and most importantly my friend. Working and chatting with you always have a lot of fun and various kinds of knowledge. Remember we will collaborate in the future, I take care of China, you take of Europe, win-win! Jianing, you are so nice, thank you very much for your guidance on the procedure and requirements of the thesis submission.

Tessa, Dorianne, Alice, Myrthe, Samara, Yi, and Marieke, my excellent students. It is a great pleasure supervising you with your thesis. I appreciate your participation and contribution to my research and project. I wish you a lot of success in your future.

Corine, Kimberley, Lisa, Charlotte, Frans, Xandra, Mike, Jelle, Nienke, Anastasia, Anita, Teresa, Nicoletta, Maryia, Josep, Pien, Sjoera, Ebru, Pieter Groen, and other FQD staff members; Loes, Joyce, Nico, Anja, Aline, Anda, Ellen, Linda, Michiel, Sylvia, Maria, and other HMI staff members, thank you all for creating an enjoyable working environment. Being part of FQD group and HMI group has been a great pleasure for me. We have a lot of nice moments, during dinners, labouting, meetings, chats, and other social activities. It is a real pleasure to meet you all and work together. Corine, Kimberley, Lisa, and Loes, thank you very much for taking care of all the administrative issues and making our PhD life easier.

Ana Maria, Femke, Mostafa, Alim, Ita, Sara, Hannah, Chunyue, Li WANG, Ling XIONG, Hao ZHANG, Geelu, Zhijun, Lijiao, Ningjing, Yuzheng, Hongwei, Eva, Yaowei, Yi SHEN, Huifang, Lawal, Pieter Dekker, Vincenzo C., Melania, Elisa, Annelies, Fabiola, Diana, Marianna, Yajing, Mohammad, Moyong, Yao CHEN, Zongyao, Keqing, Jiaying, Qing HAN, Feilong, Zekun, Qing REN, Xiangnan, Kangni, Zhe CHENG, Yifang, Peiheng, Ximeng, Yongkai, Wenyi, Julie, Fiametta, Niels, Cristina, Marialena, Luc, Swantje, Sofia, Ruth, Andrea, Laura, Lise, Pengfei, Ruth Boachie, Niels, and other FQD colleagues; Nuning, Laura, Isabela, Aisha, Arabela, Berdien, Blance, Maaïke, Oshin, Raka, and other HMI colleagues; Taojun, Chen ZHANG, Xilong, Liang FANG, Mu HE, Suo MU, Jianli, Keli, Zhaoxiang, Li XIE, Caifang, Xiaoning, and my friends, thank you all for the great time we had together and sharing the fantastic PhD journey with me. It is nice to meet you all in the Netherlands.



Tiantong and Erik, thank you very much being my paranymphs, being my side during my defense and supporting me. I deeply appreciate all the effort you put into organizing my PhD defense.

Special thanks to Prof. Yongkang Luo at China Agricultural University, being my mentor and *Bole*. Special thanks to China Scholarship Council for the financial support.

To my family, 父母在, 不远游, 游必有方。

Zhan HUANG

2023-02-07

Wageningen, The Netherlands



## About the author



Zhan HUANG was born on 26<sup>th</sup> September, 1993, in Yangzhou, Jiangsu province, China. He obtained his bachelor degree of engineering in Food Science and Engineering from HeFei University of Technology in 2016 and obtained his master degree of engineering in Agricultural Product Processing and Storage Engineering from China Agricultural University in 2018. In October 2018, he started his PhD study under the direction of Dr. Edoardo Capuano, Prof. Vincenzo Fogliano, and Prof. Jerry M. Wells at the chair groups of Food Quality & Design and Host-Microbe Interactomics, Wageningen

University & Research. Currently, he is working as a postdoctoral researcher in Sokol's Lab at Sorbonne University in Paris, France.

### Contact information:

Email: [huangzhan1993@126.com](mailto:huangzhan1993@126.com)



## List of publications

1. **Huang, Z.**, Boekhorst, J., Fogliano, V., Capuano, E., & Wells, J. M. Impact of high-fiber or high-protein diet on the capacity of human gut microbiota to produce tryptophan catabolites. (*Submitted to journal for publication*)
  
2. **Huang, Z.**, de Vries, S., Fogliano, V., Wells, J. M., van der Wielen, N., Capuano, E., & Effect of whole foods on the microbial production of tryptophan-derived aryl hydrocarbon receptor agonists in growing pigs. (*Submitted to journal for publication*)
  
3. **Huang, Z.**, Boekhorst, J., Fogliano, V., Capuano, E., & Wells, J. M. (2023). Distinct effects of fiber and colon segment on microbiota-derived indoles and short-chain fatty acids. *Food Chemistry*, 398, 133801. <https://doi.org/10.1016/j.foodchem.2022.133801>.
  
4. **Huang, Z.**, Schoones, T., Wells, J. M., Fogliano, V., & Capuano, E. (2021). Substrate-Driven Differences in Tryptophan Catabolism by Gut Microbiota and Aryl Hydrocarbon Receptor Activation. *Molecular Nutrition & Food Research*, 65(13), 2100092. <https://doi.org/10.1002/mnfr.202100092>.
  
5. **Huang, Z.**, Jia, S., Zhang, L., Liu, X., & Luo, Y. (2019). Inhibitory effects and membrane damage caused to fish spoilage bacteria by cinnamon bark (*Cinnamomum tamala*) oil. *LWT-Food Science and Technology*, 112, 108195. <https://doi.org/10.1016/j.lwt.2019.05.093>.
  
6. **Huang, Z.**, Liu, X., Jia, S., Zhang, L., & Luo, Y. (2018). The effect of essential oils on microbial composition and quality of grass carp (*Ctenopharyngodon idellus*) fillets during chilled storage. *International Journal of Food Microbiology*, 266, 52–59. <https://doi.org/10.1016/j.ijfoodmicro.2017.11.003>.
  
7. **Huang, Z.**, Liu, X., Jia, S., & Luo, Y. (2017). Antimicrobial effects of cinnamon bark oil on microbial composition and quality of grass carp (*Ctenopharyngodon idellus*) fillets during chilled storage. *Food Control*, 82, 316–324. <https://doi.org/10.1016/j.foodcont.2017.07.017>.

## Conference talks

1. Effect of fiber type on the metabolism of *ex vivo* human gut microbiota. Presented at 11<sup>th</sup> Probiotics, prebiotics & new foods, nutraceuticals and botanicals for nutrition & human and microbiota health, Rome, Italy, 2021.

## Overview of completed training activities

### *Discipline specific activities*

Annual gut day	VLAG/MIB	2018
Nutrient delivery and impact on human health	University of Udine, Italy	2019
Mediterranean diet seminar	University of Naples, Italy	2019
Intestinal microbiome of humans and animals	VLAG/MIB	2019
Big data analysis in the life sciences	VLAG/HNH	2019
Energy metabolism and body composition	VLAG/HNH&HAP	2021
Healthy food design	VLAG/FQD	2021
Reaction kinetics in food science	VLAG/FQD	2021
Modelling of habitual dietary intake	VLAG/RIVM	2021
Conference: Probiotics, Prebiotics, & New Foods	Università Urbaniana, Italy	2021

### *General courses*

VLAG PhD week	VLAG	2019
Introduction to R	VLAG	2019
Reviewing a scientific paper	WGS	2019
Posters and Pitching	WGS	2019
Scientific Writing	WGS	2019
Applied Statistics	VLAG	2019
Adobe InDesign Essential Training	WUR library	2019

Scientific Artwork - Vector graphics & images	WUR library	2019
---	-------------	------

***Optional activities***

Preparation of research proposal	VLAG/FQD	2018
FQD PhD study tour to Spain	VLAG/FQD	2022
FQD weekly group meetings	VLAG/FQD	2018-22
HMI weekly group meetings	WIAS/HMI	2018-22
Thesis supervision	VLAG/FQD	2018-22

***List of abbreviations***

VLAG: Graduate School for Nutrition, Food Technology, Agrobiotechnology and Health Sciences

MIB: Laboratory of Microbiology

FQD: Food Quality and Design group

HNH: Division of Human Nutrition and Health

HAP: Human and Animal Physiology

RIVM: Rijksinstituut voor Volksgezondheid en Milieu

WGS: Wageningen Graduate School

WUR: Wageningen University & Research

WIAS: Wageningen Institute of Animal Sciences

HMI: Host-Microbe Interactomics group





The research described in this thesis was financially supported by the Chinese Scholarship Council.

Financial support from Wageningen University for printing this thesis is gratefully acknowledged.

Cover design by ProefschriftMaken and Zhan Huang

Printed by ProefschriftMaken



